HEAT TRANSFER AND FRICTION FACTOR AUGMENTATION USING TWISTED TAPE INSERT WITH DIMPLE CONFIGURATIONS IN A DOUBLE PIPE HEAT EXCHANGER: AN EXPERIMENTAL STUDY

A Thesis

Submitted in partial fulfillment of the requirements for the award of the degree of

DOCTOR OF PHILOSOPHY

in

(Mechanical Engineering)

By

Jatoth Heeraman

(42000066)

Supervised by

Dr. Ravinder Kumar

Professor, School of Mechanical Engineering, Lovely Professional University, Punjab, India.

Co-Supervised by

Dr. Prem Kumar Chaurasiya

Professor, Department of Mechanical Engineering, Bansal Institute of Science and Technology, Bhopal, India.

LOVELY PROFESSIONAL UNIVERSITY, PUNJAB

2024

CANDIDATE'S DECLARATION

I hereby certify that the work which is being presented in this thesis, entitled "**Heat Transfer and Friction Factor Augmentation Using Twisted Tape Insert with Dimple Configurations in A Double Pipe Heat Exchanger: An Experimental Study**" for the fulfillment of the requirements for the award of the Degree of **Doctor of Philosophy (Ph .D.)** and submitted in the **School of Mechanical Engineering** of Lovely Professional University, Punjab, India is an authentic record of my own work carried out under the supervision of **Dr. Ravinder Kumar**, Professor, School of Mechanical Engineering, Lovely Professional University, Punjab, India and **Dr. Prem Kumar Chaurasiya**, Professor, Department of Mechanical Engineering, Bansal Institute of Technology, Bhopal, India. The thesis is an original piece of research work and embodies the findings made by me.

The matter presented in this thesis has not been submitted in part or in full for the award of any other degree/diploma of this or any other University/Institute.

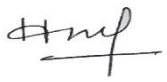

Jatoth Heeraman,
(Reg. No. 42000066),
School of Mechanical Engineering,
Lovely Professional University,
Punjab, India

CERTIFICATE

This is to certify that the thesis entitled "**Heat Transfer and Friction Factor Augmentation Using Twisted Tape Insert with Dimple Configurations in A Double Pipe Heat Exchanger: An Experimental Study"**, being submitted by **Mr. Jatoth Heeraman (Reg. No. 42000066)** to the School of Mechanical Engineering, Lovely Professional University, Punjab, India for the award of Degree of '**Doctor of Philosophy' (Ph. D.)** in Mechanical Engineering, is a bonafide research work carried out by him under my supervision and guidance. His thesis has reached the standard of fulfilling the requirements of regulations relating to degree.

The results presented have not been submitted in part or in full to any other University/Institute for the award of any other degree or diploma.

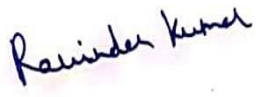

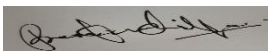

Dr. Ravinder Kumar,
Professor,
Mechanical Engineering Department,
Lovely Professional University,
Punjab, India.

Dr. Prem Kumar Chaurasiya,
Professor,
Mechanical Engineering Department,
Bansal institute of science and technology,
Bhopal, India.

ABSTRACT

Heat transfer is a fundamental concept in various applications such as refrigeration, air-conditioning, thermal power generation, food processing, and feedstock processing. The exchange of heat between two fluids at different temperatures, separated by a solid surface, has numerous applications, and the device that facilitates efficient heat transfer is known as a heat exchanger. Heat exchangers are used to transfer heat from one fluid to another, either to heat the fluid or to cool it down, and they come in various shapes and sizes depending on the application. In general, a heat exchanger consists of two fluid streams separated by a solid wall, and the heat transfer occurs through conduction, convection, and radiation. The efficiency of a heat exchanger depends on various factors such as the geometry of the heat exchanger, the fluid properties, the flow rates, and the thermal conductivity of the materials used.

Double pipe heat exchangers (DPHEs) are widely used in various industries due to their simple design, low cost, and low maintenance requirements. Compared to other types of heat exchangers, double pipe heat exchangers are the most basic in construction and design. They are commonly used in small scale industries such as food, oil, chemical, reheating, preheating, and effluent heating processes. The performance of double pipe heat exchangers is crucial in terms of system efficiency and economics. Therefore, improving the heat transfer ability of double pipe heat exchangers can be a significant step towards sustainable energy growth.

There have been many investigations, both theoretical and experimental, on the performance of heat exchangers with various types of twisted tapes, including typical, perforated, notched, jagged, center-cleared, V-cut, serrated, square cut, and helical screw. However, the present study contributes to the literature by introducing the use of dimpled twisted tape with adjacent hole, which has not been previously reported in the literature, in a heat exchanger tube under constant heat flux and turbulent flow conditions. This novelty can provide insight into the potential of this type of tape for improving heat transfer efficiency in heat exchangers.

To summarize, this study aims to investigate the effects of using twisted tapes with dimples of different diameters and diameter-to-depth ratios in a double pipe heat exchangers. For this purpose, the researchers have designed and fabricated an

experimental setup according to the ASHRAE standards. The setup consists of two circuits, a hot water closed loop circuit and a cold-water open loop circuit. The test section of the setup is made of copper for the inner pipe and Galvanized Iron for the outer pipe. Six T-type thermocouples are placed at different locations to capture the surface temperature, and thermometric wells are connected at the ends of the test section to measure the temperatures of hot and cold water. Two knobs are connected at the ends of the test section to measure the pressure drop across the test section using a U-tube manometer. The data from the thermocouples and RTDs is logged to analyze the heat transfer efficiency. This experimental setup will help in determining the effectiveness of dimpled twisted tape inserts in a double pipe heat exchangers.

The highest heat transfer coefficient (Nusselt number) is observed when using a twisted tape with a dimple diameter of 4 mm and a diameter-to-depth ratio of 3, at a Reynolds number of 13987. The value of Nusselt number is an indication of the effectiveness of the heat transfer, and a higher value indicates better heat transfer performance. The comparison of the results between plain tube and twisted tape with and without dimple allowed for a clear evaluation of the impact of the dimple on the heat transfer and friction characteristics. Overall, the results of this study suggest that the use of dimpled twisted tapes can significantly improve the heat transfer performance of double pipe heat exchangers. The highest value of Nusselt number is found to be 111 at Reynolds number =13987, for D =4 mm and D/H =3.

The results of the study suggest that the friction factor (f) is directly proportional to the depth of the dimple and increases with an increase of dimple diameter on twisted tape. The highest value of friction factor is obtained at dimple diameter 2 mm and dimple diameter to depth ratio (D/H) = 4.5. In addition, it is also observed that maximum value of PEC is found at dimple diameter of 4 mm (D/H=4.5).

The correlation has been developed by using regression analysis in terms of dimple geometry dimple diameter (D) and dimple diameter to depth ratio (D/H), Reynolds number (Re) for Heat transfer and friction factor.

Acknowledgement

It is my great pleasure to record profound gratitude to my research supervisor**, Dr. Ravinder Kumar**, Professor, School of Mechanical Engineering, Lovely Professional University, Punjab, India and **Dr. Prem Kumar Chaurasiya**, Professor, Department of Mechanical Engineering, Bansal institute of Technology, Bhopal, India, for their constant inspiration and invaluable guidance throughout the course of investigation. I gratefully acknowledge his painstaking efforts in thoroughly going through and improving the manuscript without which this work would not have been completed. The numerous discussions I had with my supervisor and co-supervisor instilled in me the confidence needed to crack formidable problems in the present field of research.

I wish to thank **Dr. Ankur Bahl**, HoS, School of Mechanical Engineering, Lovely Professional University, and **Dr. Sudhanshu Dogra**, HoD, Thermal Engineering, Lovely Professional University, for the administrative support during the execution and completion of this thesis for their kind cooperation, support and continuous guidance. I would also like to thank all the end term presentation panel members, faculty and staff members of Mechanical Engineering Department, Lovely Professional University, Punjab, India, for their valuable advice, during the completion stage. I further extended my vote of thanks to **Dr. A. Nagarjuna Reddy**, Principal, DVR College Engineering and Technology, Sangareddy, for permitting me to undergo Ph.D. from Lovely Professional University. Special gratitude to **Prof. K. Venkateswara Rao,** Prof. Nanotechnology & Registrar JNTUH Telangana, India my dedicated and inspiring professor whose unwavering guidance and intellectual mentorship propelled me through the challenging journey of earning my Ph.D.

My gratefulness, hearty and special measure of thanks is due to my parents for their patience, love, and encouragement during this course of work, just for being themselves. I also express deepgratitude to my father Jatoth Bavu Singh, mother Jatoth Badili Bai, sister Jatoth Sujatha and brother-in-law Kadavath Dhara Singh for their moral support. I would also like to thank my friends **Dr. Ch. Sandeep**, **Banoth Amala**, and all my dear friends for their support during crucial time of my research. Finally, I owe entire of my academic achievements to my parents. Before all and after all the man thanks should be to the Almighty God.

(Jatoth Heeraman)

Reg No.: 42000066

Table of Contents

List of Tables

List of Figures

Nomenclature

English Alphabets

A	Surface area of inner tube	m^2
C_p	Specific heat capacity	J/kg K
D	Diameter of dimple	m
DPHE	Double pipe heat exchanger	Dimensionless
D/H	Dimple diameter to depth ratio	Dimensionless
d	Diameter of inner tube	m
f	Friction factor	Dimensionless
H	Depth of dimple	m
h_i	Heat transfer coefficient	W/m^2K
h_1	Manometer reading	mm of Hg
k	Thermal conductivity	W/m K
L	Length of twisted tape	m
l	Length of test section	m
m	Mass flow rate	Kg/s
Nu	Nusselt number	Dimensionless
PEC	Performance evaluation criteria	Dimensionless
Q	Mean heat transfer rate	W
Q	Heat transfer rate	W
Re	Reynolds number	Dimensionless
T	Temperature	^oC

U	Mean velocity	m/s
V	Volume flow rate	m^3/s
k	Turbulent kinetic energy	m^2/s^2

Greek Symbols

$\Delta\rho$	Pressure drop	Pa
ρ_{in}	Density of hot water at inlet	kg/m^3
ρ_h	Density of hot water at bulk temperature	kg/m^3
ν	Kinematic viscosity of hot water	m^2/s
μ	Dynamic viscosity	kg/m-s
μt	Turbulent dynamic viscosity	kg/m-s
υ	Kinematic viscosity	m^2/s
φ	Heat transfer rate	W
υ	Turbulent kinematic viscosity	m^2/s
λ	Thermal conductivity	W/m K
ε	Dissipation rate of turbulence	$m^2/s3$
Γ	Generalized diffusion coefficient	
μ	Dynamic viscosity	kg/m-s

Subscripts and abbreviations

c	Cold water
h	Hot water
c_i	Cold water at inlet
c_o	Cold water at outlet
h_i	Hot water at inlet
h_o	Hot water at outlet
TT	Twisted Tape
He’s	Heat Exchangers
HT	Heat Transfer

CHAPTER-1

INTRODUCTION

1.1 Introduction

Heat transfer plays an important factor in many industrial and everyday applications. The efficient transfer of heat is important for achieving optimal performance and heat efficiency in this system, including air conditioners and refrigeration, engines, batteries, etc. To transfer heat with minimal leakage to surroundings and to increase efficiency heat exchanger systems are used through various methods. Heat Transfer augmentation techniques are commonly employed to enhance the performance of Exchanger in various industries such as air conditioning, heating and cooling systems, automotive industry, heat pumps, refrigeration, and petroleum refining, among others. By improving the efficiency of heat transfer, these techniques can help reduce energy consumption, operating costs, and environmental impact [1-3].

The output from the Double Pipe Heat Exchanger system is essential in terms of both system economics and efficiency [4-6]. As a result, boosting the rate of thermal gradient rate is important for long-term energy growth. Several techniques are used to increase their figure of merit, minimize their size, and lower their energy costs. The objective of heat transfer enrichment is to increase the heat transfer rate while maintaining or reducing the pressure drop, which leads to improved overall efficiency and reduced energy consumption. This is particularly important for applications where heat transfer is a critical factor, such as in power plants or chemical processing [7-10]. Figure. 1 shows a schematic of a Double Pipe Heat Exchanger system.

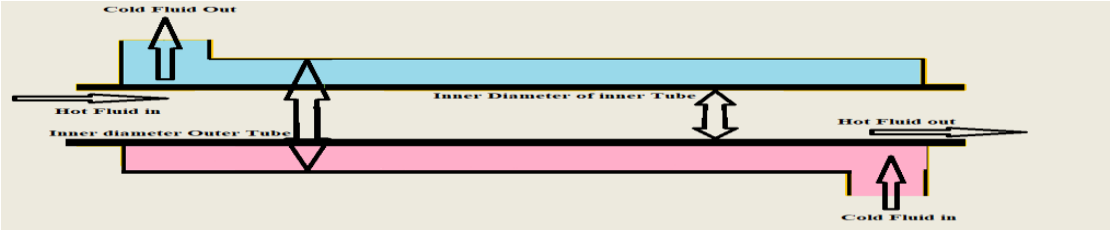

Figure.1.1. Representation of double pipe Heat exchanger system

1.2 Need for Heat Transfer Enhancement

In addition to increasing vorticity or turbulence of flow, various other techniques have been explored for heat transfer enrichment. For instance, the incorporation of inserts, such as twisted tape, wire coils, and baffles, can effectively mix and create turbulence, which enhances heat transfer rates. Similarly, surface modifications like the use of rough surfaces, porous coatings, and microchannels can also promote turbulence and enhance heat transfer efficiency. Other methods include the use of phase-change materials, nanofluids, and magnetic fields [11-13].

Over the past few years, there has been a growing interest in incorporating advanced computational techniques such as computational fluid dynamics (CFD) and artificial intelligence (AI) to design and optimize heat exchangers. These techniques can provide detailed insights into fluid flow and heat transfer characteristics, which can help in identifying best enhancement techniques for a given application. Furthermore, the use of advanced materials such as graphene and carbon nanotubes also shows promise in enhancing heat transfer efficiency [4,5,7,8,10].

Overall, heat transfer enhancement is a critical area of research with significant implications for energy conservation and sustainability. The development of novel enhancement techniques, coupled with advancements in computational and material science, holds great potential for achieving higher efficiency and compactness in heat exchangers [14-16].

1.3 Different Methods of Heat Transfer Enhancement

Three distinct types of strategies for enhancing thermal gradient rate: (a) active, (b) passive, and (c) compound methods [14,15].

1.3.1 Active Methods

In category of active methods of heat transfer enhancement, external power or energy is supplied to improve the thermal gradient rates. This can include methods such as induced pulsation using reciprocating plungers and cams, the application of electrostatic fields or magnetic fields, surface vibration, mechanical assistance, and fluid vibration to disrupt well-illuminated seeded particles in a flowing stream. Thermal conductivity holds significant importance as a parameter that necessitates

careful consideration for heat-emitting applications. Nanofluid circulated batteries are analysed for their cooling performance [17-20].

i. **Mechanical aids**: Mechanical aids can be very effective in enhancing fluid mixing, but their effectiveness depends on specific applications and properties of fluid being mixed.

ii. **Surface vibration**: It is a technique used to augment heat transfer by inducing vibrations on surface of the heat transfer equipment.

iii. **Fluid Vibration**: Fluid vibration refers to motion of fluid particles induced by external forces, such as acoustic waves, pressure waves, or flow-induced vibration. These vibrations can augment heat transfer by increasing mixing and turbulence within the fluid.

iv. **Electrostatic Fields**: Electrostatic fields can be used to improve heat transfer in fluids. The method involves the application of an electric field to the fluid which causes the fluid molecules to become polarized and align themselves in a specific direction

v. **Injection:** It is a technique used in fluid mixing that involves introducing a stream of one fluid into another to enhance mixing. The injected fluid can be either a gas or a liquid, and the rate of injection can be adjusted to control the degree of mixing. Injection is often used in industrial applications such as chemical processing, where it is used to promote chemical reactions and achieve uniform product quality.

vi. **Suction**: It is a technique used in mixing to draw fluid or material into a mixer or a process vessel using a vacuum or negative pressure. This technique is commonly used in industries such as food processing, pharmaceuticals, and chemical processing. Suction can be achieved using a variety of methods, including vacuum pumps, ejectors, and educators.

vii. **Jet impingement:** It is a heat transfer technique that involves the use of high-velocity jets of fluid impinging on a surface to augment rate of heat transfer. In this technique, a high-velocity fluid jet is directed at a solid surface, typically a flat plate or a curved surface, to increase rate of heat transfer.

1.3.2 Passive Methods

The passive approach is widely preferred due to its ability to improve heat transfer characteristics without requiring external power. Several passive techniques are commonly utilized to augment thermal gradient rates and extended surfaces. These techniques rely on their inherent design and surface properties to promote efficient heat transfer without the need for additional energy input. By leveraging these passive methods, heat transfer can be significantly improved in various applications [21-25].

i. Treated surfaces: In this technique, use of surface modifications to alter the surface characteristics of a material to enhance its performance. In fluid mechanics, treated surfaces are used to modify surface of a solid wall to influence behavior of fluid flow. The surface modifications can be in the form of coatings, textures, roughness, or patterned structure.

ii. Extended surfaces: In this technique, is used to increase heat transfer area by creating an extended surface on the solid wall of heat transfer equipment. The extended surface can take various forms, such as fins, pins, wires, plates, etc. The Extended surfaces find common application in various contexts in heat exchangers, where they can increase heat transfer rate amidst two fluids by enhancing the convective heat transfer coefficient.

iii. Displaced enhancement devices: In this technique, use of inserts or obstacles are placed within the fluid flow path to disrupt laminar flow and enhance heat transfer.

iv. Swirl flow devices-: It is a type of heat transfer augmentation device that utilizes the swirling motion of fluid to improve heat transfer rates. The devices typically consist of a set of vanes or blades arranged in a helical pattern inside a tube or pipe.

v. Coiled tubes-: In this technique, are used as an enhancement device for heat transfer in various applications such as heat exchangers, and condensers. The coiled tube increases heat transfer area and induces turbulence in flow, resulting in higher heat transfer coefficients.

vi. Surface tension devices-: It is a type of passive heat transfer enrichment

technique that works by manipulating surface tension of fluid. These devices can be used to promote the formation of thin liquid films, which increases the effective surface area available for heat transfer.

1.3.3 Compound Methods

Compound techniques are a mix of active and passive approaches (e.g., fluid vibration on rough surfaces) [1-3]. As a result, with a low pumping power, an optimum thermal gradient rate is achieved. Among the approaches below the passive method is the pipe additions technique. Twisted tape, helical springs, ribs, conical nozzles, conical rings, corrugated tubes, and other tube inserts in heat exchanger systems are only a few examples [26-30].

Twisted tape inserts are most often utilized as tube inserts, and they've been carefully researched and investigated by researchers all around the world. To improve thermal gradient rate figure of merit, they created new designs and devised new methods such as coarsening the energy exchanger system surface [31-34]. Figure 2 show depicts a typical twisted tape.

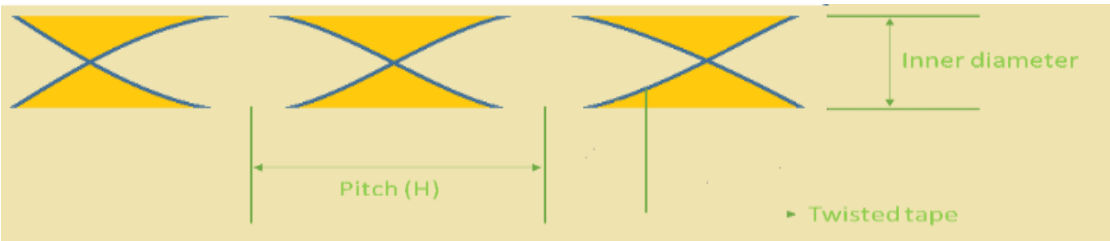

Figure.1.2. Structure of typical twisted tape

1.4 Twisted Tape Inserts Technique in Passive Methods

Twisted tape inserts, which produce swirling movement, are extensively implemented techniques with passive modes for increasing thermal gradient rate. Because of rotating flow generated near wall boundaries, tubes implanted with twisted tapes outperform simple tubes. The addition of dimple patterns at the back end of each twist of tapes is illustrated in Fig.3 below. As well as the development of new techniques such as coarsening of the energy exchanger system surface to enhance thermal gradient rate efficiency are both novel aspects of the current improvement approach. Figure 3 shows depict an example of dimple-twisted tape [35-38].

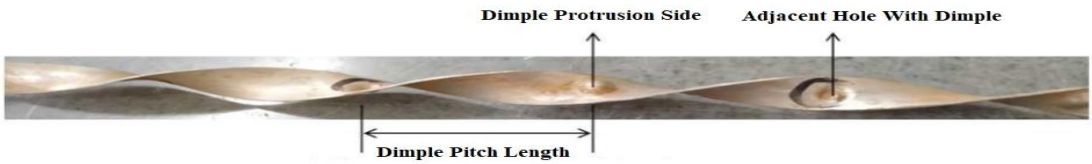

Figure.1.3 Twisted tape insert with dimples Configuration

Thermal performance of Twisted tape heat exchangers systems has been studied extensively since the 1960s, both theoretically and practically. Twisted tapes can be made in a variety of patterns, including standard, and more, utilizing a variety of methods [39-42], as indicated in Table 1.1.

(i) The twist ratio is a geometric measurement that quantifies the spatial relationship between successive points on a configuration, measured twisted tape is oriented parallel to the axis. It is calculated by dividing half of the twist pitch by the total hydraulic tube diameter.

$$TR = \frac{\left(\frac{P}{2}\right)}{D} \tag{1.1}$$

(ii) Reynolds Number is ratio of dynamic viscosity of fluid to a product of tube's hydraulic diameter, mean fluid velocity, and density.

$$Re = \frac{U \times d}{\vartheta} \tag{1.2}$$

(iii) Nusselt Number - The convective thermal gradient rate coefficient multiplied by the tube diameter is proportional to the thermal conductivity.

$$Nu = \frac{(h\, d_e)}{k} \tag{1.3}$$

(iv) Friction Factor is proportionality between product of tube's total pressure decrease and corresponding Inner Tube Diameter to product of density, characteristic linear dimension, and square of tube's average fluid velocity. It is represented by f.

$$f = \frac{2d(\Delta P)}{4\rho L V^2} \tag{1.4}$$

(v) Performance Evaluation Criteria is defined as the ratio of Nusselt number ratio (N_{uT}/N_{u0}) [Ratio of Nusselt number with twisted tape insert (N_{uT}) to without twisted tape (N_{u0})] to that of cubic root of friction factors ratio $\left(f_T/f_0\right)^{1/3}$ [Ratio of

friction factors with twisted tape insert (f_T) to without twisted tape (f_0)] when pumping power is constant

$$(PEC) = \frac{\left(\frac{N_{uT}}{N_{uo}}\right)}{\left(\frac{f_T}{f_o}\right)^{0.33}} \qquad [14] \qquad (1.5)$$

All these metrics are dimensionless in nature and are widely used to evaluate twisted tape figure of merit in a double pipe heat exchanger. The thermal performance factor is most widely utilized metric among all afore mentioned measures.

Table 1.1. Schematic geometry of various twisted tape arrangements

Name	**Configuration**	**Reference**
Dimple twisted tape	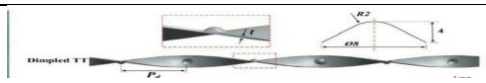	Toygan Dagdevr et al, 2021 [11]
Two Wire coil with twisted tape	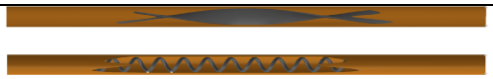	Abdussamet Subasi, et al, 2021 [12]
Novel Double-Perforated Inclined Elliptic twisted tape		M.E. Nakhchi, et al, 2021 [13]
Several Square Perforations twisted tape	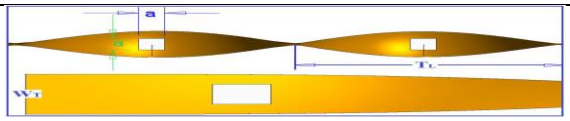	Amar Raj Singh Suria et al, 2017 [16]
Regularly spaced quadruple twisted tape		P. Samruaisin et al, 2018 [17]

Without Multiple Square twisted tape	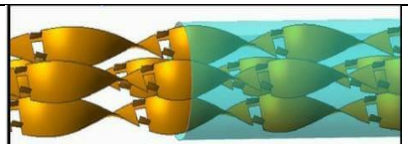	Suri et al, 2017 [44]
Regularly spaced twisted tape		Zhang et al, 2012[45]
Triple twisted tape		Yuxiang Hong et al, 2012 [47]
Conventional twisted tape		Mokkapati et al, 2014 [48]
Semicircular groove twisted tape		Zhang et al, 2016 [49]
Helical twisted tape		Nanan et al, 2013[50]
Twisted tape with V-winglet		Promvonge et al, 2014 [51]
Helical screw tape	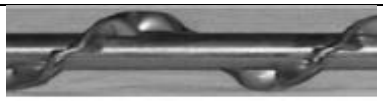	Suhas et al, 2014 [52]
Regularly spaced twisted tape		Eiamsa-ard et al, 2014 [53]
Square cut twisted tape	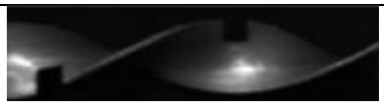	Murugesan et al, 2010 [30]
Elliptic cut twisted tape	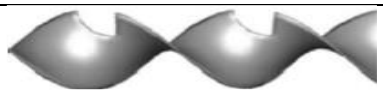	Zhang et al, 2016 [54]
Peripherally cut v		Eiamsa-ard et al, 2013 [28]

Twisted tape composed of alternating axes and central wings		Eiamsa-erd et al, 2010 [32]
Twisted tape with circular rings		Eiamsa-erd et al, 2013 [59]
Serrated twisted tape		Eiamsa-erd et al, 2010 [57]
Ribbed spiky twisted tape		Chang et al, 2012 [58]
Twisted tape with alternate axes		Eiamsa-erd et al, 2013 [59]
Triple twisted tape		Bhuiya et al, 2013 [60]
V-cut twisted tape		Murugesan et al, 2011 [61]
Double twisted tape		Bhuiya et al, 2014 [62]
Center cleared twisted tape	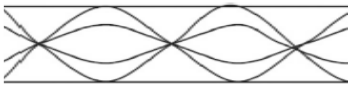	Bhattacharya et al, 2013 [63]
Twisted tape with geometrical progression ratio		Maddah et al, 2014 [64]
Twisted tape with wire nails	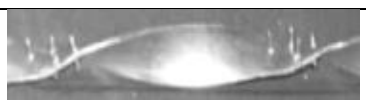	Murugesan et al, 2010 [65]
Perforated twisted tape		Bhuiya et al, 2013 [66]

Typical twisted tape	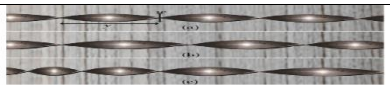	Man et al, 2017 [67]

1.5 impact of Inserts with Twisted Tape on Transfer of Heat and Friction Factor

Classification of twisted tape inserts based on their design highlights major experimental and numerical studies conducted by numerous investigators on each respective geometry [43-45].

1.5.1 Effect of Conventional Twisted Tape

The performance of a heat exchangers is influenced not only by geometrical parameters including twist ratio, width, and length of twisted tape but also by position and number of twisted tapes. Studies have shown increasing the length of the twisted tape results in an increase in Nusselt number, friction factor, and performance evaluation criteria at all values of Reynolds number [46-50]. When other parameters are held constant, an increase in the number of twisted tape enhances Heat exchangers performance, specifically improving heat transfer characteristics. Additionally, placing twisted tapes of short length at the beginning of the tube increases the convective heat transfer coefficient and frictional losses. Twisted tapes are found to be higher effective in laminar flow conditions compared to turbulent flow conditions, and it has also been reported that the twist ratio of the twisted tape inversely affects friction factor and Nusselt number [51-54].

The primary mechanism responsible for the improved heat transfer in a double pipe heat exchanger due to inserts like twisted tape is reduction in hydraulic diameter, resulting in increased flow velocity and swirl, which maximizes wall shear stress. Twisted tape blocks the flow path, resulting in boundary layer thickness near tube surface being reduced, while velocity experiences an increase [55-58]. The induced vortex flow improves fluid mixing in the mid-zone, and the aim of researchers should be to achieve higher convective heat transfer by reducing formation of the layer near tube surface. Twisted tape acts as a vortex generator, reducing adhesion between the fluid and solid surface. This induces turbulence, overlaid with vortex motion, leads to a thinner boundary layer, thereby enhancing heat transfer [59-62].

1.5.2 Effect of Self-Rotating Twisted Tape

Numerous studies have investigated effectiveness of rotating twisted tape in terms of antifouling, descaling, and heat transfer enrichment. Table 1.1 shows the different configurations of twisted tape that have been studied. The rotational speed of the tape is influenced by the axial velocity of the flowing fluid [63-65]. Heat transfer improvement at twist ratios (TR) of 10 or greater is primarily due to enhancements in the velocity of the flowing medium near tube surface and reduction in tube equivalent diameter [66-70]. However, at twist ratios of less than 10, the helical flow effect becomes a major factor, while secondary flow recirculation is the primary element at twist ratio values of 1 or less. Scaling is a combination of particulate and crystallization scaling, and the rate of crystallized salt formation on heat transfer tubes can be very rapid, with layers growing several millimeters in just an hour [71-74].

1.5.3 Effect of Materials of Twisted Tape

Several researchers have investigated the effect of twisted tape material on heat transfer performance and concluded that polypropylene twisted tapes outperform aluminum twisted tapes [75-79]. Additionally, impact of twisted tape porosity on heat transfer parameters such as Nusselt number, friction factor, and performance evaluation criteria has been studied, and it has been found that there exists an inverse relationship between porosity and these parameters [80-84].

1.5.4 Effect of Multi Twisted Tape and Twisted Tape with Slots, Holes, and Cuts

Multiple twisted tape inserts placed inside the tube have been found to induce strong vortex motion, resulting in improved heat transfer characteristics according to several studies [85-89]. Additionally, modifying the geometry of the inserts, such as adding slots, holes, or cuts, has been shown to induce strong turbulence near the tube wall, further enhancing heat transfer and reducing pressure drop. Several researchers have conducted studies on various types of geometry both experimentally and numerically using tape inserts [90-92].

1.5.5 Effect for using inserts in turbulent Flow

Using inserts in turbulent flow cases provides several advantages, including increased heat transfer rates, reduced fouling, improved energy efficiency, and the potential for compact and retrofit-friendly designs. These benefits make inserts a popular choice for enhancing heat exchanger performance and optimizing fluid handling systems in

various industrial and engineering applications.

1.5.6 The Heat Transfer Performance with Flow Visualization

Flow visualization plays a crucial role in enhancing our understanding of fluid dynamics and its impact on heat transfer processes. By providing visual insights into the fluid flow behavior, flow visualization techniques enable engineers and researchers to optimize heat transfer performance, improve system efficiency, and develop more effective heat transfer solutions.

CHAPTER -2

LITERATURE REVIEW

2.1 Introduction

A comprehensive literature review has been carried out to investigate recent developments in enhancing heat transfer characteristics. This method of improving heat transfer has been gradually developed over the years and has been employed in various Heat exchangers applications. The goal of this survey is to explore different advancements in heat exchanger design that aim to reduce size, cost, and improve performance in terms of energy efficiency. There are three methods of improving heat transfer performance: active methods, passive methods, and a combination of both. Passive methods are particularly popular and widely used to intensify heat transfer characteristics. These methods include surface coating, the use of extended surfaces, inserts in the flow field, nanoparticles, phase change materials etc...

Inserts are passive method that have been widely used to improve heat transfer characteristics of heat exchangers. By placing inserts in the flow field, they create a swirl flow that improves the convective coefficient, albeit with an increase in pressure drop. Researchers have investigated various designs and geometries of inserts to determine their effect on the performance characteristics of Heat exchangers.

2.2 Experimental Investigations on Twisted Tapes

Numerous researchers have conducted experiments to investigate effect of twisted tape inserts on heat transfer enhancement and friction factor. In this section, we will discuss some notable contributions in the field of heat transfer and friction factor characteristics of twisted tape insets.

Kumar, et al, 2024 [1] utilization of twisted tape inserts in tubular heat exchangers has proven highly effective in enhancing overall thermal performance. Twisted tape inserts induce turbulence within the fluid flow, thereby augmenting heat transfer rates and friction factors. The present experimental study, the focus lies on mitigating the associated increase in friction factor to achieve superior thermal performance. Various design modifications to twisted tape inserts, including Simple Twisted Tape (STT), Double V-Cut Twisted Tape (DVCTT), and Perforated Double V-Cut Twisted Tape (PDVCTT), with different twist ratios (TR) ranging from 3 to 5, are investigated. The

design modifications entail features such as V-cut with specific dimensions (width of cut - wc: 5 mm, depth of cut - dc: 4 mm) and perforations of 5 mm diameter within the twisted tape structure. Water serves as the working fluid for the experimentation. Data related to Nusselt number and friction factor is collected within the turbulent flow regime, encompassing Reynolds numbers ranging from 4000 to 16,000. The results indicate significant enhancements in both Nusselt number and friction factor, with respective maximum increases recorded at 2.44 times and 3.71 times that of a plain tube at a Reynolds number of 4000, specifically for TR = 3. The PDVCTT configuration demonstrates the highest decrement in Nusselt number and friction factor, exhibiting reductions of 3.83% and 27.35%, respectively, compared to DVCTT. The maximum thermal performance achieved is 1.71 for PDVCTT with a TR of 3 at a Reynolds number of 4000.

Jawarneh, Ali M., et al, 2023 [2] conducted an experimental study suggest that inducing vortex flow in Heat exchangers was an effective technique for enhancing heat transfer rates. Implemented 4 different entrance flow angles 0, 30, 45, and 60 degrees, as well as 4 hot Reynolds numbers (Reh) and 4 cold Reynolds numbers (Rec) at varying levels. To measure the temperature along Heat exchangers, thirty-four thermocouples were employed on both the tube and shell sides. Results indicate that as entrance swirl angle (θ) and Re increase, local Nu, overall heat transfer coefficient (U), and ratio of f experience an increase. Nusselt number shows a percentage increase ranging from 10% to 82% swirl flow exhibits notable distinctions compared to axial flow. Similarly, the overall heat transfer coefficient exhibits an increase of 7% to 32%, depending on the inlet flow angle

Hozaifa A. Mohamed, et al, 2023 [3] conducted an experimental study use of Al_2O_3 nanofluid to enhance heat transfer inside a double pipe heat exchanger. The findings revealed a significant improvement in the heat transfer coefficient inside the tube of the Heat exchangers when using Al_2O_3 nanofluid. The addition of Al_2O_3 nanoparticles to the nanofluid further enhanced the Nusselt number, with maximum enrichment observed at a volume concentration of 0.1%. This improvement can be attributed to the increased thermal conductivity, decreased specific heat at constant pressure, and elevated temperature associated with the nanofluid. However, a further increase in nanoparticle concentration resulted in a minor decline in Nu, possibly due to the

formation of a fouling layer that impeded heat transfer. The study also provided empirical correlations that describe relationship between Nu, friction factor, and relevant parameters for nanofluid flow within the double pipe heat exchanger.

Dandoutiya, et al, 2022 [4] conducted an experimental analysis to investigate the behavior of the Nu and f in a double pipe heat exchanger using a W-cut twisted tape. The study considered Re range of 5500 to 16,000 and varied depth of the W-cut to width of twisted tape ratio, including values of 0.2, 0.4, and 0.6. Additionally, the effects of the twist ratio were examined by varying it between 5, 10, and 15. The study identified that the peak enhancement in Nusselt number and friction factor occurred at a Reynolds number of 5500, with a depth of W-cut of 6 mm and a twist ratio of 5. Under these conditions, the Nusselt number showed an improvement of 105.47%, while friction factor increased by 301%. The maximum TPF and friction factor were observed at the same operating parameters. In current investigation, the extreme TPF achieved was 1.35.

M. Soltani, et al, 2022 [6] experiment tests were conducted to examine the influence of twisted tape insert geometry on heat transfer and pressure drop in inner pipe of outer surface of double pipe heat exchanger was kept adiabatic, and water was used as the working fluid under turbulent flow conditions. Among torsional turbulent studied, the louvered twisted tape inserts with dimples exhibited highest thermal performance (at a value of 1.24). Compared to other twisted tape inserts without dimples, the inclusion of dimples as a result, there was an observed increase in both heat transfer and friction factor values by 5.58% and 8.73%, respectively. The study examined typical, continuous, continuous winglet, and discontinuous louvered twisted tape inserts, with the dimpled louvered twisted tape exhibiting a heat exchanger value of 1.24 at a Reynolds number of 5300 for water under conditions of $5000 \leq Re \leq 9500$.

Dan Zheng, et al, 2022 [7] conducted an experimental study on DTHE was evaluated by analysing effects of applied nanofluids inside inner tube and incorporated corrugation structures on the outer surface of the inner tube. Among four fluids considered, SiC-water nanofluid exhibited the highest increase in Nusselt number, while SiO_2-water nanofluid showed the least. DTHE with a small thread pitch demonstrated superior thermal performance compared those with a large thread pitch.

The study specifically focused on corrugated DTHE's, with various range of flow rate is 60 to 200 L/h.

Mehdi Noorbakhsh, et al, 2022 [8] assessed the impact of nanofluids, involved Al_2O_3/water, CuO/water, and SiO_2/water, at a Reynolds number of 3343 resulting in a 4.1%, 4.6%, and 2.5% increase in thermal performance, respectively, compared to using pure water. At a higher Reynolds number of 5492, use of nanofluids led to an even greater increase in thermal performance, with Al_2O_3/water, CuO/water, and SiO_2/water resulting in 6.6, 7, and 5% enhancement, contrasted to pure water. Among nanofluids studied, CuO/water at a Reynolds number of 5492 demonstrated maximum thermal performance enrichment of 7%, while SiO_2/water at a Reynolds number of 3343 exhibited minimum enhancement of 2.5% compared to using pure water. The study also investigated the use of twisted tape as a swirl generator on both sides of CuO/water nanofluid at a Reynolds number of 5492 and the SiO_2/water nanofluid at a Reynolds number of 3343.

Ke Chen, et al, 2022 [9] perform a study to assess heat transfer and influencing factors of 2 different borehole heat exchanger (BHE) models that were simulated under various working conditions. D-U BHE model was improved and replaced by cross-sectional area of a buried pipe that is equivalent to create an enhanced coaxial BHE. Under winter and working-specific conditions, average heat transfer per linear meter of an enhanced coaxial BHE was found to be 1.46 and 1.45 times that of equivalent U BHE, respectively. The study utilized numerous layers of rock and soil to create 3-D geometric models of both the D-U BHE and the improved coaxial BHE with spiral ring fins intermittently installed. During simulation, inlet temperature of pipe was kept constant at 5 and 35°C during winter and summer operational conditions, respectively, with a stable inlet flow rate of 1.5 m3/h.

Zi Ding, et al, 2022 [10] The study found that heat transfer performance of TiO_2-H_2O nanofluids surpassed that of pure water, across all three mass fractions tested (0.1, 0.3, and 0.5). Heat transfer capacity of nanofluid as cold fluid was slightly improved when the flow increased. They found that corrugated pipe disrupted fluid flow, leading to destruction of the boundary layer and formation of eddy currents. As a result, there was an enhancement in heat transfer capacity. However, it also led to an increase in flow resistance within corrugated pipe. An pipes is of temperature

distribution within Heat exchangers pipes revealed that heat transfer between the cold and hot fluids was more prominent in corrugated double pipe heat exchanger. This confirmed that corrugated pipe provided a higher heat transfer capability compared to smooth pipe. Overall, the study highlights the potential of TiO_2-H_2O nanofluids and corrugated double pipe heat exchanger for improving heat transfer performance.

Toygun Dagdevir, et al, 2021 [11] investigated performance of twisted tape inserts with dimples and perforations in heat transfer enrichment. It was found that dimpled twisted tape with a pitch ratio of 0.25 had best heat transfer performance. The addition of ethylene glycol to water increased heat transfer rate thermal performance but had no significant influence on friction factor at the same Reynolds number. New correlations were established for Nusselt number and friction factor for twisted tape with perforations and dimples with validity for Twist Ratio of 5.88, Pitch Ratios of 0.25, 0.5, and 1.0, Reynolds number of 5219-22,757, and Prandtl number of 5.5–36.2. Thermo-hydraulic performance for dimpled twisted tape implanted tubes were 1.42, 1.17, and 1.05 at the most fundamental fluid Reynolds numbers of (0:100), (20:80) and (40:60). The study mixture of ethylene glycol and water was utilized with pitch ratios of 0.25, 0.5, and 1.0 (Pp/y and Pd/y) with a Twist Ratio (H/D) of 5.88 with perforations and dimples.

Abdussamet Subasi, et al, 2021 [12] comparison between twisted tape and wire coil inserts showed that twisted tape had better thermal and hydraulic performance, but the wire coil had a larger Pareto front range. This means that wire coil could be used in situations where a higher heat transfer rate thermal performance is required, but at cost of a maximum friction factor. The study also found that a fusion nanofluid of water-based CNT-Fe_3O_4 performed better than other types of nanofluids in terms of thermal and hydraulic performance. Best configuration parameters of heat transfer rate enhancement method were found to be (Re; h/d; Pr) = (20,000; 0.27%; 10; 5.50) for case abbreviated as twisted tape-CNT-Fe_3O_4, which exhibited the highest thermal-hydraulic performance. The study emphasized the importance of carefully selecting criteria weights in ranking alternatives, and the technique used in the study could be applied to multi-objective optimization issues in various disciplines, not just heat transfer rate improvement research. The study also identified the design parameters

that maximize Nusselt number while minimizing friction factor.

M.E. Nakhchi, et al, 2021 [13] carried out the use of perforated elliptic vortex generators, specifically DPIE turbulators, which can significantly increase heat transfer and improve thermal efficiency of double pipe heat exchanger tubes. The perforations in the elliptic inserts increase recirculation flows and vortex generation, leading to increased heat transfer compared to smooth pipes without vortex generators. Thermal boundary-disturbances are identified as fundamental physical reasons for this increased heat transfer. The test findings show that DPIE turbulators with d/b = 0.25 can increase heat transfer by 217.4% compared to a smooth pipe without vortex generators. However, the use of perforated elliptic turbulators can also result in increased friction factor (f), which may need to be considered in the design. The highest Nusselt number (Nu) was achieved with DPIE turbulators with tilt angle of 25° and d/b = 0.25 at a Reynolds number is 18,000. Overall, use of DPIE turbulators with specific design parameters (inclination angle, perforation diameter, etc.) can enhanced thermal efficiency of double pipe heat exchanger tubes. By given information also suggests that average Nusselt number and friction loss can be calculated as functions of design factors using proposed correlations. **Sanjay Kumar Singh & Arvind Kumar, 2021 [14]** performed an experimental evaluation of twisted tape inserts with dimple configurations has shown that these inserts can significantly improve the friction factor and Nusselt number compared to twisted tape inserts without dimples and plain tubes. Nusselt number generally increases as dimple progresses along its path, depth gradually its moves from D/H ratios of 6 and 3, and subsequently reductions depth increases among D/H ratios of 3 and 1. The resulting in increased contact surface resistance and flow area. The dimple depth is closely related to the friction factor, as it reduces flow area while increasing contact surface resistance. The impact of Reynolds number on the twisted tape with dimples is prominently proportional to both friction factor and Nusselt number. Research found that smallest friction factor for a normal tube configuration without twisted tape enclosure was computed. With a D = 5 mm and a D/H of 3, Performance Evaluation Criterion was at its highest, indicating that Nusselt number takes precedence over friction factor. The friction factor and Nusselt number, PEC performance of system was assessed by employed various evaluate of twisted tape with various diamter and

D/H ratio is 4, 5 and 7 mm and 1.5, 3, and 6 Respectively, which were constantly. twisted tape had a twist ratio of 5.5 and were made of aluminum with a thickness of 1mm Overall, the research demonstrated that the use of twisted tape with dimples can significantly improve heat transfer in various industries, making it an important area for further research and development.

Prem Kumar Chaurasiya, et al, 2021 [15] conducted experimental study of inner and outer corrugated tubes can enhance heat transfer rates compared to smooth tubes, especially at low Reynolds number. However, optimal helix angle for achieving highest heat transfer rate depends on whether corrugation is located on the inside or outside of the tube. For inner corrugation tubes, highest increase in friction factor is achieved at a helix angle of 25°, whereas for outer corrugation tubes, the highest increase in friction factor is achieved. Performance Evaluation Criteria of outer corrugated tubes with helix angle of 15° is superior to other combinations tested within the range of Reynolds numbers studied. A correlation has been formulated to predict Nusselt number, friction factor, and helix angle based on Reynolds number. However, there may be some deviations between the computed and mathematical values, with a range of ±5% to ±10%. Both internally corrugated inner tubes and externally corrugated inner tubes have been tested with three different helix angles (15°, 20°, and 25°). The influence of helix angle on heat transfer coefficient, frictional cost coefficient, pressure drop, and thermal gradient rate has also been studied. **P. Samruaisin, et al, 2018 [17]** compared experimental study to performance of RS-QTT tapes with different configurations to conventional twisted tapes. The thermodynamic enhancement factor (TEF) was observed to be higher in the cross-arrangement of RS-QTT, while the co- and stand-arrangements reflected subordinate thermodynamic enhancement factor. This was attributed to the decrease in free space ratio in RS-QTT, which resulted in a reduction in heat transfer rate of Nusselt number, friction cost, and thermodynamic enhancement factor. The peak thermal enhancement factors were observed in the cross-arrangement of RS-QTT through s/y = 0.654, 1.92, 2.56, and 2.81 values, which resulted in TEF values of 1.27, 1.25, 1.22, and 1.2, respectively. The RS-QTT were implemented with constant drop as heat flux boundary condition and consisted of twisted tape with (y/w) = 2.5 and consistently move apart QTT parameters are (s/y) of 0.5, 1.0, 1.5, and 2.0. The study evaluated the

thermodynamic enhancement factor, Nusselt number, and pressure loss for RS-QTT.

Chamoli, et al, (2017) [18] investigated the impact of multiple twisted tape with perforated rings on heat transfer and friction factor. Experiment was conducted with four twisted tape, for ratio of 1 to 3 as well a twist ratio of 2 to 4. The Reynolds number varied from 6400 to 22800. The researchers found that lower range for Nu_t/Nu and f_t/f was perceived with lower range of pitch ratio. It's unclear from the information provided what Nu_t/Nu and f_t/f refer to, but it's possible that they are ratios of Nusselt number to average Nusselt number and friction factor to average friction factor, respectively. These ratios may be used to compare the performance of different Heat exchangers enrichment methods. **Lin, et al, (2017) [19]** conducted experiment investigated on impact of twisted tape on PWVG were employed at various spacing on double pipe heat exchanger heat transfer, friction factor, and performance evaluation criteria. The experiment used air as working fluid, and Reynolds number is among 50 to 600. Space between the winglets was 0.83, 1.0, 1.25, and 1.67D. Experiment revealed the enrichment in Nusselt number is 0.76 to 1.90 times, while the friction factor increased is 1.791 to 2.893 times. Performance of the twisted tape along parallelogram winglet vortex generators increased when space among winglets was smaller.

Man, et al, (2017) [20] analyzed twisted tape effect with alternate twist and different lengths in a double pipe heat exchanger can lead to enhanced heat transfer rates. The alternation of clockwise and anticlockwise twist has been shown to provide higher heat transfer rates in comparison to conventional twisted tape. It is interesting to note that the highest heat transfer was at full length of insert. Performance Evaluation Criteria was reported to be 1.42 at Reynolds number 3700, which indicates that the use of twisted tape with alternate twist and different lengths can improve overall performance of Heat exchangers. Additionally, Nusselt number and friction factor were found to be improved in comparison to the plain twisted tape. **Man, et al, (2016) [21]** performed on investigated the impact of twisted tape length on performance of double pipe heat exchanger using water as the working fluid. 4 different lengths of twisted tape's, namely 600, 1200, 1800, and 2400mm, were tested at various Reynolds numbers ranging from 11000 to 27000. Results were equated with those of a plain twisted tape. The study found as length of the twisted tape increased, Nusselt

number increased. Specifically, Nusselt number values for four different lengths (600, 1200, 1800, and 2400mm) is found 1.15-1.37, 1.18-1.45, 1.23-1.55, and 1.45-1.90 rates more than plain twisted tape, respectively. In addition, study found that friction factor increased as length of twisted tape increased. The friction factor values for four different twisted tape lengths (600, 1200, 1800, and 2400mm) were estimated to be 1.21-1.31, 2.15-2.75, 2.30-4.48, and 3.69-5.75 times greater than plain twisted tape, respectively.

Tamna, et al, (2016) [22] performed experimental study on double V-ribbed twisted tape in a double pipe heat exchanger. It appears that the study found that Nusselt number and friction factor increased with Reynolds number with extreme Nusselt number and friction factor observed were a blockage ratio of 0.19. The study also reported that performance evaluation criteria retched its maximum value was 1.41 for ratio of 0.09, whereas it was 1.08 for the twisted tape without rib. **Singh, et al, (2016) [23]** examined multiple twisted tape inserts with solid rings to investigate impact of this configuration on thermal behavior of a Heat exchangers. They varied pitch ratios of solid ring turbulators at 1 and 2, and twist ratios of the twisted tape at 2, 3, and 4. They collected heat transfer data at different Reynolds number ranging from 6300 to 22500. Results shows Nusselt number values were in range of 107-293, friction factor values were in range of 0.93-0.99, and performance evaluation criteria ranges are 1.46-1.61 was the solid ring turbulators. The highest value of performance evaluation criteria was reported at pitch ratio of 1.0 and twist ratio of 2, with a value of 1.61. Concluded that quadruple co-twisted tape inserts outperformed the other tested configurations in their study.

Nanan, et al, (2016) [24] experimental investigation on impact of transverse twisted baffles on performance of double pipe heat exchanger, specifically on performance evaluation criteria. The study varied the baffle width ratio and baffle twist ratio and found performance evaluation criteria was positive correlation with baffle width ratio and inverse correlation with baffle twist ratio. Highest performance evaluation criteria was observed with a baffle twist ratio of 2, which was 4.7-6.1% higher were Reynolds number is 6000 to 20000 with air as working fluid. **Skullong, et al, (2016) [25**] performed an effect with delta-wing twisted tape were angle 30, 45 and 60 degrees as well as different ratios 2.5, 1.5, 1, 0.5. Study focused on examining the impact of the

delta-wing tape on heat transfer rate and pressure drop of working fluid, which was air, with a Reynolds number ranging from 4200 to 25500. Results of the study demonstrated Nusselt number, which is a measure of heat transfer, increased by 50.5% with the use of delta-wing tape, while friction factor, which is a measure of the pressure drop, increased by 69%.

Hasanpour, et al, (2016) [26] study evaluated the impact of V-cut and U-cut on performance of twisted tape in regarding Nusselt number and friction factor. Conducted experiments with various twist ratios (3, 5, and 7) and width to depth ratios of the cut (0.3 to 0.6). Results showed Nusselt number ratio of modified twisted tape to conventional twisted tape was greater than one for all experiments, with the highest value observed for V-cut twisted tape at a depth ratio of 0.45, width ratio of 0.3, and twist ratio of 3. Furthermore, increase in Nusselt number for both V-cut and U-cut was indicated that values were higher with depth ratio and decreased with the ratio of width. Overall, the study demonstrated that modifying twisted tape with V-cut or U-cut can augment the heat transfer performance of Heat exchangers. **Patil, et al, (2014) [27]** evaluated thermal performance of a double pipe heat exchanger. Results revealed incidence for direct relationship between Nusselt number and Reynolds number, indicating that increasing Reynolds number results in an increase in Nusselt number. However, an inverse relationship was observed between Nusselt number and twist ratio, suggesting that increasing the twist ratio results in a decrease in Nusselt number. Values of Nusselt number is 3.64-18 rates higher than plain twisted tape, indicating that the use of twisted tape inserts improves heat transfer performance of Heat exchangers. Similarly, friction factor was found to be 3.64-18 times higher than plain tube, indicating that use of twisted tape inserts also results in an increase in pressure drop across Heat exchangers.

Eiamsa-ard, et al, (2013) [28] conducted an experimental study to investigate effect of circular rings and twisted tape inserts on thermo-hydraulic performance of tubes in turbulent flow conditions. They found the combined setup of circular rings and twisted tape inserts resulted in notable enhancement in thermal-hydraulic performance, with values of PEC, friction factor and Nusselt number being enhanced by 6.3%, 82.8%, and 25.8% respectively when compared to using circular ring alone. The study also showed a reduction in dynamic pressure due to flow restriction by the

circular ring and twisted tape inserts. These factors were reported to contribute to the observed enhancements in thermal-hydraulic performance of system. **Zhang, Zhen., et al, (2012) [29]** experimental study investigated an effect of twisted tape inserts with triangular grooves on thermal performance of a Heat exchangers. Twist ratios are 5 and 7, were tested. Researchers found that triangular grooves disturbed the boundary layer and increased the rotational speed. Additionally, study examined impact of frequently spaced twisted tape inserts on thermal performance. Results showed increasing number of twisted tape inserts improved heat transfer rate and increased pressure drop. Findings suggested that use of twisted tape inserts with triangular grooves and frequent spacing can enhance the thermal performance of Heat exchangers.

Murugesan, et al, (2010) [30] experimental investigated on effect of different geometry of twisted tape in a tube on heat transfer. Experimental data were collected and compared with conventional tape under identical operating conditions. Results showed that, regardless of type of cut, heat transfer rates were improved by 1.2 times at lower Reynolds number. This suggests that use of twisted tape inserts in Heat exchangers can significantly enhance heat transfer rates, and geometry of tape can also play a role in performance enhancement. Further analysis may be needed to fully understand the relationship between twisted tape geometry and heat transfer enhancement. **Sarada, et al, (2010) [31]** analyzed investigation on, performance of a Heat exchangers was evaluated while varying width of twisted tape inserts. The range of width considered for the twisted tape inserts was 10 to 22mm. The Reynolds number range for experiments was 6000 to 13500. The study reported an increase in heat transfer performance of Heat exchangers with twisted tape inserts when the width of the tape was increased to 22mm. This suggests that wider twisted tape inserts can improve heat transfer performance of Heat exchangers. **Eiamsa-ard, et al, (2010) [32]** evaluated impact of regularly-spaced dual twisted tape with varying space and twist ratios on heat transfer performance in a tube. Experimental data was collected and compared with single and dual twisted tape of full length under similar operating conditions, Reynolds number from 4000 to 19000. Results showed dual twisted tape with variable spacing and twist ratio improved heat transfer performance compared to single and dual twisted tape of full length. Furthermore, the optimal space and twist

ratio combination was identified to achieve the maximum heat transfer enrichment.

Yadav, et al, (2009) [33] performed on investigation with thermal performance of a U-bend double pipe heat exchanger with half-length twisted tape. They found that use of half-length twisted tape led to a significant improvement in heat transfer rate, with an enrichment of 40% compared to a smooth tube lacking inserts. However, the performance of the modified Heat exchangers was found to be 1.3 to 1.5 rates lower than that of a plain twisted tape. Overall, study suggests that use of half-length twisted tape can enhance thermal performance of a U-bend double pipe heat exchanger, but performance should be evaluated carefully considering the type of performance criterion used. **Rama Krishna, et al, (2009) [34]** investigated impact of modified configurations of full-length inserts with different spacer distances on heat transfer performance characteristics. Examined heat transfer data for different values of Reynolds number and detected appreciable enrichment in Nusselt number as the spacer distance was decreased. Maximum value of Nusselt number was at a spacer length was reduced; no significant changes were observed beyond a distance of 2 inches. Additionally, study reported that extreme performance ratio was found at a Reynolds number of 2550, regardless of type of insert used. Overall, the study suggests that the modified configurations of full-length inserts can improve heat transfer performance of system. **Promvonge (2008) [35]** performed an investigation to combined effect of wire coil and twisted tape inserts on heat transfer characteristics. Reynolds number in experiment ranged is 3000 to 18000. Three different spring pitch ratios of 4, 6, and 8 for the coil and two different D/H was 4 and 6 for twisted tape were used in experiment. Heat transfer data were collected for the modified configuration and compared with conventional twisted tape or wire alone. The results showed a significant improvement in heat transfer rates, which were reported to be twice as compared with the coil and wire alone. It was also reported that the modified configuration with lesser pitch and turn ratios yielded greater heat transfer rates under the same operational conditions.

Li, et al, (2008) [36] investigated effect of rotation with and without a spiral of the thickness of crystallized salt in a continuous production process. The results showed that using a spiral resulted in a significant reduction in thickness of crystallized salt over time, from 5.4 to 2 mm. Additionally, the study may have also estimated the

convective coefficient, which is a measure of heat transfer rate between a solid surface and a fluid, in the process. **Chang, et al, (2007) [37]** investigated effect of using broken twisted tape inserts compared to conventional twisted tape inserts under similar operating conditions. Four different twist ratios were considered in the experiment Reynolds number was 1000 to 40000. Results showed that broken twisted tape inserts had better performance compared to plain twisted tape inserts. Thermal performance factor, fanning factor, and heat transfer coefficient of broken twisted tape inserts were found to be 0.99 to 1.8, 2.0 to 4.7, and 1.28 to 2.4 times higher, respectively, compared to conventional twisted tape inserts. **Promvonge and Eiasma-ard (2007) [38]** study impact of two different devices that generate swirl flow in a tube, using air as working fluid and twist ratios 3.75 and 7.5. Reynolds number range tested was 6000 to 26000. Results revealed that incorporated a conical-ring device there was a notable increase in Nusselt number, with a 366.9% increase for twist ratio of 3.75 and a 349.9% increase for twist ratio of 7.5, contrasted to a plain tube.

Mengna, et al, (2007) [39] an experimental investigation was carried out on effect of converging-diverging tubes on heat transfer characteristics by experimenting with different combinations of twist ratio and rotation angle. Twist ratio and rotation angle combinations used in experiment were (y=2.22, θ= 180o), (y=2.22, θ= 270o), (y=4.72, θ= 180o), and (y=4.72, θ= 270o). heat transfer data were collected for a range of Reynolds number from 3400 to 20000 and were compared with the plain twisted tape and converging-diverging tube without an insert. Results showed that the combination of a twist ratio was 4.72 and a rotation angle was 180^{o} most effective in all the arrangements. Moreover, the researchers observed heat transfer efficiency index increased with Reynolds number. **Naphon et al. (2006) [40]** conducted experimental investigation to evaluate effects of inserts in a double pipe heat exchanger on heat transfer rate and pressure drop. The inserts used in study were made of aluminum and had a thickness of 1 mm. The study compared heat transfer rate and pressure drop between double pipe heat exchanger with inserts and without inserts. Results showed that the double pipe heat exchanger with inserts had a significant improvement in heat transfer rate compared to Heat exchangers without inserts. However, it was also observed that pressure drop increased with use of

twisted tape inserts. Study demonstrated that use of inserts in a double pipe heat exchanger can improve heat transfer rate but at cost of increased pressure drop.

Noothong et al. (2006) [41] analyzed study to found that a lower twist ratio in twisted tape resulted in better heat transfer performance in heat exchanger. The twist ratio refers to ratio of distance traveled by tape in one complete twist to its width. The researchers experimented with twist ratios of 5.0 and 7.0 and tested them in a range of Reynolds number with water as the working medium. They found presence of twisted tape induced a swirling flow that reduced thickness of boundary layer of working fluid, leading to improved heat transfer. The enhancement efficiency and Nusselt number was found to rise as twist ratio reduced. This was attributed to the formation of a secondary flow due to presence of twisted tape, which increased overall heat transfer coefficient of Heat exchangers. **Yu et al. (2005) [42]** investigated the use of oblique teeth twisted tape inserts for Heat exchangers and their effect on fouling. The first study found that the moment of force, which is the twisting force created by the twisted tape, increased by 75% to 101% compared to a smooth twisted strip. This increase in twisting force resulted in improved heat transfer and reduced fouling in the Heat exchangers. The second study also found that oblique teeth twisted tape inserts were effective in reducing fouling, with a decrease in fouling resistance of up to 47% compared to smooth twisted tape inserts. Summary of literature is shown in Table.2.1.

2.3 SUMMARY OF LITERATURE REVIEW

Table.2.1 Following major findings have been observed from the Literature review.

Finding	Summary
(a)	Increasing the length of twisted tape in heat exchangers results in higher Nusselt number, friction factor, and performance evaluation criteria across all Reynolds number ranges.
(b)	Increasing the number of twisted tapes can enhance heat transfer performance in heat exchangers, leading to higher Nusselt number, friction factor, and overall performance evaluation criteria under constant parameters such as Reynolds number and tape geometry.
(c)	Twisted tape exhibits higher effectiveness for laminar flow compared to turbulent flow in terms of convective heat transfer coefficient enhancement.

Finding	Summary
(d)	Higher twist ratios of twisted tape lead to lower Nusselt number and higher friction factor.
(e)	Special designs like U-cut, V-cut, etc., in twisted tape inserts enhance convective heat transfer coefficient, increase friction factor, and improve performance evaluation criteria compared to regular twisted tape designs.
(f)	Using multiple short-length twisted tapes with the same twist ratio results in a smaller pressure drop compared to a single full-length twisted tape.
(g)	Twisted strip inserts are equally favoured in both turbulent and laminar flow regimes if frictional losses are not considered.
(h)	The choice of shape of tube inserts is an important factor to consider for experimental investigation.
(i)	Helical screw tape inserts show higher heat transfer enrichment rates compared to twisted tape inserts based on experimental investigations.
(j)	Nusselt number and friction factor are directly proportional to depth ratios and inversely proportional to width ratios of twisted tape with cuts on their surfaces.
(k)	A decrease in the width of twisted tape leads to an increase in Nusselt number and friction factor values.
(l)	Performance evaluation criteria of twisted tape exhibits an inverse relationship with Reynolds number for all types of twisted tape.
(m)	Novel twisted tape designs can generate stronger swirl flow and offer better heat transfer performance compared to conventional twisted tape inserts.
(n)	Selection of a superior twisted tape configuration is often based on a higher magnitude of the performance evaluation criteria.

2.4 RESEARCH GAP

After an extensive literature review, it has been determined that multiple authors have examined various types of twisted tape inserts in their experimental and modelling studies. However, few experimental study has been done so far a lack of experimental research specifically focused on evaluating heat transfer using twisted

tape with dimple inserts and investigating influence of dimple depth on heat transfer and friction factor in a double pipe heat exchanger.

- As per current up-to-date global survey's on twisted tape energy exchanger system with dimple configuration setup, no research investigations pertaining to experimental aspects of thermal transfer are neither performed nor available.
- Also, information unavailability about influence of dimple depth on thermal transfer gradient as well as friction factor are lacking on above mentioned test configuration.

2.5 AIM AND OBJECTIVES

1. To explore effect of geometrical variables on the rate of heat transfer and friction factor in a double pipe heat exchanger in an experimental environment. To experimentally investigate the effect of geometrical parameters such as the size of dimple diameter (D) and diameter-to-depth ratio (D/H) of dimple on heat transfer rate and friction factor in a double pipe heat exchanger.
2. To compare Nusselt number and friction factor ratio's of twisted tape inserts with dimple configurations to plain tube arrangements using Perforamnce Evaluation Crireria.
3. To evaluate Perforamnce Evaluation Crireria, in order to balance Ratio of Nusselt number and friction factor with twisted tape inserts to that of plain tube arrangement respectively obtained through Efficiency (η) and flow conditions viz., Reynolds number.
4. To develop new correlations for Performance Evaluation Criteria in terms of Nusselt number, friction factor, Reynolds number, Dimple diameter (D), for given set of flow- and geometrical- parameters.

2.6 Life Span of Twisted Tape, Pressure drop and Scaling

Twisted tape inserts can significantly enhance heat transfer performance in heat exchangers. However, they may experience fouling and scaling issues over time, affecting their long-term efficiency. It is crucial to consider trade-offs between improved heat transfer rates and potential scaling-related challenges when designing Heat exchangers with twisted tape inserts. Proper maintenance and periodic cleaning are essential to extend the lifespan and maintain optimal performance

CHAPTER - 3

DETAILS OF EXPERIMENTAL SETUP

3.1 Introduction

Twisted tape produces secondary motion (swirling flow) in flowing fluid inside a tube which enhances heat transfer rate between the fluids therefore it is widely used in heat exchangers [48-50]. Twisted tape employing now a days are also used in the various solar equipment like solar water heaters and parabolic trough heaters for augmenting the heat transfer rate from the existing heat exchanger devices and for reduction in size and performance improvement during the designing of new heat exchanging devices [41,47,78]. These inserts are placed inside the tubes of the heat exchanging devices. The prevalent twisted tape inserts being used are an aid to improve the thermal performance by increasing the heat transfer rate, but it is associated with frictional losses. In general performance of heat exchangers device is influenced by usage of twisted inserts on account of an increase in frictional losses which in turn enhances impelling power requirement [67-71].

Experimental setup developed in this study considering usage of twisted tape inserts in various industrial applications. As the various industrial heat exchanging devices involve the usage of twisted insert inside the circular tube; a similar test facility has been developed as per ASHRAE standards [14,67,83] for various range of dimple characteristics (diameter of dimples and diameter-to-depth ratio of dimples) on twisted tape. Experimental results(data) have also been collected for plain tube under similar conditions for comparison. Arrangements have been made for temperature measurement at various locations to calculate the enhanced heat transfer as well as for frictional loss measurement to determine the extra pumping power requirement. In the current investigation, water has been used as working fluid. Experimental set-up consists of two circuit viz. hot water close loop circuit and cold-water open loop circuit. Hot water circuits include tank, stirrer, centrifugal pump, rotameter, test section and valves whereas cold water circuit consists of cold-water tank, centrifugal pump, rotameter, test section and valves.

Test section used in experiment is a double pipe heat exchanger. Inner pipe of test section was made up of copper and six T-type thermocouples placed at different

locations of inner pipe surface to measure the surface temperature of inner pipe. Outer pipe was made up of Galvanised Iron and at the ends both pipes were connected together by the help of sockets. Thermometric wells are installed at the entry and exit points of the test section to measure the temperatures of the hot and cold water using RTDs. Moreover, two knobs are connected at entry and exit of test section to find pressure drop due to frictional losses across test section by U-tube manometer. One end of all RTDs is dipped in their corresponding thermometric well and the other ends are connected with data logger. Similarly, one end of all T-type thermocouples is attached with inner tube surface whereas other ends are connected with data logger.

Experimental setup of hot water circuit consists of a heating source of 10 kW to heat the water tank, RTD to measure the tank water temperature, Solid-state relay (SSR) to control the fluctuation in hot water temperature. Hot water tank is connected with another tank which is equipped with stirrer, with the help of pipe using valve. Outlet of stirrer tank is further joined with centrifugal pump whereas the outlet of centrifugal pump is linked with rotameter with valve. Further outlet of rotameter is connected with entry of test section and outlet of test section linked with hot water tank. In cold water circuit, source of water is cold water tank, and it is connected to inlet of centrifugal pump. The outlet of centrifugal pump is linked to rotameter with valve whereas the outlet of rotameter is connected to the test section. The experimental setup is depicted in the schematic diagram, and a corresponding photograph is provided as well in Figure 3.1(a) & (b) and model of dimple twisted tape depicted in Figure 3.4 and 3.5. The main features of the experimental setup and instrumentation are summarized methodology below: and shown in Table.3.1.

3.2 METHODOLOGY

To achieve the objectives, the sequence of steps followed have been given below:

1. Fabrication of double pipe heat exchanger experimental setup
2. Validation of experimental setup
3. Fabrication of twisted tape with dimples of different geometry
4. Data collection
5. Data processing
6. Correlations for Nusselt number and friction factor.

Table 3.1 Methodology

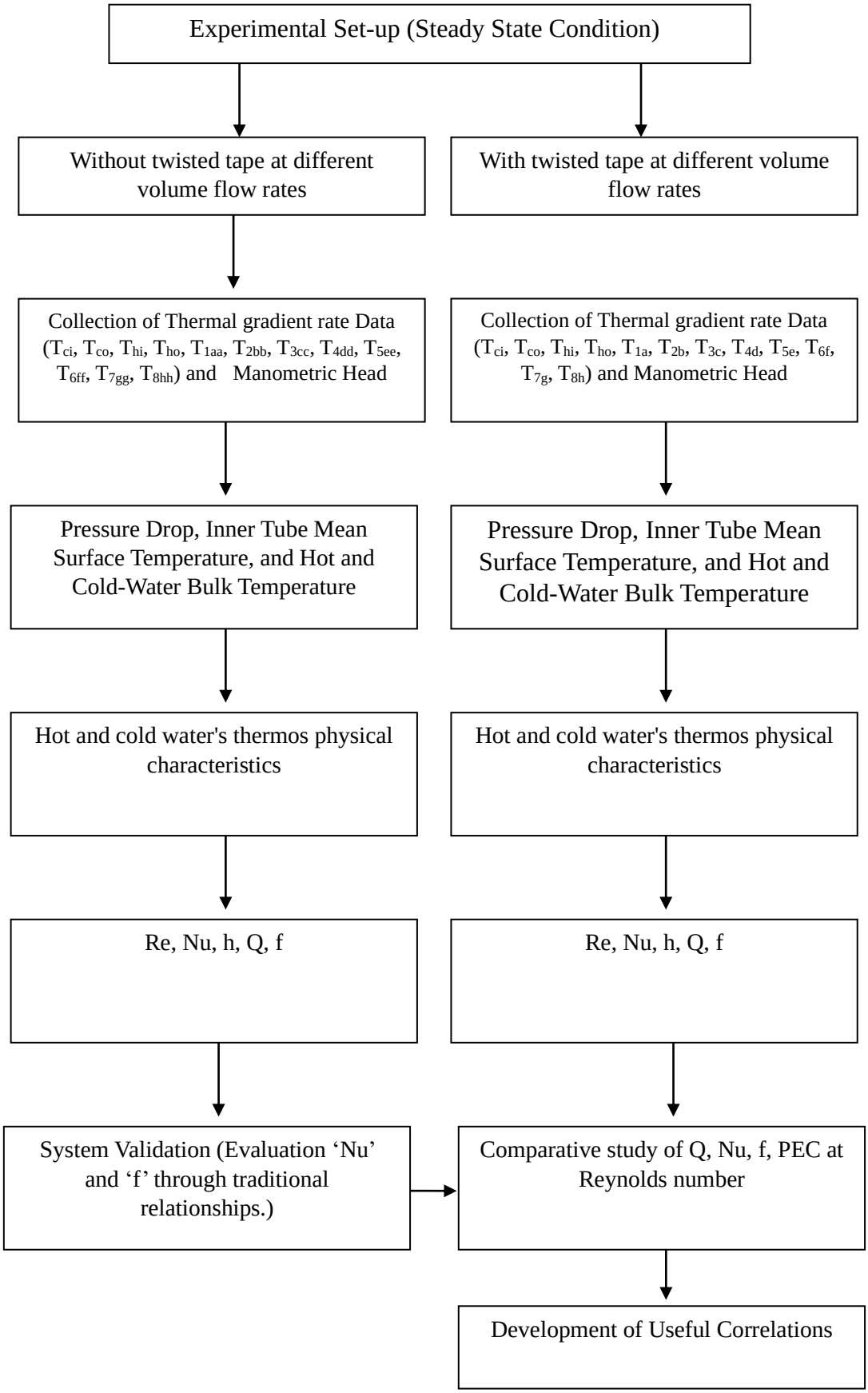

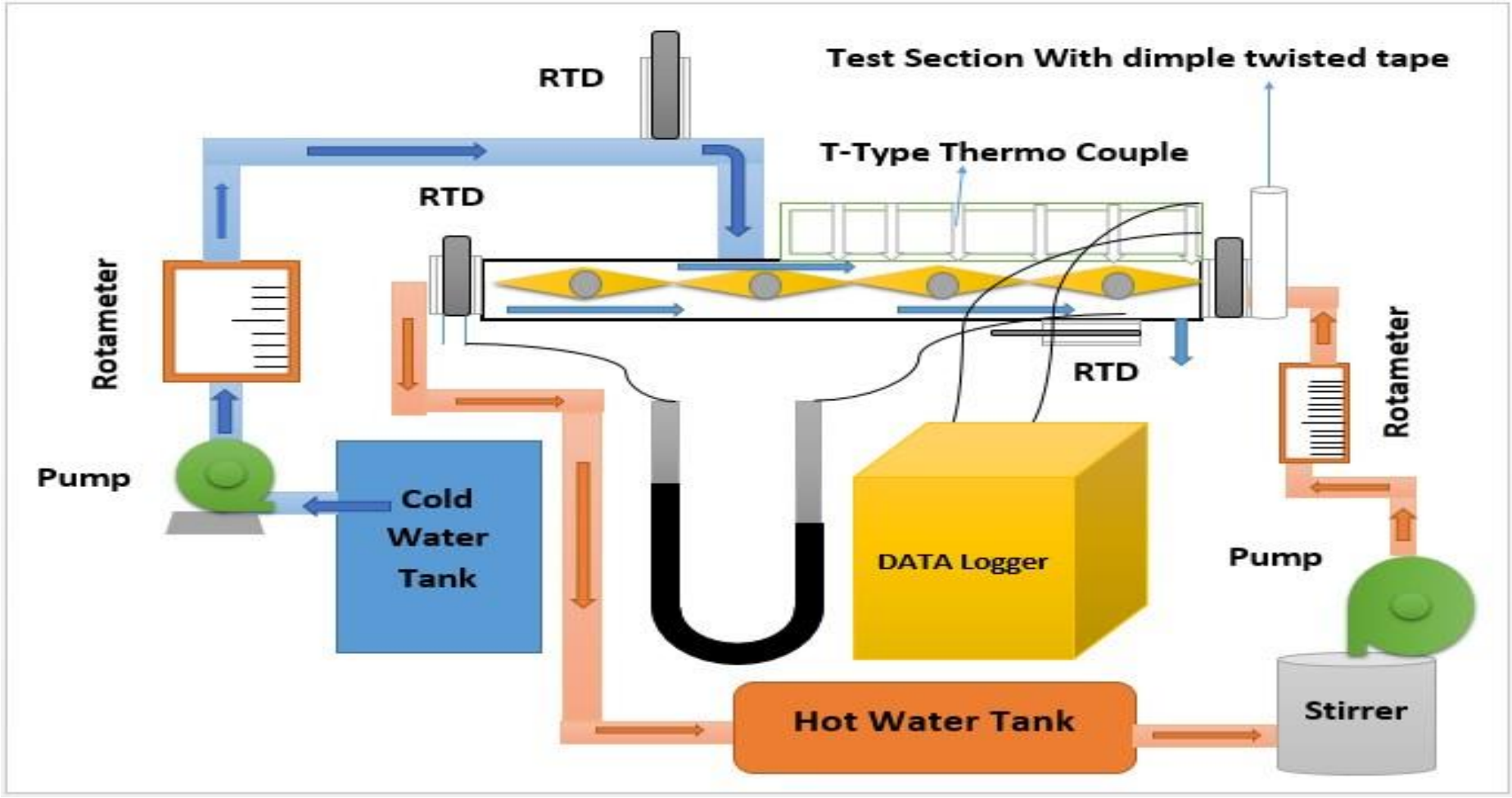

Fig.3.1. (a) Schematic diagram of the experimental set-up

Fig.3.1.(b) Photograph of the experimental set-up

3.3 Details of Experimental Setup

3.3.1 Test Section

Test section used in experiment is a concentric tube double pipe heat exchanger of length 1500 mm, inside pipe is made up of copper whereas outside pipe is made of Galvanised Iron. Smaller diameter of inside tube is 16mm and thickness 2 mm whereas outside tube is 32mm and thickness 3mm. Dimensions of the tubes used for the test section are chosen as per the literature survey [14,55,56]. Six T- type thermocouples have been placed at upper surface of inside tube at same distance to measure surface temperature of inner tube and four RTD has been used to compute temperatures of hot and cold water at the entry and exit. Experiments have been carried out in counter flow arrangement. Test section is fully insulated with glass wool insulator in effort to reduce heat loss. Pictographic view of test section is shown in Fig.3.2 and direction of flow of water and heat flow are depicted in Fig. 3.3. Inner pipe of test section is depicted in Figure 3.6, inner pipe with thermocouple is depicted in Fig.3.8 and outer pipe is depicted in Fig. 3.7.

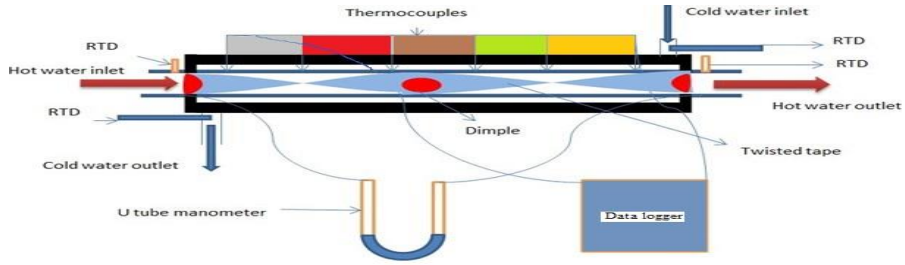

Fig. 3.2 Pictorial view of test section

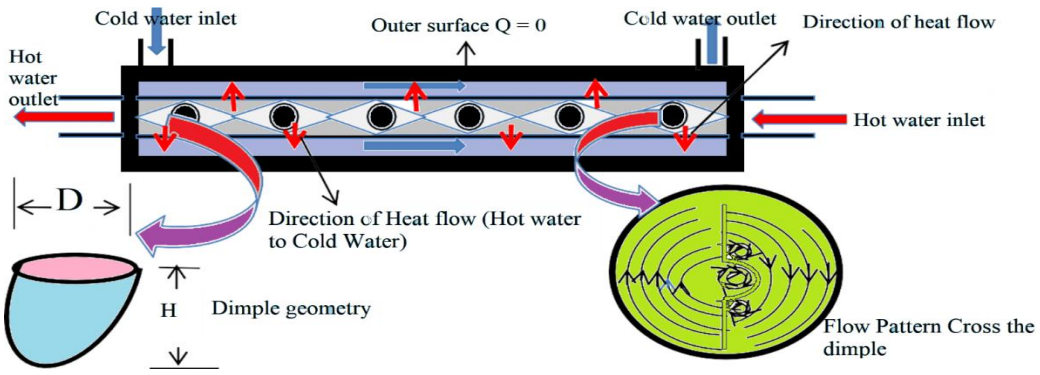

Fig. 3.3 Representation of test section with dimpled twisted tape

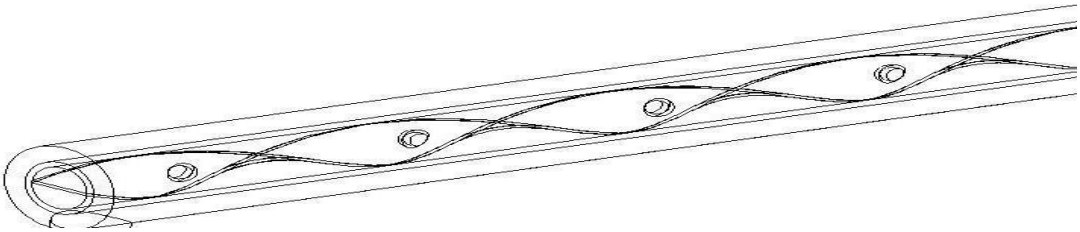

Fig. 3.4 Wire frame model of double pipe heat exchanger with dimpled twisted tape

Fig. 3.5 Twisted tape with dimples

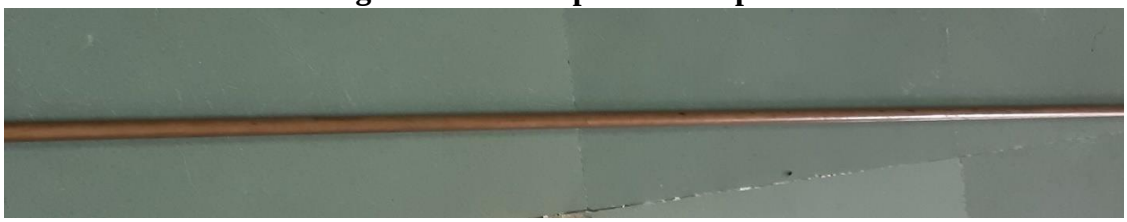

Fig.3.6 Photograph of Inner Copper pipe

Fig.3.7 Photograph of Outer GI pipe

Fig.3.8 Photograph of Inner tube with thermocouple

3.3.2 Developing and Calming Section

The pipe length has been extended at entry and exit of test section to confirm proper growth and calm flow conditions at the beginning and end of test suggested by Nikuradse J. [81] for turbulent flow. Proper insulation using glass wool has been applied to both sections.

Estimation of the length of developing section has been done through following correlation; For turbulent flow

Nikuradse suggested that L = (25 to 40) d [81] (3.1)

3.3.3 Temperature Measurements

To calculate heat transfer rate between flowing fluids in test section, temperatures of inner tube surface and of flowing fluids at inlet and outlet are required to be measured. To place thermocouples on tube surface, blind hole of one mm depth has been made on outer surface of inner tube by CNC machine. Six blind holes were made throughout length of tube each at a distance of 250 mm and at an angle of 60^{o}. T-type thermocouple (copper/constantan) has been used in each hole to measure average surface temperature of inner tube at six various places and four RTD has been used to measure temperatures of cold and hot water at entrance and exit. After fixing the thermocouples they were tested to show the consistency in temperature measurement. All the thermocouples and RTD were calibrated before use in the experimental setup. Arrangements of thermocouples are shown in Fig.3.9 and RTDs can be seen in Fig.3.10.

Fig.3.9 Photograph of T-type thermocouples used in experiment

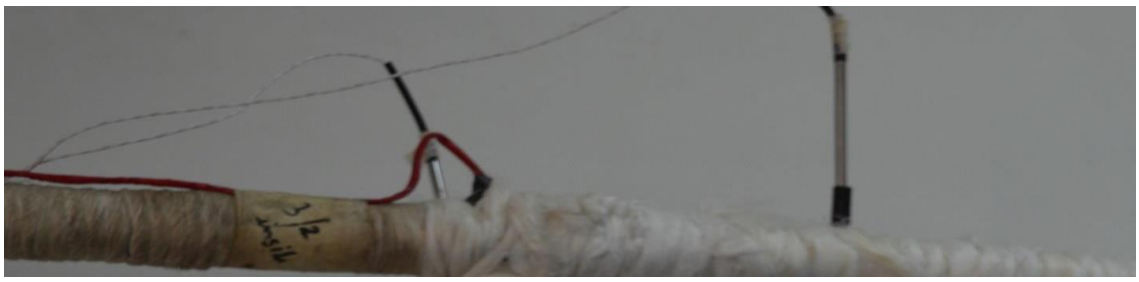

Fig.3.10 Photograph of RTDs used in experiment

3.3.4 Hot Water Tank

Hot water tank of 200 litters capacity with proper insulation has been used in the experiment and it is equipped with electrical heater of 10 kW capacities to heat the tank water. Water level indicator has been used to locate level of water inside tank. To maintain flow rate of hot water, ball valves have been used at inlet and exit of the tank. To know the temperature of tank water one calibrated RTD has been used. To control fluctuation in temperature of hot water tank, solid-state relay (SSR) has been used which senses the temperature up to ± 0.1OC. The details of solid-state relay (SSR) are given in Table 3.2. Hot water tank with accessories have been fabricated by Steam Thermo Boiler Pvt. Ltd. Govind Pura, Bhopal, India.

Table 3.2 Details of Solid-state relay (SSR)

Solid-state relay (SSR) Details	
Company	Unison
Input	12-270VAC/DC
Output	24-480VAC
PIV	1200
Current	90Amp
Body insulation	4kV
Input-Output insulation	6kV

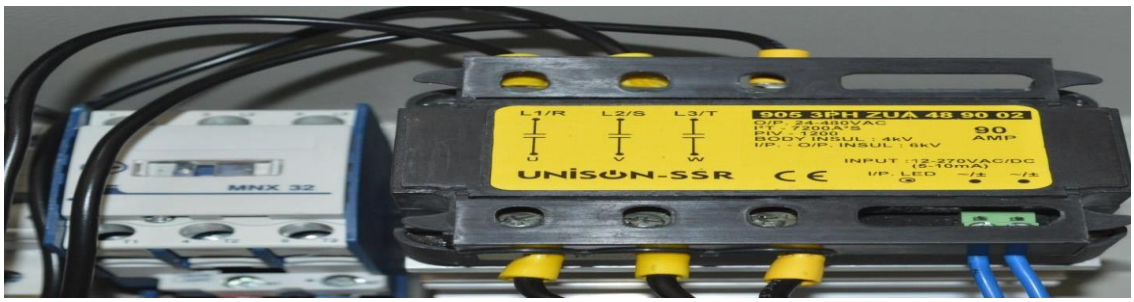

Fig.3.11 Photograph of Solid-state relay (SSR)

Fig. 3.12 Photograph of water level indicator

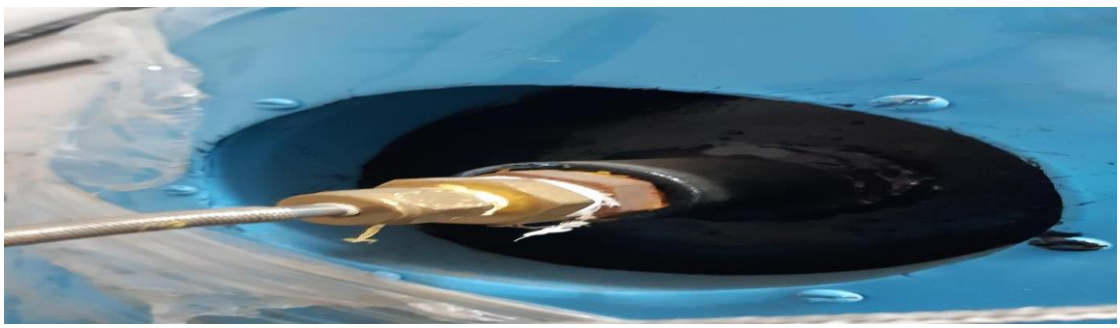

Fig.3.13 Photograph of RTD used in hot water tank

Fig.3.14 Photograph of water heater

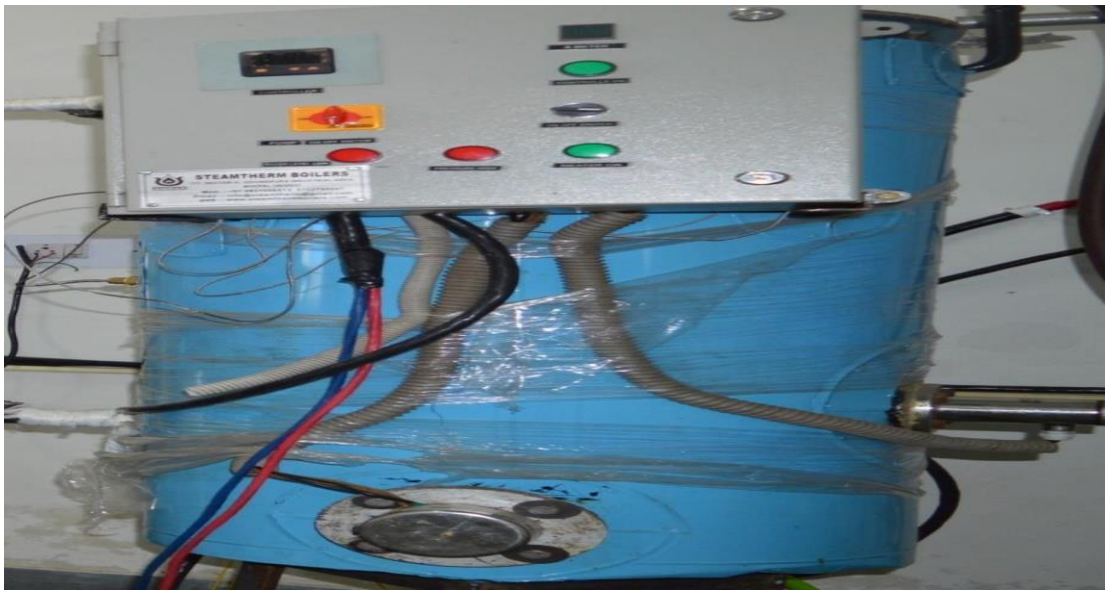

Fig.3.15 Photograph of Hot water tank

3.3.5 Mechanical Stirrer

Solid-state relay (SSR) used in the tank equipped with heater can only control the variation in temperature of hot water up to ± 0.1oC but in order to further reduce variation in temperature of hot water mechanical stirrer has been used. A mechanical stirrer is placed on top of the tank and its upper end is connected with low-speed electrical motor whereas lower end is placed in water. Stirrer stirs tank water in order to decrease temperature variation and in this way, it helps to achieve the steady state condition. Tank equipped with stirrer is shown in Fig.3.16 and it is fabricated by Megha Roto-Tech Pvt. Ltd., Ahmedabad, India.

Fig. 3.16 Photograph of Tank with stirrer

3.3.6 Flow Measurement

In order to conduct experiments for turbulent flow with “Re” range (6000 to 14000) and to calculate Re, the measurement of rate of flow is required. In the experimental setup, two calibrated rotameters have been used. Each rotameter is made to measure flow rates from 0 to 500 LPH with a least count of 10 LPH in shown Figure 3.17. In both cases, water enters from bottom and leaves from top of rotameter and measuring scale is fixed along the length of rotameter to measure the flow rate. Needle- type float has been used in both cases whose upper surface is flat whereas needle is pointed at the bottom and upper surface of float shows flow rate of flowing fluid. Both rotameters are fabricated by the Flow tech Pvt. Ltd., Baroda, India.

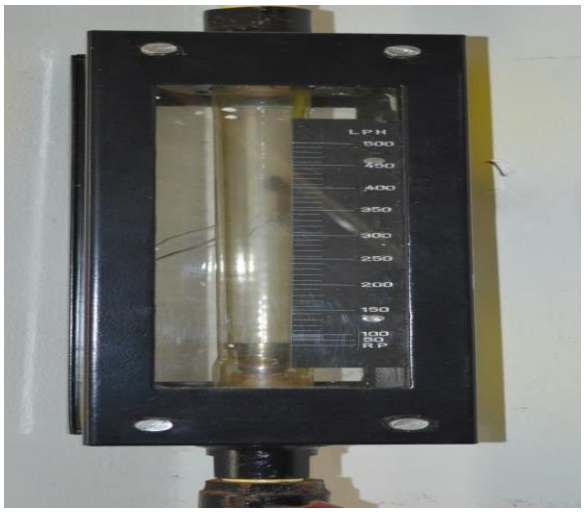

Fig. 3.17 Photograph of Rotameter

3.3.7 Pressure Drop Measurement

In pipe flow system friction loss between flowing fluid and tube surface is the main reason of pressure drop. As discussed earlier; twisted tape enhances heat transfer rate in association with frictional losses. To calculate frictional losses associated with the twisted insert with and without dimples pressure drop is required to be measured. In the test setup, a glass U-tube manometer full of mercury has been used to measure pressure drop due to frictional losses across the test section. For greater accuracy in calculation of pressure difference, U-tube manometer can also be used in inclined position, for few sets of readings. Fig.3.18 shows the U- tube used in the experiment.

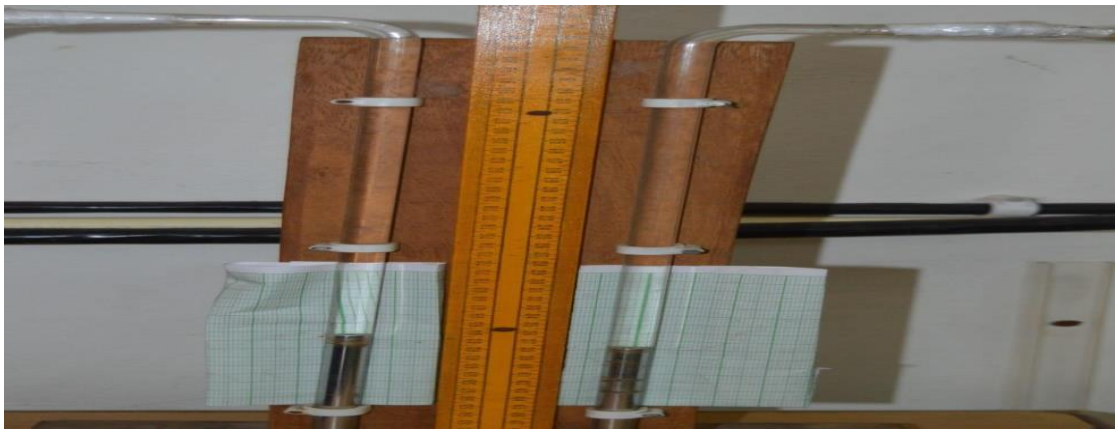

Fig.3.18 Photograph of U-Tube manometer

3.3.8 Data Acquisition System

Function of data acquisition system is to read, display and store the output of thermocouples and RTD at constant intervals of time. To record the values of temperature at various locations/ sections a 16- channel data acquisition system (Uni Log 8/16) manufactured by PPI has been used as shown in Fig.3.19. System comprises of a microprocessor-based temperature scanner equipped with built-in memory was employed to record and store data. Temperature can be seen on at the front panel screen of the data logger. In addition, the data stored in system can be transferred to other devices (for e.g., USB stick) for further use, since it is a USB version data logger.

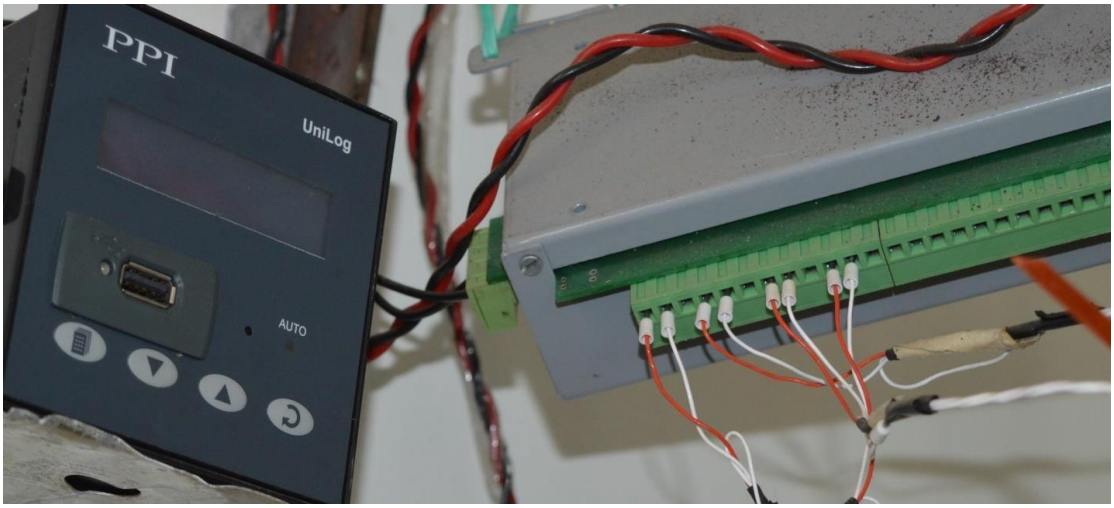

Fig.3.19 Photograph of a 16-channel temperature data logger

3.3.9 Centrifugal Pump

The centrifugal pumps of same capacity have been used for both the fluids to control the rate of flow. In hot water circuit, centrifugal pump has been placed between hot water tank and rotameter whereas in cold water circuit, centrifugal pump is placed between cold water tank and rotameter. Centrifugal Pumps manufactured by Kirloskar Pumps Pvt. Ltd. each of 0.5 HP have been used in the experiment as shown in Fig. 3.20.

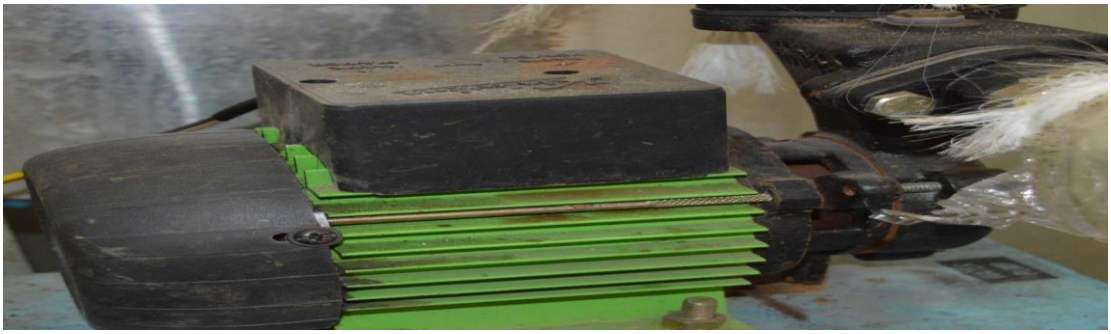

Fig.3.20 Photograph of Centrifugal Pump

3.3.10 Thermal Insulation

To minimise heat loss from system to surroundings, thermal insulation is necessary. In experimental setup, hot water circuit which includes hot water tank,

piping and test section are required to be insulated for proper functioning. Hot water tank is properly insulated by glass wool sheet and of thickness 40 mm whereas glass wool tape has been used to insulate test section and piping. Hot water circuit with insulation is shown in Fig. 3.21.

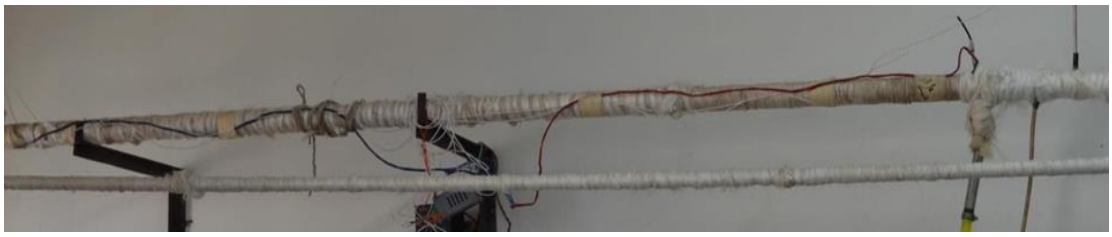

Fig.3.21 Photograph of Test section insulated with glass wool tape

3.4 FABRICATION OF TWISTED TAPE USED

twisted tape inserts are most popular tube inserts and are therefore extensively studied by authors from around the world. Mainly two types of twisted tape have been used in the experiment and they are plain twisted insert and twisted insert with dimples.

3.4.1 Fabrication of Plain Twisted Tape:

A plain twisted tape made from an aluminum sheet was created according to Figure 3.22. The aluminum sheet had a thickness of 1mm, a width of 16mm, and a length of 1500mm. Initially, the aluminum strip was secured between two vices with a distance greater than 1500mm. One vice is fixed, while other is free and both were attached to a lead screw. Free vice is rotated twenty-four times to achieve a twist ratio of 5.5, resulting in the production of the twisted tape.

Fig.3.22 Photograph of Plain twisted tape

3.4.2 Fabrication of Dimpled Twisted Tape:

Initially nine sets of dies and punches of different dimensions were made to generate dimple shape on aluminum strip and these sets of dies and punches were made by Bend Joint Pvt. Ltd., Bhopal, India. Details of measurements of dimples are

given in Table 3.3. With help of die and punches dimples were generated on aluminum strip. To make the dimpled twisted tape same procedure was followed as discussed earlier for plain twisted tape.

Since width of twisted tape fabricated for experiment was 16mm and it was not possible to make dimple of more than 6mm diameter on 16mm aluminum strip, and the dimple of diameter less than 2mm may give similar effect as plain tape on heat transfer characteristics. By considering the above limitations is shown in Table 3.4, the maximum diameter of dimple has been taken as 6 mm and minimum diameter as 2, various type and size of dimple twisted tape shown in from Figure 3.23 to 3.31.

Table3.3. Details of Dimple dimension

Dimple diameter (mm)	(D/H)		
2	1.5	3	4.5
4	1.5	3	4.5
6	1.5	3	4.5

Fig. 3.23 Photograph of twisted tape with dimples (D =2 mm D/H=4.5)

Fig. 3.24 Photograph of twisted tape with dimples (D =2 mm D/H=3)

Fig.3.25 Photograph of twisted tape with dimples (D =2mm D/H=1.5)

Fig. 3.26 Photograph of twisted tape with dimples (D =4 mm D/H=4.5)

Fig. 3.27Photograph of twisted tape with dimples (D =4 mm D/H=3)

Fig. 3.28 Photograph of twisted tape with dimples (D =4 mm D/H=1.5)

Fig.3.29 Photograph of twisted tape with dimples (D =6 mm D/H=4.5)

Fig.3.30 Photograph of twisted tape with dimples (D =6 mm D/H=3)

Fig.3.31 Photograph of twisted tape with dimples (D =6 mm D/H=1.5)

Table 3.4 Range of parameters for experimental investigation

Inlet temperature of hot water	70^{o}C
Inlet temperature of cold water	30- 32^{o}C
Volume flow rate of hot water	120-260 LPH
Reynolds number	6000-14000
Twist ratio	5.5
Diameter of dimple (D)	2, 4, 6 mm
D/H	1.5, 3 and 4.5

The boundary conditions, including material properties, fluid flow rates and temperatures, and geometric dimensions, directly influence heat transfer behavior in the heat exchanger system. Considering boundary conditions is essential for obtaining meaningful insights into the heat transfer performance of twisted tape inserts with dimples, as investigated in the study.

CHAPTER - 4

DATA REDUCTION AND SAMPLE CALCULATION

4.1 Introduction

This section deals with how to use experimental data to calculate Nusselt number, friction factor and performance evaluation criteria. It also discusses the correlations which were used to validate experimental setup. Step-wise procedure to calculate heat transfer characteristics from experimental data has been discussed below [4, 14]. Heat transfer from hot water to surrounding is shown in Fig. 4.1.

Heat lost by the hot water = Heat gained by the cold water due to convection+ Heat transfer through outer tube to surrounding by convection + Heat transfer by radiation

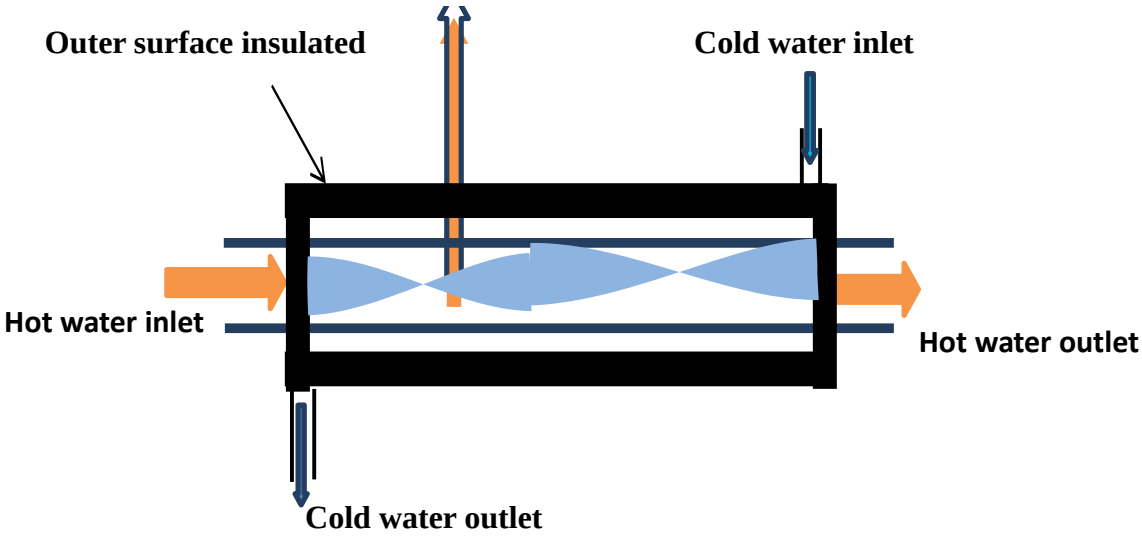

Figure 4.1 showing the heat transfer from hot water to surroundings

$$Q_{\text{Heat lost by hot water}} = Q_{\text{Heat gained by cold water due to convection}}$$

$$+ Q_{\text{Heat transfer through outer tube to surrounding by convection}}$$

$$+ Q_{\text{Heat transfer by radiation}}$$

Since, outer surface of the test section is shielded, heat transfer through outer surface to surrounding by convection is small and it is neglected and also heat transfer by radiation is small and it is neglected [4, 11, 14, 39].

$$\text{So, } Q_{\text{Heat lost by hot water}} = Q_{\text{Heat gained by cold water due to convection}}$$

$$Q = h_i \times A_s \times (T_h - T_w) \quad (4.1)$$

4.2 Calculation of Nusselt Number

As discussed earlier, six thermocouples is placed on surface of inner tube to measure surface temperature and four RTDs were used to measure entrance and exit temperatures of both hot and cold water. After obtaining steady state condition, data acquired from the experimental work has been processed using the relations given below.

4.2.1 Calculation of hot water bulk temperature

Hot water bulk temperature (t_h) is the average temperature of hot water at entrance and exit of measuring portion and it is calculated as

$$t_h = \frac{(t_{hi}+t_{ho})}{2} \quad (4.2)$$

4.2.2 Calculation of cold-water bulk temperature

Cold water bulk temperature (t_c) is the average temperature of cold water at entrance and exit of the measuring portion and it is calculated as

$$t_c = \frac{(t_{ci}+t_{co})}{2} \quad (4.3)$$

4.2.3 Calculation of mean surface temperature of inner tube surface (t_w)

Mean surface temperature of inner tube surface (t_w), It is the mean of thermocouples reading which were placed on inner tube surface and is calculated as

$$t_w = \frac{t_1+t_2+t_3+t_4+t_5+t_6}{6} \quad (4.4)$$

4.2.4 Calculation of mean velocity of hot fluid (U_h)

When fluid flows through the tube; its velocity is not uniform in radial direction due to formation of boundary layer. On account of formation of boundary layer, velocity of flowing fluid is maximum at the center and minimum or zero at periphery. So, it is required to calculate the mean velocity of flowing fluid for further calculation. Mean velocity of flowing fluid can be calculated as

$$U_h = \frac{V_h \times \rho_{in}}{\left(\frac{\Pi d^2 \times \rho h}{4}\right)} \tag{4.5}$$

4.2.5 Calculation of Reynolds number (Re)

Reynolds number is used to classify whether flow is laminar or turbulent.

$$R_e = \frac{U_h \times D_I}{V} \tag{4.6}$$

4.2.6 Calculation of heat lost by hot fluid (Q$_h$)

In heat exchangers transfer of heat takes place from hot fluid to cold fluid where hot fluid loses its heat whereas cold fluid receives the heat.

$$Q_h = \rho_h \times V_h \times C_p (T_{hi} - T_{h0}) \tag{4.7}$$

4.2.7 Calculation of heat gain by cold fluid (Q$_c$)

The heat captivated by the cold water is given by the equation given below.

$$Q_c = \rho_c \times V_c \times C_{pc} (T_{co} - T_{ci}) \tag{4.8}$$

4.2.8 Calculation of mean heat transfer rate (Q)

Mean value is taken into consideration for further calculations.

$$Q = \frac{(Q_h + Q_c)}{2} \tag{4.9}$$

4.2.9 Calculation of convective heat transfer coefficient (h_i)

Convective heat transfer coefficient is mathematically ratio between the heat flux to change in temp.

$$Q = \frac{(Q_h + Q_c)}{2} = h_i \times A_s \times (T_h - T_w) \tag{4.10}$$

4.2.10 Calculation of Nusselt number (Nu)

The physical interpretation of Nusselt number is heat transfer enhancement due to convection over conduction alone. If Nu =1, then fluid is static and total transfer of heat takes place only by conduction. With Nu>1, the fluid motion augments heat transfer by convection.

$$(N_u) = \frac{h_i D}{K_h} \tag{4.11}$$

4.3 Calculation of Friction Factor

Friction factor is a measure of resistance to the fluid flow of a duct or tube. Mathematically,it calculated by the equation given below.

$$(f) = \frac{2(\Delta P)}{4\rho_h L V_{h^2}} \tag{4.12}$$

Where ΔP is calculated as $\Delta p = (\rho_m - \rho_w) g \Delta h$

4.4 Performance Evaluation Criteria & Its Calculation

The performance evaluation criteria based on trade-off between increased heat transfer and friction factor is most widely used criteria and it is comparison of heat transfer coefficients between plain tube (without twist) to that for a tube fitted with twist under constant pumping power condition, which is defined as the ratio of Nusselt number within enhanced pipes against importance of heat transfer to pressure drop in Heat exchangers.

$$(PEC) = \frac{\left(\frac{N_{uT}}{N_{uo}}\right)}{\left(\frac{f_T}{f_o}\right)^{0.33}} \tag{4.13}$$

4.5 Experimental Procedure

The experimental setup was developed to analyse result of twisted insert and dimpled twisted insert on heat transfer characteristics. For the accuracy and sensitivity of the experimental results, utmost attention was taken in the fabrication and testing of the experimental setup at every step. For minimization of errors and for better accuracy of the experimental results calibration of temperature and flow measuring devices was performed. Experiments were conducted on fabricated experimental setup. Initially both the tanks were filled with water. Water of tank was heated by the electrical heater. The required temperature of hot water was fixed by the control panel while solid-state relay (SSR) maintained this temperature with ± 0.1^{o}C variation. After achieving the desired temperature of hot water, both hot and cold water were permitted to pass through test section at desired flow rate. For each case readings were taken for eight different flow rates after achieving the steady state condition.

4.6 Assumptions Made for Experimental Analysis

Following assumptions have been consider during the experimental analysis

a. Flow is fully developed (L/D > 60)

b. Flow is turbulent (Re > 2300)

c. Working medium is water

d. Radiation heat loss is neglected

4.7 Error Analysis of Experimental Results

We hardly ever get the exact same results when we repeat an experiment. Instead, it is thought that repeated measurements cover a range of values due to the precise limitations of measuring equipment. This range of experimental data is called error and it can be found by the uncertainty analysis of experimental data. In the present work, after uncertainty analysis it was found that the error in Reynolds number, Nusselt number and friction factor. Error in "Re" and Nusselt number are represented by the error bars and it is shown in Fig. 4.2 whereas the error bar representation of "Re" with friction factor is shown in Fig. 4.3.

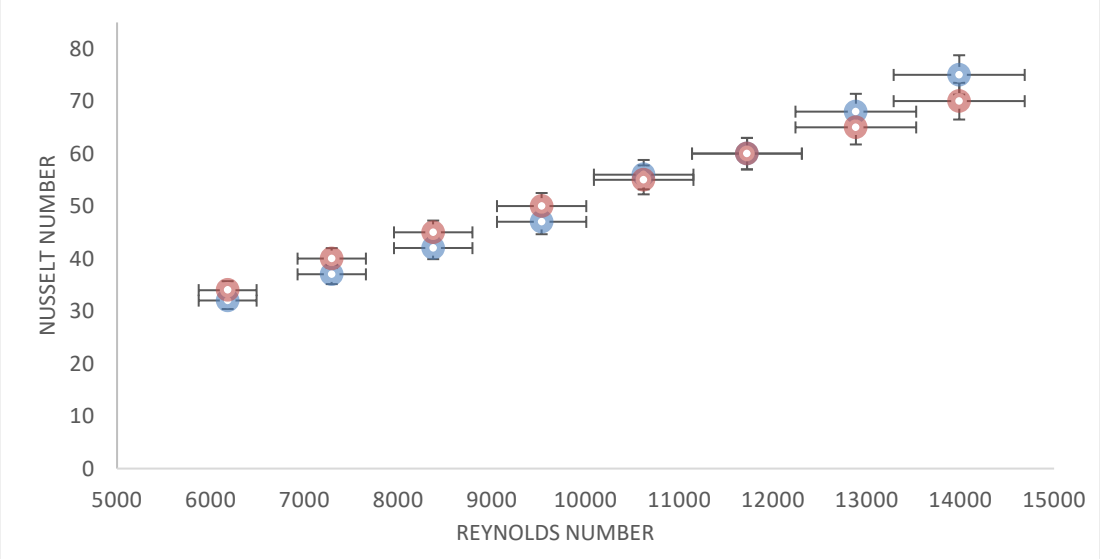

Fig.4.2 Plot of percentage error representation in Reynolds number and Nusselt number

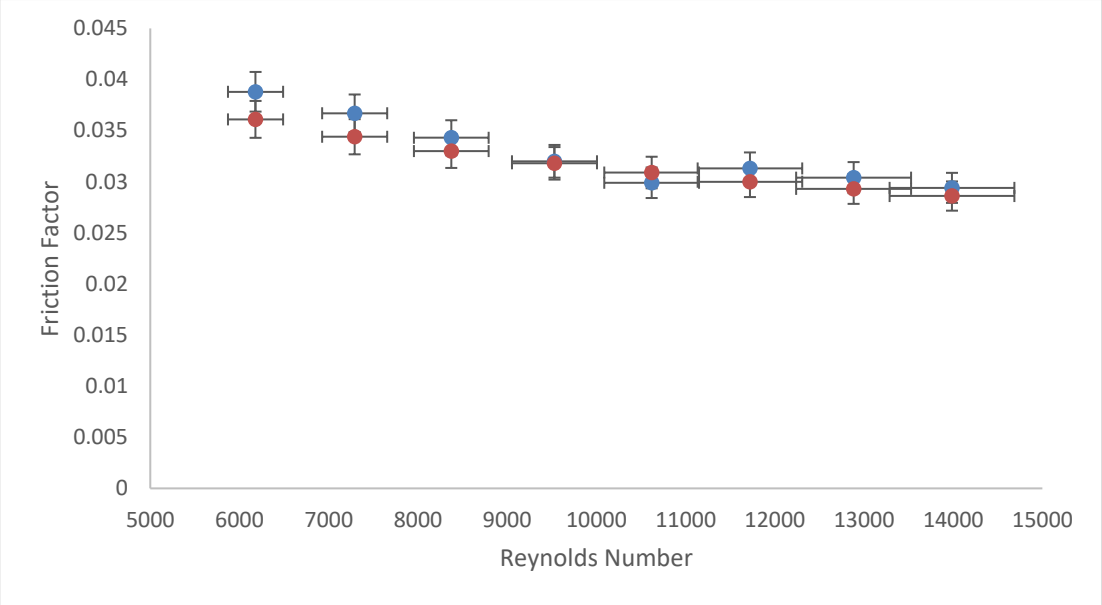

Fig.4.3 Plot of percentage error representation in Reynolds number and Friction factor

4.8 Validation of Experimental Setup

Before investigating the effect of dimple diameter (D) and dimeter to depth ratio (D/H) on heat transfer characteristics, it is necessary to validate the test setup. Validation of test setup helps to check accuracy of all data collected from experiments. Validation is performed by matching the experimental results with theoretical result obtained by well-known correlations. It represents the ratio between experimental and theoretical values' percentage deviations. Deviation should be in acceptable range as suggested by different authors. In present work test set-up is validated by comparing it against standard correlations as recommended by the authors [14,55,56], to verify the correctness of data collected shown in Table 4.1 and 4.2.

Nusselt number and friction factor values in study on pipe without insert are matched with the Gnielinski and Filonenko correlations for turbulent flow regime respectively.

Gnielinski correlation

$$Nu_f = \frac{\left(\frac{f}{8}\right)(Re - 1000)Prf}{\left[1 + 12.7\left(\frac{f}{8}\right)^{1/2}\left((Pr)^{0.66} - 1\right)\right]\left[1 + \left(\frac{d}{L}\right)^{2/3}\right]} C_1 \quad (4.14)$$

For Liquid $C_1 = \frac{Pr_f}{Pr_w} = 0.05\ to\ 20$

Where, Pr_f = Prandtl Number of Fluid

Pr_w = Prandtl Number of Water

Filonenko correlation

$$f = (1.82\ln\ R_e - 1.64)^{-2} \quad (4.15)$$

4.8.1 Sample Calculation for Set-up Validation

Table- 4.1 Parameters and test data used for Sample calculation

Parameters	Symbol	Data
Sectional size of the test	L	1500 [mm]
Tube diameter	d	16 [mm]
Pressure drop	ΔP	2.2 [mm of Hg]
Hot water exit temp	t_{ho}	63.3 [°C]
Hot water inlet temp	t_{hi}	73.8 [°C]
Cold water inlet temp	t_{ci}	25.2 [°C]
Cold water outlet temp	t_{co}	51.8 [°C]
Volume flow rate	V	240 [lph]
Surface temperature	t_1	62.7 [°C]
Surface temperature	t_2	62 [°C]
Surface temperature	t_3	62 [°C]
Surface temperature	t_4	62.7 [°C]
Surface temperature	t_5	62.7 [°C]
Surface temperature	t_6	62.6 [°C]

Data Processing

A). Hot water average temperature,

$$t_h = \frac{(t_{hi}+t_{ho})}{2} \qquad \frac{(73.8+63.3)}{2} = 68.55°C \tag{4.16}$$

B). Cold water average temperature,

$$t_c = \frac{(t_{ci}+t_{co})}{2} \qquad \frac{(25.2+51.8)}{2} = 38.5°C \tag{4.17}$$

C). Mean temperature of wall

$$t_w = \frac{t_1+t_2+t_3+t_4+t_5+t_6}{6} \qquad \frac{62.7+62+62.7+62+62.7+62.6}{6} = 62.45°C \tag{4.18}$$

Table 4.2. Thermo physical properties of water

Parameters	Symbol	Data
Specific heat of hot water at bulk temperature	C_{Ph}	4066 [J/Kg K]
Heat conductivity	k	0.66153 [W/m K]
Density of hot water at inlet temperature	ρ_{in}	975.1 [kg/m^3]
Density of hot water at bulk temperature	ρ_h	978.2 [kg/m^3]
Density of cold water at bulk temperature	ρ_c	992.36 [kg/m^3]
Prandtl number of hot waters at bulk Temperature	P_r	2.4693
Kinematic viscosity of hot water at bulk Temperature	v	3.132 x10^{-7} [m^2/s]
Specific heat of cold water	C_{Pc}	4067.6 [J/Kg K]

(D). Mean velocity of hot water

$$U_h = \frac{(\mathrm{V}_h \times \rho_{in})}{\left(\frac{\pi d^2 \times \rho_h}{4}\right)} \qquad \frac{\left(\frac{150}{3600\times1000}\times 975.1\right)}{\left(\frac{3.14\times0.016^2\times978.2}{4}\right)} = 0.27383 \text{ m/s} \tag{4.19}$$

(E). Reynolds number (Re)

$$R_e = \frac{U_h \times \mathrm{d}}{v} \qquad \frac{0.27383\times0.016}{3.132\times10^{-7}} = 13987 \tag{4.20}$$

(F). Heat released by hot water

$$Q_h = \rho_h \times V_h \times C_{ph}(t_{hi} - t_{ho})$$

$$= 978.2 \times 4.16 \times 10^{-5} \times 4066(73.8 - 63.3)$$

$$= 1737.311 \text{ W} \tag{4.21}$$

(G). Heat gained by cold water

$$Q_c = \rho_c \times V_c \times C_{pc}(t_{co} - t_{ci})$$

$$= 992.36 \times 1.32 \times 10^{-5} \times 4067.6(51.8 - 25.2) = 1417.304 \text{ W} \tag{4.22}$$

(H). Convective heat transfer coefficient

$$Q = \frac{(Q_h + Q_c)}{2} = h_i \times A_s \times (T_h - T_\mathrm{w})$$

$$\frac{(1737.311+1417.304)}{2} = h_i \times \pi \times 0.016 \times 1.5 \times (68.55 - 62.45)$$

$$= 3431.241 \text{ W/m}^2 \text{ K} \tag{4.23}$$

(I) Nusselt number

$$N_u = \frac{(h_i \times \mathrm{d})}{K_h} \qquad \frac{(3431.241\times0.016)}{0.66153} = 82.98 \tag{4.24}$$

(J). Friction factor

$$f = \frac{2d(\Delta P)}{4\rho L U^2} \qquad \frac{2\times0.016(265.7939)}{4\times978.2\times1.5\times0.27383^2} = 0.0214 \tag{4.25}$$

(K). Gnielinski correlation

$$Nu_f = \frac{\left(\frac{f}{8}\right)(\mathrm{Re}-1000)_{prf}}{\left[1+12.7\left(\frac{f}{8}\right)^{1/2}((\mathrm{Pr})^{0.66}-1)\right]\left[1+\left(\frac{d}{L}\right)^{2/3}\right]} C_1$$

$$\frac{\left(\frac{0.0214}{8}\right)(13987-1000)\times 2.4693}{\left(1+12.7\left(\frac{0.0214}{8}\right)^{0.5}(2.4693)^{0.66}-1\right)\left(1+\left(\frac{0.016}{1.5}\right)^{0.66}\right)} = 69 \qquad (4.26)$$

(L). Filonenko correlation

$$f = (1.82\ln 13987 - 1.64)^{-2} = 0.0286 \qquad (4.27)$$

Table 4.3 Calculation table for plain tube within specified eight Reynolds number range 6000<Re<14000

S. No	V_h (LPH)	Re	U_h (m/s)	$h_{experimental}$ (W/m^2K)	Δp (Pa)	$Nu_{experimental}$	$Nu_{theoretical}$	$f_{experimental}$	$f_{theoretical}$
1	120	6180	0.1651	1340	84	32	34	0.0388	0.0361
2	140	7291	0.1926	1556	108	37	40	0.0367	0.0344
3	160	8374	0.2202	1767	133	42	45	0.0343	0.0330
4	180	9531	0.2478	1981	157	47	50	0.0320	0.0318
5	200	10620	0.2754	2343	181	56	55	0.0299	0.0309
6	220	11722	0.3030	2517	229	60	60	0.0313	0.0300
7	240	12884	0.3306	2824	265	68	65	0.0304	0.0293
8	260	13987	0.3582	3125	302	75	69	0.0214	0.0286

Validation of experimental setup against standard correlations is an important step to ensure the correctness of the experimental data. This is typically done by comparing experimental results with predicted by existing correlations in available literature. [11,

14,55,56]. Gnielinski and Filonenko correlations are used to match values of Nusselt number and friction factor that were discovered from research on tubes without inserts. Findings demonstrate that experimental values fall within acceptable bounds, confirming experimental design. Largest divergence discovered is ±7.5% for friction factor and ±7% for Nusselt number.

Table 4.4 . Calculation table for plain twisted tape (without dimple configuration)

S.No	V_h(LPH)	Re	t_h (^{O}C)	t_c(^{O}C)	t_w(^{O}C)	Δp (Pa)	$h_{experimental}$ (W/m^{2}K)	$Nu_{experimental}$	$f_{experimental}$	PEC
1	120	6300	64.45	42.20	57.61	302	1668	40	0.1387	0.8189
2	140	7400	65.20	42.85	58.65	399	1824	44	0.1344	0.7648
3	160	8600	65.95	43.20	59.80	483	2030	49	0.1246	0.7513
4	180	9700	66.50	43.45	60.81	592	2266	54	0.1206	0.7396
5	200	10900	67.15	43.60	62.11	725	2670	64	0.1195	0.7376
6	220	12000	67.40	44.10	62.52	785	2811	68	0.1070	0.7451
7	240	13200	67.65	44.20	63.11	906	3107	75	0.1037	0.7353
8	260	14400	68.05	45.05	63.90	1003	3428	82	0.0977	0.7390

A. Impact of Flow measurement on heat transfer for plain tube

Variation of Nusselt number with Reynolds number for a plain tube with 16 mm of inner diameter, without any twisted tape or dimples shown in figure 4.4. It exhibits difference of Nusselt number as a function of tube diameter at Eight (8) different volume flow rates V_h (LPH) and Reynolds number values as reflected from Table 4.3 and 4.4. It is evident from the plot that value of Nusselt number has experienced a noticeable increase with subsequent increase in the value of Reynolds number. Through comparative experimental investigation variable Nusselt number reached its maximum value 77 (for Reynolds number = 14000) and 31.576 (for Reynolds number = 6000).

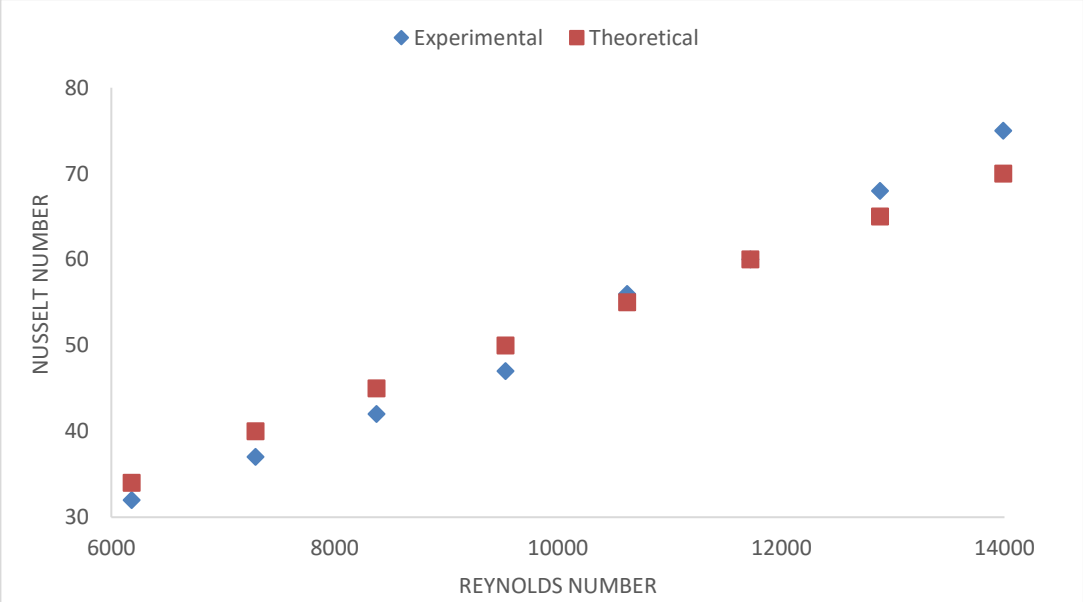

Fig 4.4 Assessment of present experimental and theoretical values for Nusselt number for plain twisted tape

B. Impact of Flow measurement on friction factor for plain tube

Variation of friction factor with Reynolds number for plain twisted tape (without twisted tape as well as without dimples) as inner tube diameter of d = 16 mm is given in Figure 4.5. It exhibits difference of friction factor as a function of tube diameter at Eight (8) different volume flow rates V_h (LPH) and Reynolds number values as reflected from Table 4.3 and 4.4. It is evident from the plot that there is a

reduce in value of friction factor with subsequent increase in value of Reynolds number. Through comparative experimental analysis conducted, friction factor had minimum value of 0.0336 (for Reynolds number = 14000) and 0.038 (for Reynolds number = 6000).

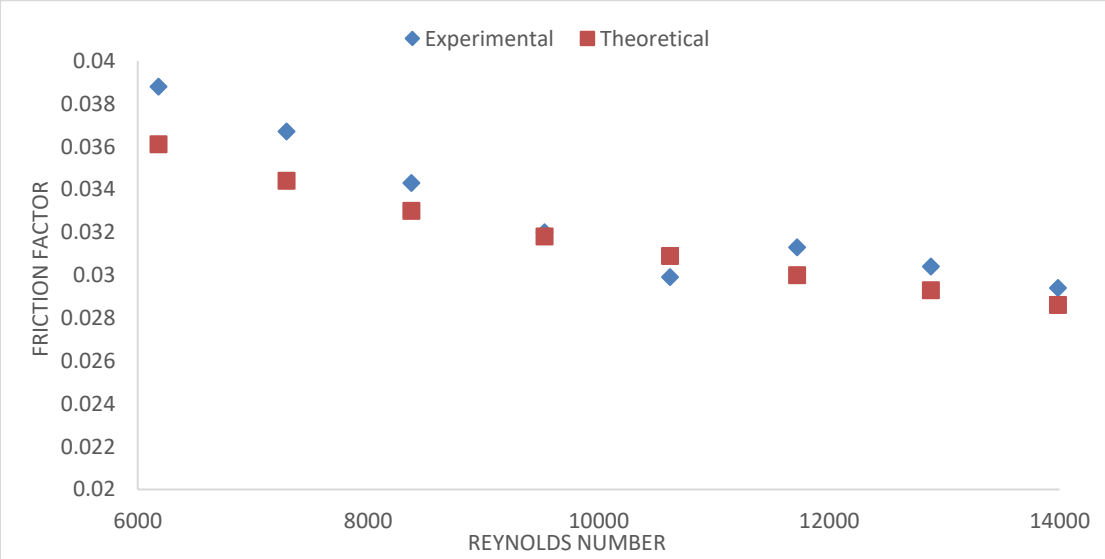

Fig 4.5. Assessment of present experimental and theoretical values for friction factor for the plain twisted tape

CHAPTER - 5

RESULTS AND DISCUSSION

5.1 Introduction

The main objective of the study is to investigate influence of dimpled twisted tape on heat exchanger performance, providing useful information for engineers to improve their Heat exchangers designs. The details of experimental setup, experimental procedure, validation of experimental setup (comparison of theoretical and experimental results) and data reduction have been discussed in previous chapters. A dimple protrusion surface, accompanied by a hole configuration placed adjacent to it, has been incorporated solely on the front face of the tube along its entire length of 1500 mm.

Thermo-hydraulic performance evaluation is one of the criteria which helps to decide the usefulness of inserts. Hence, thermo-hydraulic behavior of dimpled twisted tape in a tube of circular cross-section has been investigated in turbulent flow regimes under constant heat flux conditions. Results of this experimental study have been presented and discussed. This research has broadly highlighted the benefits and utility of dimpled twisted tape in accordance with industry applications.

Objective: 1

5.2 The Effect of Dimple Diameter (D) and Dimple Diameter to Depth Ratio (D/H) on heat transfer has been studied experimentally

Deviation of Nusselt number with Reynolds number for twisted tape without dimple and with dimple (Dimple Diameter (D) = 2, 4, and 6 mm to dimple diameter to depth ratio (D/H) = 1.5, 3 and 4.5) is described in figures.5.1, 5.3 and 5.5 respectively. Observed in study that all cases, Nusselt number increases with the increasing Reynolds number. The above statement means that using a tube with inserts, specifically with dimples, leads to an increase in heat transfer compared to using a plain tube or tube with inserts but without dimples. In other words, presence of dimples in tube inserts enhances heat transfer efficiency of tube. Suggests that Nusselt number, which is a dimensionless number used to quantify the heat transfer rate, increases for dimple diameter between 2 to 4 mm. However, the value of Nusselt

number decreases for diameter between 4 to 6 mm, for the range of Reynolds number that were studied. This means that the optimum range of dimple diameter for maximizing the heat transfer rate lies between 2 to 4 mm.

General trend based on experimental analysis reflects a substantial improvement for dimple diameter (D) =2 for dimple diameter to depth ratio (D/H) =1.5, 3 and 4.5. In a sense, from smaller to larger dimple diameter to depth ratio (D/H) convective heat transfer rate is improvising at a faster rate, whereas if dimple diameter to depth ratio (D/H) is further increased then there a downward trend. Nusselt number had the maximum value of it is observed that for specific diameter with dimple diameter (D) = 2 mm, Nusselt number initially has a lower value compared to same at dimple diameter to depth ratio (D/H) = 3. Subsequently as dimple diameter to depth ratio (D/H) is increased to D/H = 4.5 The Nusselt number decreasing or dropping. Therefore, Optimum value for higher Nusselt number is benchmarked or standard for discussion at dimple diameter to depth ratio (D/H) = 3 for different diameter as it 90 (Re = 13987) and 48 (Re = 6180) where dimple diameter (D) and dimple diameter to depth ratio (D/H) are 2 mm and 3 respectively.

General trend based on experimental analysis reflects a substantial improvement dimple diameter (D) =4 for dimple diameter to depth ratio (D/H) =1.5, 3 and 4.5. In a sense, from smaller to larger dimple diameter to depth ratio (D/H) convective heat transfer rate is improvising at a faster rate, whereas if dimple diameter to depth ratio (D/H) is further increased then there a downward trend. Nusselt number had the maximum value of it is observed that for specific diameter with dimple diameter (D) = 4 mm, Nusselt number initially has a lower value compared to same at dimple diameter to depth ratio (D/H) = 3. Subsequently as dimple diameter to depth ratio (D/H) is increased to dimple diameter to depth ratio (D/H) = 4.5 The Nusselt number decreasing or dropping. Therefore, Optimum value for higher Nusselt number is benchmarked or standard for discussion at dimple diameter to depth ratio (D/H) = 3 for different diameter as it 111 (Re = 13987) and 58 (Re = 6180) where dimple diameter (D) and dimple diameter to depth ratio (D/H) are 4 mm and 3 respectively.

General trend based on experimental analysis reflects a substantial improvement for dimple diameter (D) =6 for dimple diameter to depth ratio (D/H)

=1.5, 3 and 4.5. In a sense, from smaller to larger dimple diameter to depth ratio (D/H) convective heat transfer rate is improvising at a faster rate, whereas if dimple diameter to depth ratio (D/H) is further increased then there a downward trend. Nusselt number had the maximum value of it is observed that for specific diameter with dimple diameter (D) = 6 mm, Nusselt number initially has a lower value compared to same at dimple diameter to depth ratio (D/H) = 3. Subsequently as dimple diameter to depth ratio (D/H) is increased to dimple diameter to depth ratio (D/H) = 4.5 The Nusselt number decreasing or dropping. Therefore, Optimum value for higher Nusselt number is benchmarked or standard for discussion at dimple diameter to depth ratio (D/H) = 3 for different diameter as it 94 (Re = 13987) and 60 (Re = 6180) were dimple diameter (D) and dimple diameter to depth ratio (D/H) are 6 mm and 3 respectively.

Beyond this range, increasing the dimple diameter decreases heat transfer rate. Nusselt number, which is used to quantify the heat transfer rate, depends on dimple diameter to depth ratio (D/H) of dimple in addition to other factors. Specifically, the Nusselt number increases for a dimple diameter to depth ratio (D/H) between 4.5 to 3, and it is dropping for a dimple diameter to depth ratio (D/H) between 3 to 1.5 in all circumstances. This means that optimum dimple diameter to depth ratio (D/H) for maximizing the heat transfer rate lies between 4.5 to 3. Beyond this range, decreasing or increasing the dimple diameter to depth ratio (D/H) leads to a decrease in heat transfer rate. Therefore, dimple diameter to depth ratio (D/H) is an important factor to consider when designing dimpled surfaces for heat transfer applications. It was observed that maximum value of Nusselt number is observed to be 111 (as Reynolds number =14000) and 58 (as Reynolds number = 6000) for Dimple Diameter (D) is 4 mm and dimple diameter to depth ratio (D/H) is 3**.**

Dimples are a type of concavity that are known to enhance heat transfer while minimizing the associated pressure drop. Dimpled surfaces have been shown to be effective in improving heat transfer coefficient, which is measure of how efficiently a surface transfers heat. The diameter of the dimple from 2 to 4 mm and changing the dimple diameter to depth ratio (D/H) from 4.5 to 3 leads to a clear increase in Nusselt number. Improved fluid flow, in turn, leads to better heat transfer rates and an overall

enhancement in the Nusselt number. The use of a dimpled surface in this scenario is compared to a plain twisted tape, which likely has a lower heat transfer coefficient due to the absence of dimpled surface.

By introducing the dimpled surface, the efficiency of heat transfer system is improved, leading to more efficient and effective operation. The reason for the decrease in Nusselt number for dimple diameter (D) and dimple diameter to depth ratio (D/H) are 4 to 6 mm and ratio between 3 to 1.5 is due to concave structure with sharp contours reduces occurrence of boundary layers and boosts fluid velocity. The presence of this concave structure creates a situation where operating fluid gets trapped at bottom of dimple. As a result, rate of flow decreases, which adversely affects the overall heat transfer efficiency. Additionally, flow on convex side of dimple is separated, further reducing Nusselt number value. Sharp concave structure of dimple may cause flow to become turbulent, which can reduce heat transfer coefficient and increase resistance flow. Overall, dropping in Nusselt number is due to negative effects of sharp concave structure on fluid flow, which results in a reduction in heat transfer efficiency. fig.5.2, 5.4 and 5.6 exhibits deviation on Nusselt number as examined for dimple diameter to depth ratio (D/H) value of dimple diameter (D) at different range of Reynolds number is shown in Tables 5.1, 5.2 and 5.3.

The Nusselt number increases from a dimple diameter to depth ratio (D/H) is 1.5 to 3, and then falling from 3 to 4.5. Highest rate of Nusselt number is observed at dimple diameter to depth ratio (D/H) is 3 evaluated to other two ratios in each case for all rates of Reynolds number. This indicates that the optimal dimple diameter to depth ratio (D/H) for maximum heat transfer efficiency lies between 1.5 to 3.0. Furthermore, it can be observed that rate Nusselt number dimple diameter (D) and dimple diameter to depth ratio (D/H) are 4 mm and 3 is more compared to varying two (2) dimple diameter (D) and dimple diameter to depth ratio (D/H) for Reynolds number. This suggests that dimple diameter (D) and dimple diameter to depth ratio (D/H) are 4 mm and 3 respectively is the optimal combination for maximizing heat transfer efficiency. Overall, these observations highlight importance of carefully selecting dimensions of dimple surface for optimal heat transfer performance.

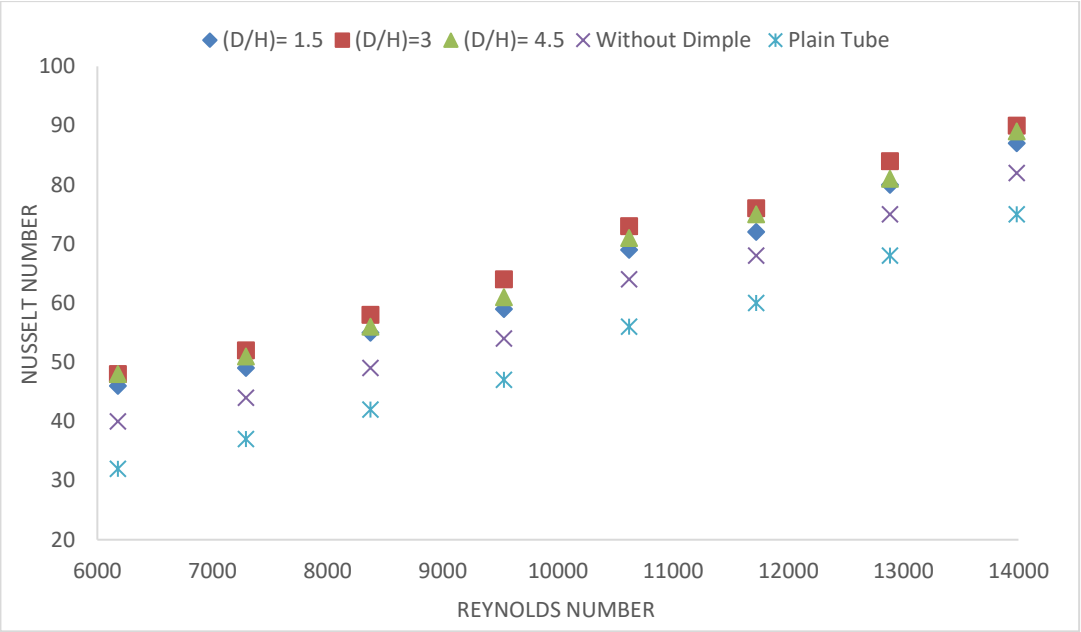

Figure: 5.1. Experimental values for Nusselt number Vs Reynolds number with Dimple Diameter to Depth Ratio (D/H) where (D = 2 mm)

The incorporation of twisted tape inserts with dimple configurations does indeed affect the pressure drop across the heat exchanger. The introduction of dimples disrupts the flow pattern and increases turbulence, consequently leading to a higher pressure drop compared to conventional setups. While this higher pressure drop may result in increased energy consumption due to elevated pumping power requirements, it is offset by the enhanced heat transfer efficiency facilitated by the dimpled twisted tape inserts. Therefore, when implementing such configurations, careful consideration of the adjustments between heat transfer enhancement and pressure drop increase is necessary to optimize overall system performance and energy efficiency.

Table 5.1. Calculation table for plain twisted tape with configuration of dimple

Reynolds number	Experimental Nusselt number (D=2mm)				
	Plain tube	Without dimple twisted tape	(D/H)=1.5	(D/H)=3	(D/H)=4.5
13987	75	82	87	90	89
12884	68	75	80	84	81
11722	60	68	72	76	75
10620	56	64	69	73	71
9531	47	54	59	64	61
8374	42	49	55	58	56
7291	37	44	49	52	51
6180	32	40	46	48	48

Table 5.2. Calculation table for plain twisted tape with configuration of dimple

Reynolds number	Experimental Nusselt number (D=4mm)				
	Plain tube	Without dimple twisted tape	(D/H)=1.5	(D/H)=3	(D/H)=4.5
13987	75	82	98	111	99
12884	68	75	94	97	95
11722	60	68	89	91	90
10620	56	64	78	87	79
9531	47	54	74	78	75
8374	42	49	66	71	67
7291	37	44	61	65	62
6180	32	40	54	58	55

Table 5.3. Calculation table for plain twisted tape with configuration of dimple

Reynolds number	Experimental Nusselt number (D=6mm)				
	Plain tube	Without dimple twisted tape	(D/H)=1.5	(D/H)=3	(D/H)=4.5
13987	75	82	90	94	92
12884	68	75	82	86	83
11722	60	68	74	79	75
10620	56	64	71	75	73
9531	47	54	61	65	63
8374	42	49	56	60	58
7291	37	44	51	55	54
6180	32	40	47	52	49

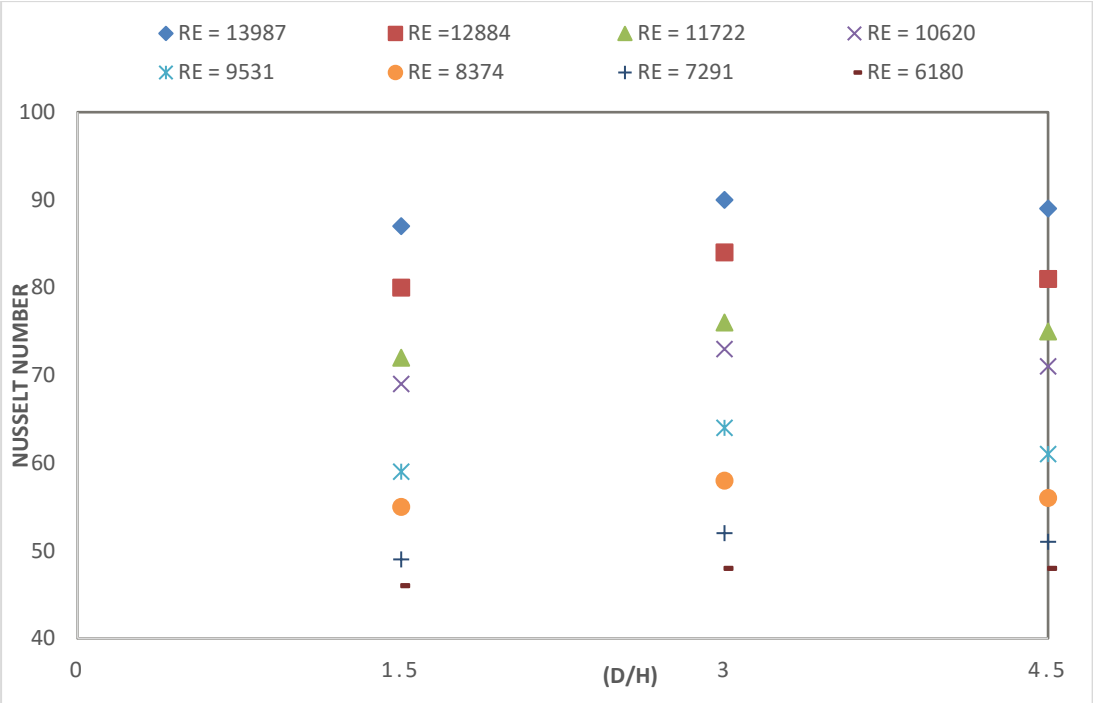

Figure: 5.2. Experimental values for Nusselt number Vs Dimple Diameter to Depth Ratio (D/H) with Reynolds number where (D = 2 mm)

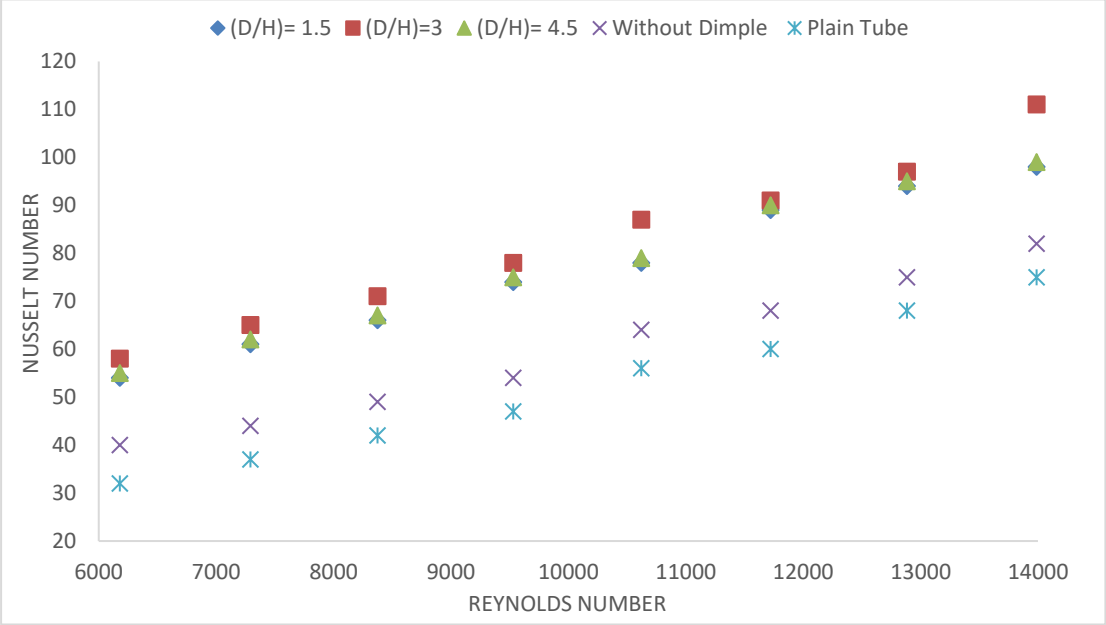

Figure: 5.3. Experimental values for Nusselt number Vs Reynolds number with Dimple Diameter to Depth Ratio (D/H) where (D = 4 mm)

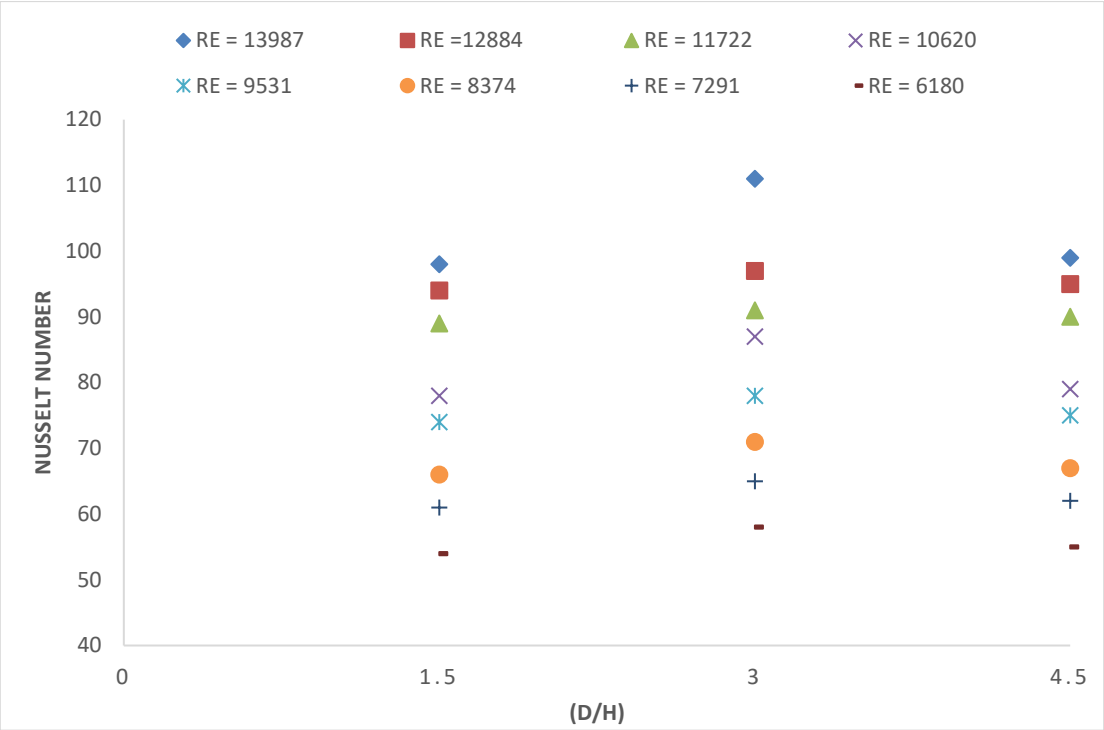

Figure: 5.4. Experimental values for Nusselt number Vs Dimple Diameter to Depth Ratio (D/H) with Reynolds number where (D = 4 mm)

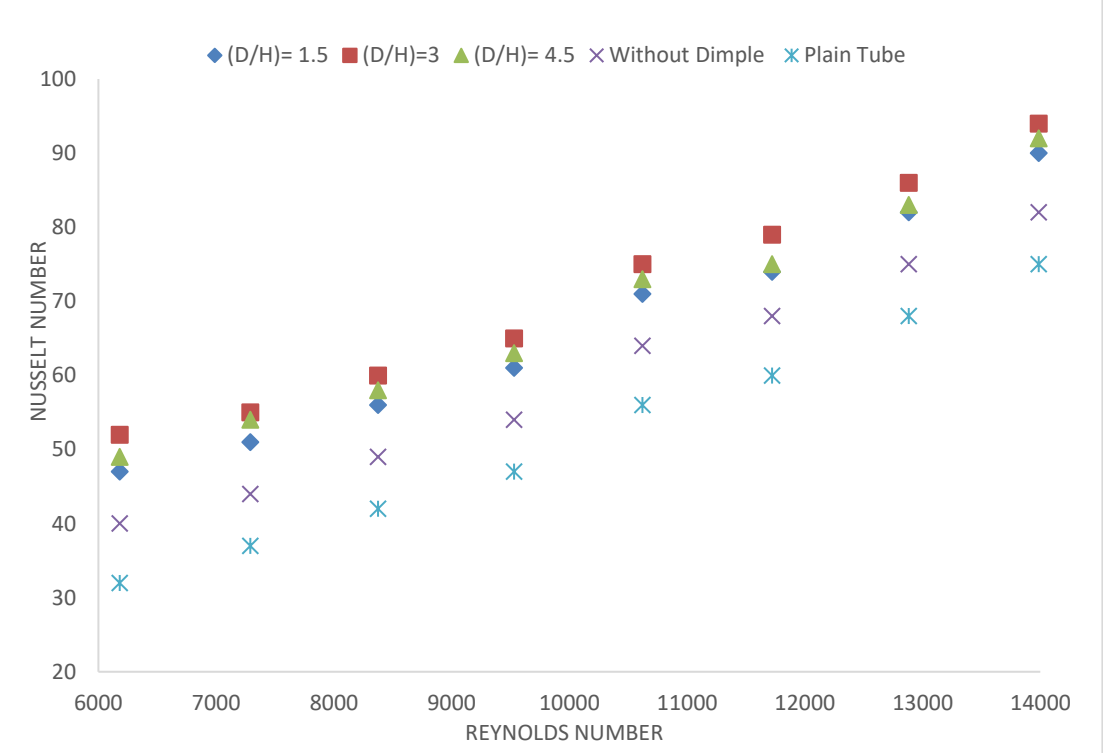

Figure: 5.5. Experimental values for Nusselt number Vs Reynolds number with Dimple Diameter to Depth Ratio (D/H) where (D = 6 mm)

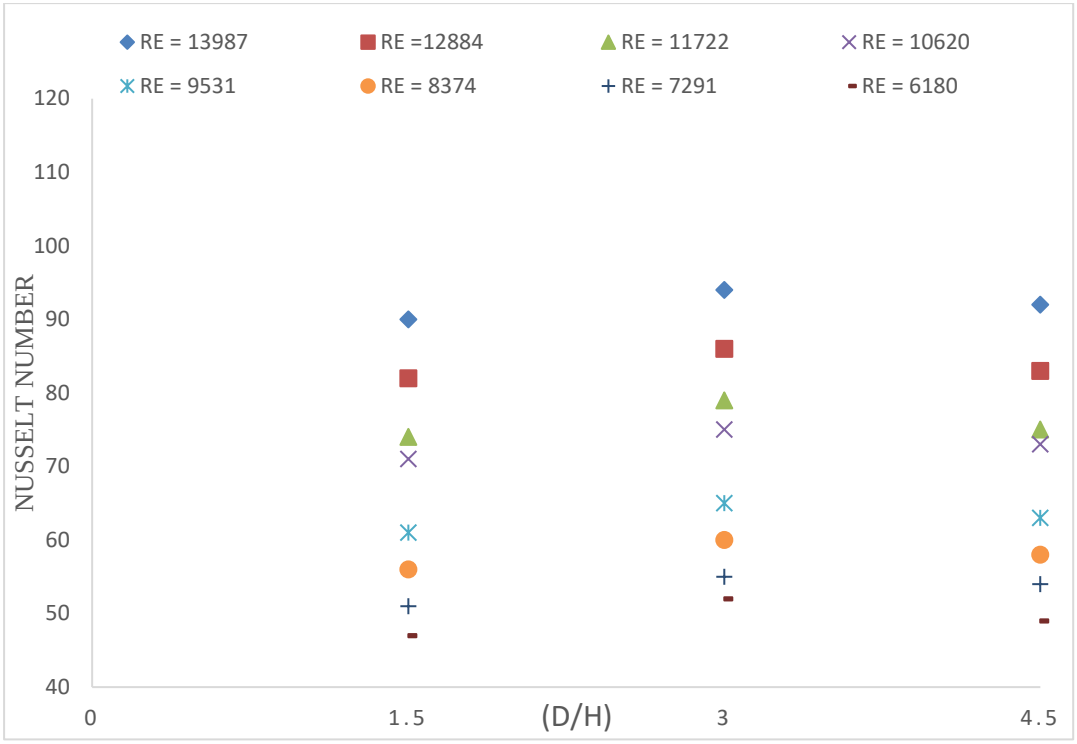

Figure: 5.6. Experimental values for Nusselt number Vs Dimple Diameter to Depth Ratio (D/H) with Reynolds number where (D = 6 mm)

5.3 The Effect of Dimple Diameter (D) and Dimple Diameter to Depth Ratio (D/H) on friction factor has been Studied Experimentally

General trend based on experimental analysis reflects a substantial improvement for dimple diameter (D) =2 for dimple diameter to depth ratio (D/H) =1.5, 3 and 4.5. In a sense, from smaller to larger dimple diameter to depth ratio (D/H) friction factor is improvising at a faster rate, whereas if dimple diameter to depth ratio (D/H) is further increased then there a downward trend. Minimum value of Friction factor is observed that for specific diameter with D = 2 mm. Initially it has a lower value compared to the same at dimple diameter to depth ratio (D/H) = 4.5. Subsequently as dimple diameter to depth ratio (D/H) is increased to 3 friction factor is increasing. Therefore, optimum value for lower friction factor is benchmarked for discussion at dimple diameter to depth ratio (D/H) = 4.5 for different diameter as it 0.1033 (for Reynolds number = 13987) and 0.1437 (for Reynolds number = 6180)

General trend based on experimental analysis reflects a substantial improvement for dimple diameter (D) =4 for dimple diameter to depth ratio (D/H) =1.5, 3 and 4.5. In a sense, from smaller to larger dimple diameter to depth ratio

(D/H) friction factor is improvising at a faster rate, whereas if dimple diameter to depth ratio (D/H) is further increased then there a downward trend. Minimum value of Friction factor is observed that for specific diameter with dimple diameter (D) = 4 mm. Initially it has a lower value compared to the same at dimple diameter to depth ratio (D/H) = 4.5. Subsequently as dimple diameter to depth ratio (D/H) is increased to 3 friction factor is increasing. Therefore, optimum value for lower friction factor is benchmarked for discussion at dimple diameter to depth ratio (D/H) = 4.5 for different diameter as it 0.1153 (for Reynolds number = 13987) and 0.1551 (for Reynolds number = 6180).

General trend based on experimental analysis reflects a substantial improvement for dimple diameter (D)=6 for dimple diameter to depth ratio (D/H) =1.5, 3 and 4.5. In a sense, from smaller to larger dimple diameter to depth ratio (D/H) friction factor is improvising at a faster rate, whereas if dimple diameter to depth ratio (D/H) is further increased then there a downward trend. Minimum value of Friction factor is observed that for specific diameter with dimple diameter (D) = 6 mm. Initially it has a lower value compared to the same at dimple diameter to depth ratio (D/H) = 4.5. Subsequently as dimple diameter to depth ratio (D/H) is increased to 3 friction factor is increasing. Therefore, optimum value for lower friction factor is benchmarked for discussion at dimple diameter to depth ratio (D/H) = 4.5 for different diameter as 0.1521 (for Reynolds number = 13987) and 0.1656 (for Reynolds number = 6180).

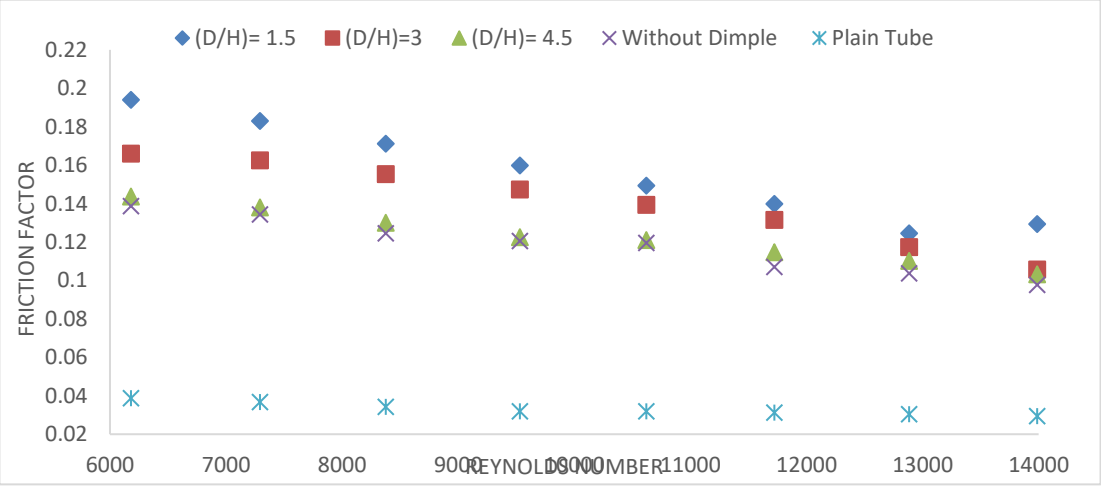

Figure:5.7. Experimental values for friction factor Vs Dimple Diameter to Depth ratio(D/H) where (D = 2 mm)

Table 5.4. Calculation table for plain twisted tape with configuration of dimple

Reynolds number	Experimental friction factor (D=2mm)				
	Plain tube	**Without dimple twisted tape**	**(D/H)=1.5**	**(D/H)=3**	**(D/H)=4.5**
13987	0.0294	0.0977	0.1294	0.1058	0.1033
12884	0.0304	0.1037	0.1245	0.1174	0.1102
11722	0.0313	0.1070	0.1398	0.1315	0.1148
10620	0.0319	0.1195	0.1493	0.1393	0.1211
9531	0.0320	0.1206	0.1598	0.1473	0.1226
8374	0.0343	0.1246	0.1712	0.1554	0.1301
7291	0.0367	0.1344	0.1830	0.1625	0.1380
6180	0.0388	0.1387	0.1940	0.1660	0.1437

Table 5.5. Calculation table for plain twisted tape with dimple configuration

Reynolds number	Experimental friction factor (D=4mm)				
	Plain tube	**Without dimple twisted tape**	**(D/H)=1.5**	**(D/H)=3**	**(D/H)=4.5**
13987	0.0294	0.0977	0.176526	0.140423	0.115341
12884	0.0304	0.1037	0.183871	0.145087	0.118756
11722	0.0313	0.1070	0.190882	0.148051	0.120101
10620	0.0319	0.1195	0.193132	0.149287	0.123321
9531	0.0320	0.1206	0.196742	0.159786	0.127871
8374	0.0343	0.1246	0.199321	0.171241	0.137023
7291	0.0367	0.1344	0.203465	0.183097	0.142361
6180	0.0388	0.1387	0.221814	0.194021	0.155189

Table 5.6. Calculation table for plain twisted tape with dimple configuration

Reynolds number	Experimental friction factor (D=6mm)				
	Plain tube	**Without dimple twisted tape**	**(D/H) =1.5**	**(D/H) =3**	**(D/H) =4.5**
13987	0.0294	0.0977	0.2112	0.1734	0.1521
12884	0.0304	0.1037	0.2207	0.1756	0.1517
11722	0.0313	0.1070	0.2247	0.1796	0.1475
10620	0.0319	0.1195	0.2267	0.1789	0.1689
9531	0.0320	0.1206	0.2456	0.1832	0.1588
8374	0.0343	0.1246	0.2412	0.1856	0.1708
7291	0.0367	0.1344	0.2368	0.2027	0.1621
6180	0.0388	0.1387	0.2716	0.2486	0.1656

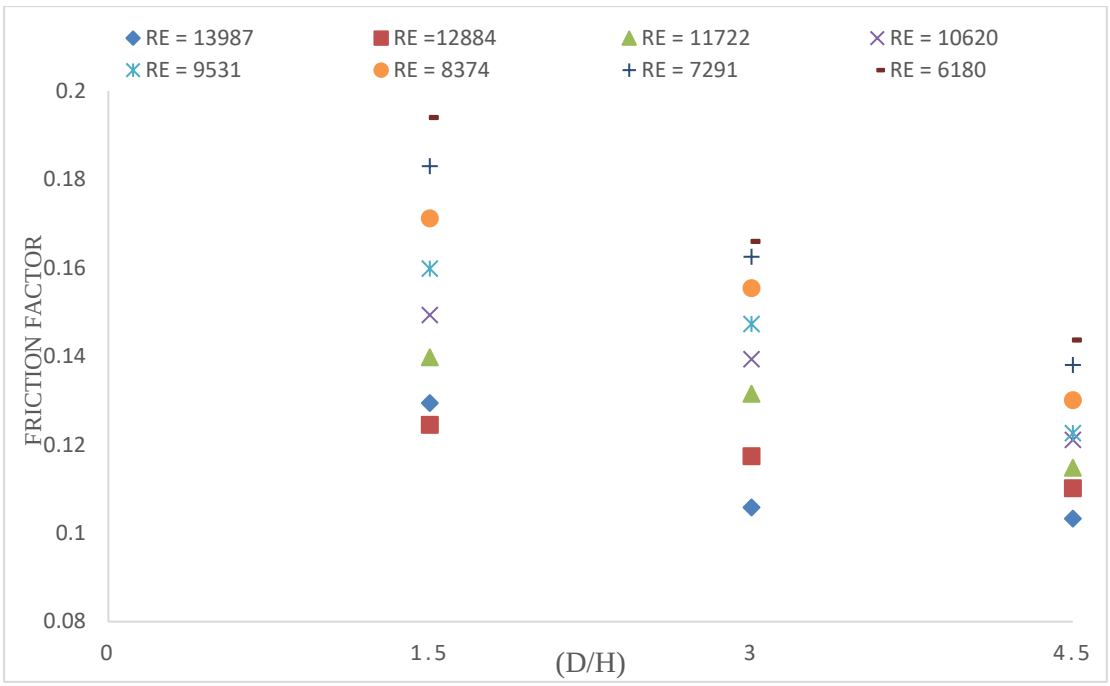

Figure: 5.8. Experimental values for friction factor Vs Dimple Diameter to Depth ratio(D/H) with Reynolds number where (D = 2 mm)

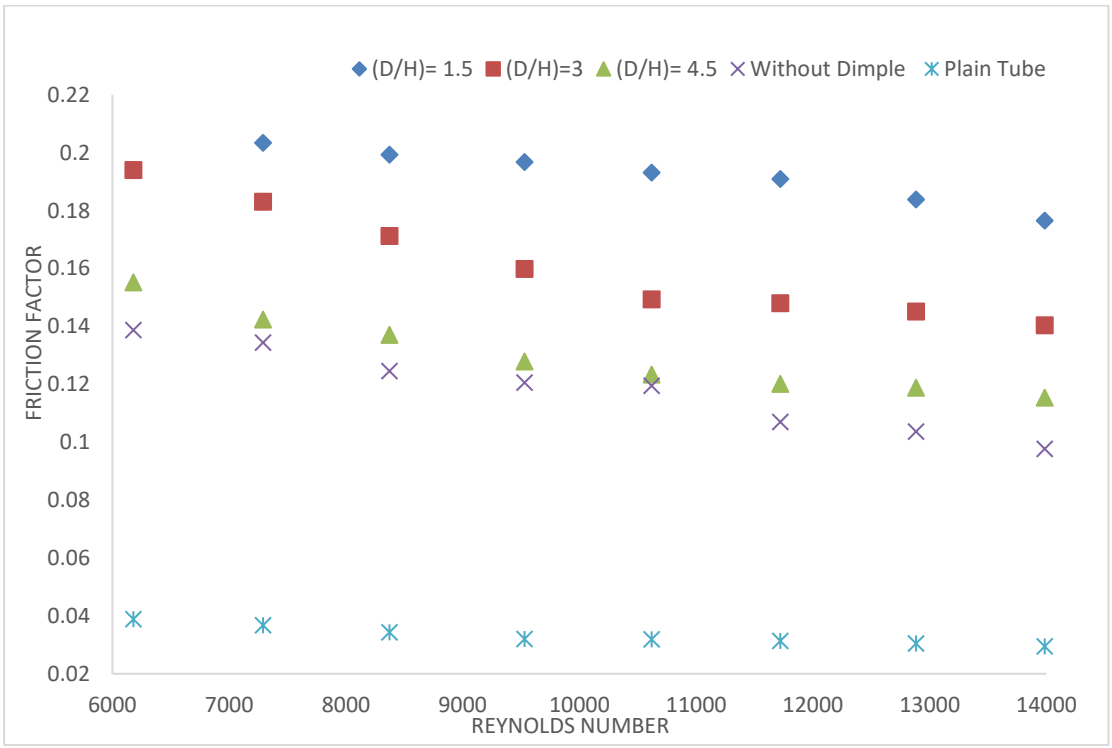

Figure:5.9 Experimental values for friction factor Vs Reynolds Number where (D = 4 mm)

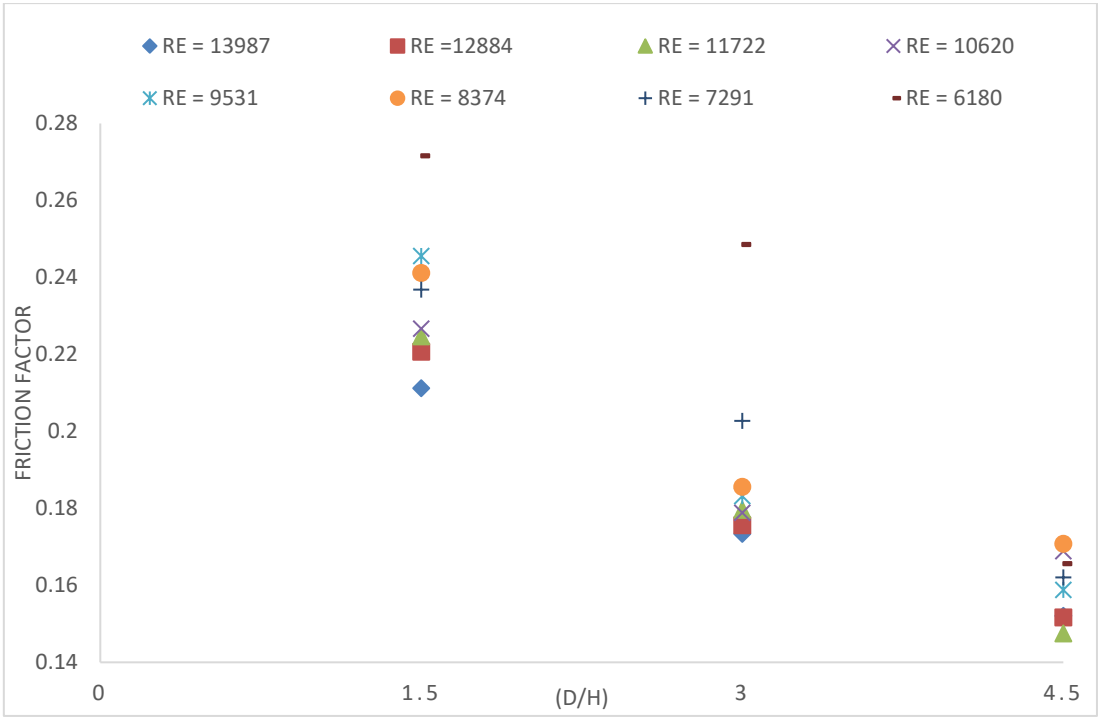

Figure: 5.10. Experimental values for friction factor Vs Dimple Diameter to Depth ratio(D/H) with Reynolds number where (D = 4 mm)

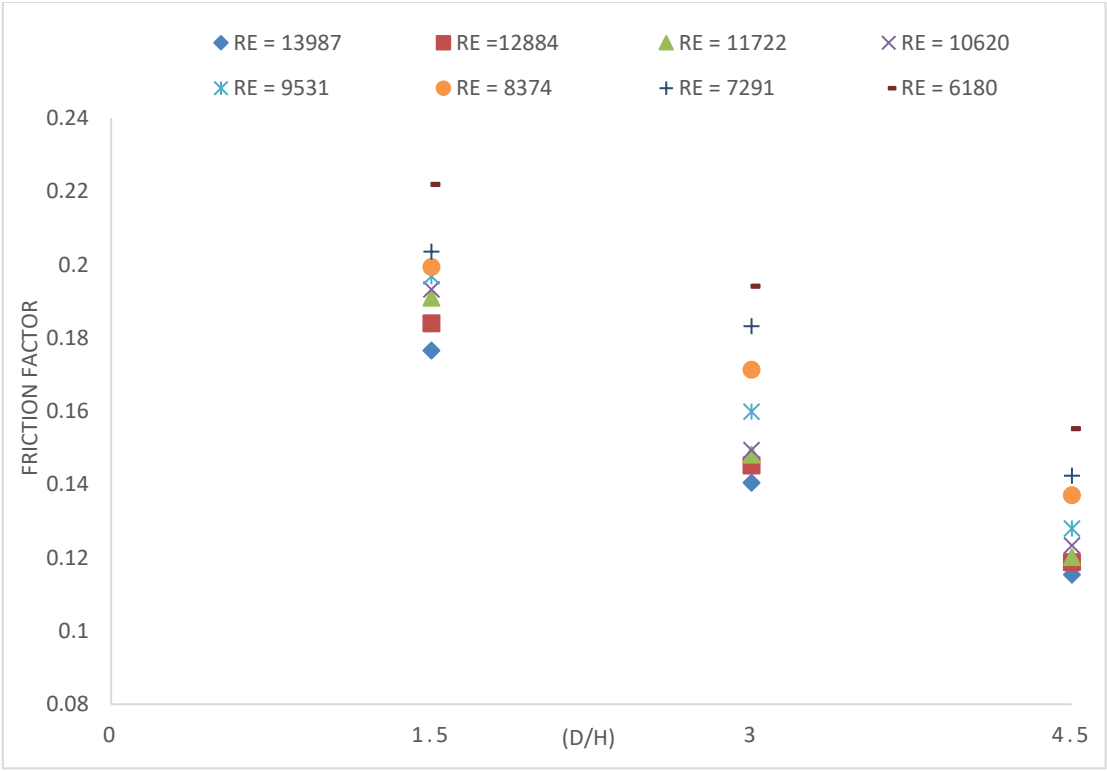

Figure: 5.11. Experimental values for friction factor Vs Dimple Diameter to Depth ratio(D/H) with Reynolds number where (D = 6 mm)

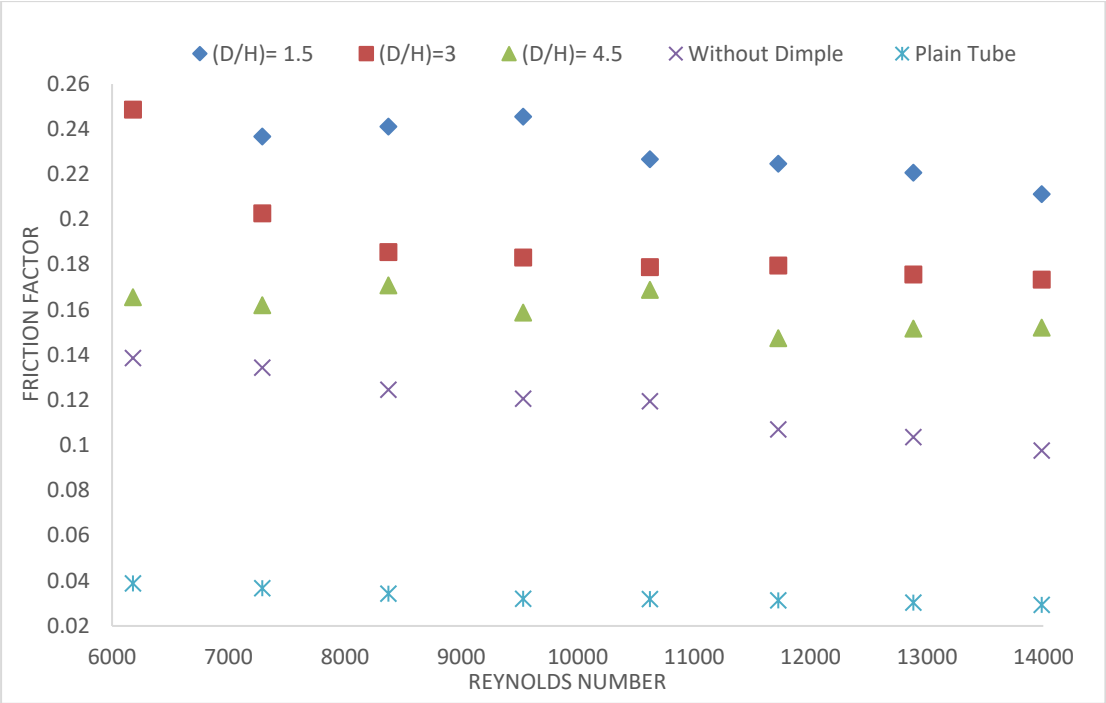

Figure:5.12. Experimental values for friction factor Vs Reynolds number where (D = 6 mm) with Dimple Diameter to Depth ratio(D/H)

Based on the given information, observed that friction factor decreases with increasing Reynolds number in every case, including tube without insert, twisted tape without dimple and twisted tape by dimple for dimple diameter (D)and dimple diameter to depth ratio (D/H) are 2, 4, 6 mm and 1.5, 3, 4.5 respectively is shown in Figures.5.7., 5.9 and 5.11 respectively. Additionally, it can be seen that the twisted tape with dimples have lower friction factors compared to twisted tape without dimples, indicating that presence of dimples on twisted tape surface can enhance flow characteristics and reduce frictional losses. Overall, results suggest that use of twisted tape with dimples can result in lower friction factor and hence, lower energy losses in fluid flow applications compared to conventional smooth tubes or twisted tape without dimples. However, it is important to consider the appropriate design parameters such as dimple diameter and dimple diameter to depth ratio (D/H) to optimize the flow characteristics and maximize energy savings. The friction factor is directly proportional to depth of dimple. It is observed that for all cases, friction factor reduces for dimple diameter to depth ratio (D/H) = 1.5 to 3 and also from 3 to 4.5 with 4.5

having minimum rate of friction factor. In calculation, friction factor falling from dimple diameter (D) = 6 to 4 mm with least rate is 2 mm. The rate of friction factor with dimple diameter (D) and dimple diameter to depth ratio (D/H) are 2 mm and 4.5 respectively is obtained 0.1033 (Reynolds number = 13987) and 0.1437 (Reynolds number = 6180).

The decrease in flow area of dimples leads to an increase in contact surface resistance, which results in an increase in friction factor figures. 5.8, 5.10 and 5.12 Tables 5.4, 5.5 and 5.6, shows. Additionally, decrease in friction factor from dimple diameter to depth ratio (D/H) =1.5 to 3 and 3.0 to 4.5 can be credited to modifications in secondary flow patterns and degree of flow obstruction caused by the dimples at different dimple diameter to depth ratio (D/H). The inverse proportionality between friction factor and dimple diameter to depth ratio (D/H) can also be explained by the increase in contact surface resistance with decreasing flow area.

Objective: 2

5.4 A Comprehensive Assessment of Dimpled twisted tape Involves Evaluating Its Performance Based on Various Parameters

The Nusselt number rises in twisted tape with dimple twisted tape insert with dimple diameter to depth ratio (D/H) of increased ranges 1.5 to 3, and then dropping from dimple diameter to depth ratio (D/H) =3 to 4.5 for all cases. This behaviour is because of changes in secondary flow patterns and degree of flow obstruction caused by dimples at different dimple diameter to depth ratio (D/H). The increase in Nusselt number with increasing dimple diameter to depth ratio (D/H) up to a certain point can be credited to improvement in secondary flow patterns and turbulence intensity induced by the dimples. As examined earlier, Nusselt number is observed highest (111 were Re = 13987 and 58 were Re = 6180) with dimple diameter (D) and dimple diameter to depth ratio (D/H) are 4 mm and 3 respectively is indicated fig.5.13. Maximum rate of Nusselt number is 1.81 times (Smallest) and 1.48 times (Extreme), 1.35 times (Smallest) 1.45, 48 times (Extreme), times larger values than Nusselt number for simple tube, dimpled twisted tape, without dimple twisted tape, with dimple diameter to depth ratio (D/H) = 3 and dimple diameter (D) = 4 mm respectively. Whereas dimple diameter with twisted tape is 2 mm is observed 1.08–1.2

where dimple diameter to depth ratio (D/H) is 4.5, as well 1.09–1.2 where dimple diameter to depth ratio (D/H) is 1.5 as well 1.06–1.15 where dimple diameter to depth ratio (D/H) is 3 rates correspondingly more than Nusselt number for tube twisted tape without insert. Conversely, Nusselt number for dimple diameter with twisted tape 4 mm is found to be 1.20–1.37 where dimple diameter to depth ratio (D/H) is 4.5, as well 1.35–1.45 where dimple diameter to depth ratio (D/H) is 3, as well 1.19–1.35 where dimple diameter to depth ratio (D/H) is 1.5 rates respectively, while twisted tape with dimple diameter (D) = 6 mm is deliberate to be 1.12–1.22 where dimple diameter to depth ratio (D/H) is 4.5, as well 1.14–1.30 where dimple diameter to depth ratio (D/H) is 3 as well 1.09–1.17 where dimple diameter to depth ratio (D/H) is 1.5 rates respectively more than Nusselt number for plain pipe.

The experimental data shows that the highest Nusselt number is found for dimple diameter (D) and dimple diameter to depth ratio (D/H) is 4 mm and 3. The dimple with these dimensions induces maximum rise in secondary flow compared to plain twisted tape and twisted tape with other configurations used in the experiments. Effect of secondary flow on heat transfer depends on various parameters such as the flow rate, geometry of surface, fluid properties, and boundary conditions. Fig. 5.14, 5.15 and 5.16 shows variation of Nusselt number based on dimple diameter (D) and dimple diameter to depth ratio (D/H) of Reynolds number. Observe Nusselt number raising where D is 2 to 4 mm and then falling where dimple diameter (D) is 4 to 6 mm. Moreover, maximum Nusselt number was initiate where dimple diameter (D) is 4 mm with respect to other two (2) dimple diameter (D) in value of Reynolds number. which means that dimple diameter (D) = 4 mm and dimple diameter to depth ratio (D/H) = 3 provides most efficient heat transfer performance among the tested configurations.

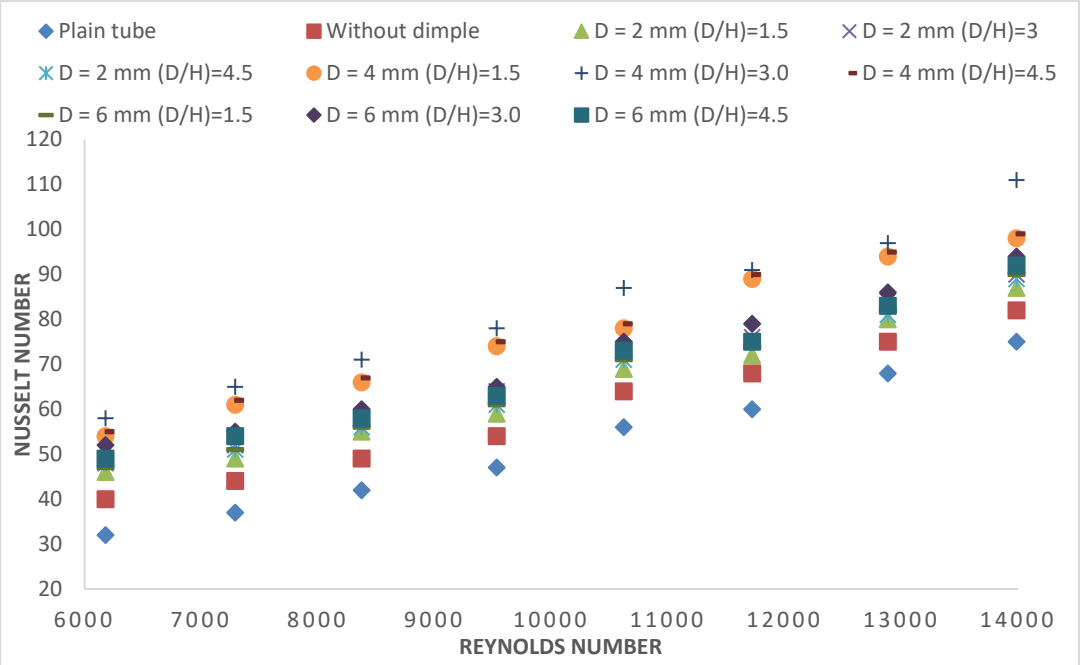

Figure: 5.13. Experimental values of Nusselt number Vs Reynolds number with Dimple Diameter to Depth Ratio (D/H) of Dimple Diameter

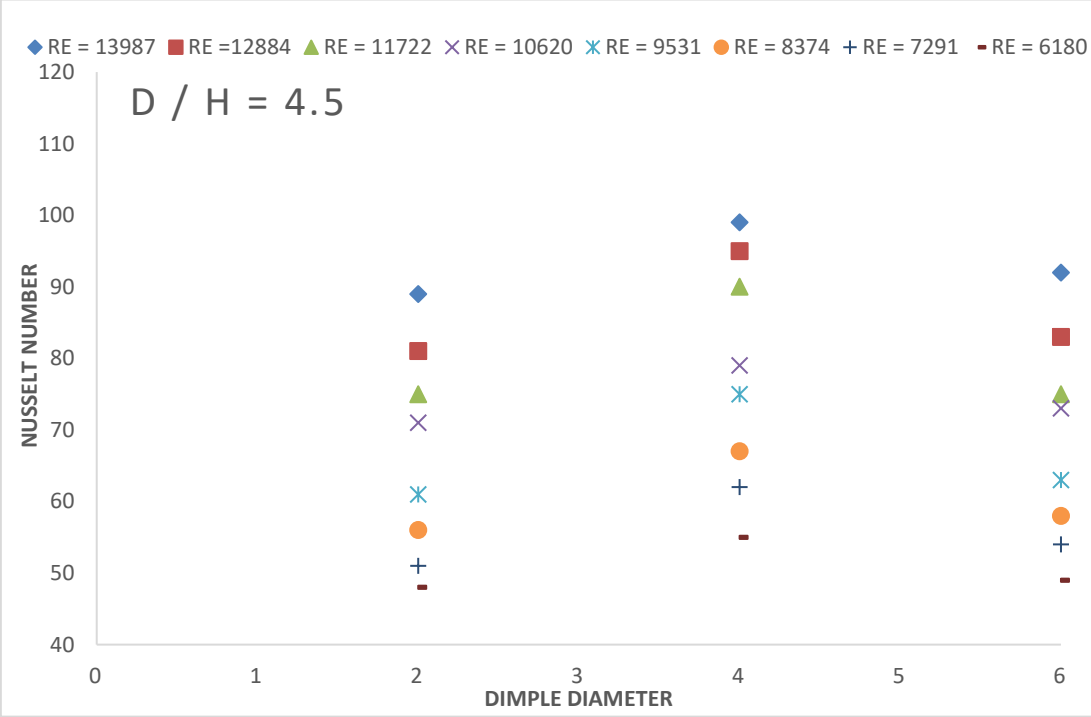

Fig.5.14 Nusselt number with Dimple diameter at various Reynolds number of Dimple Diameter to Depth Ratio (D/H) 4.5

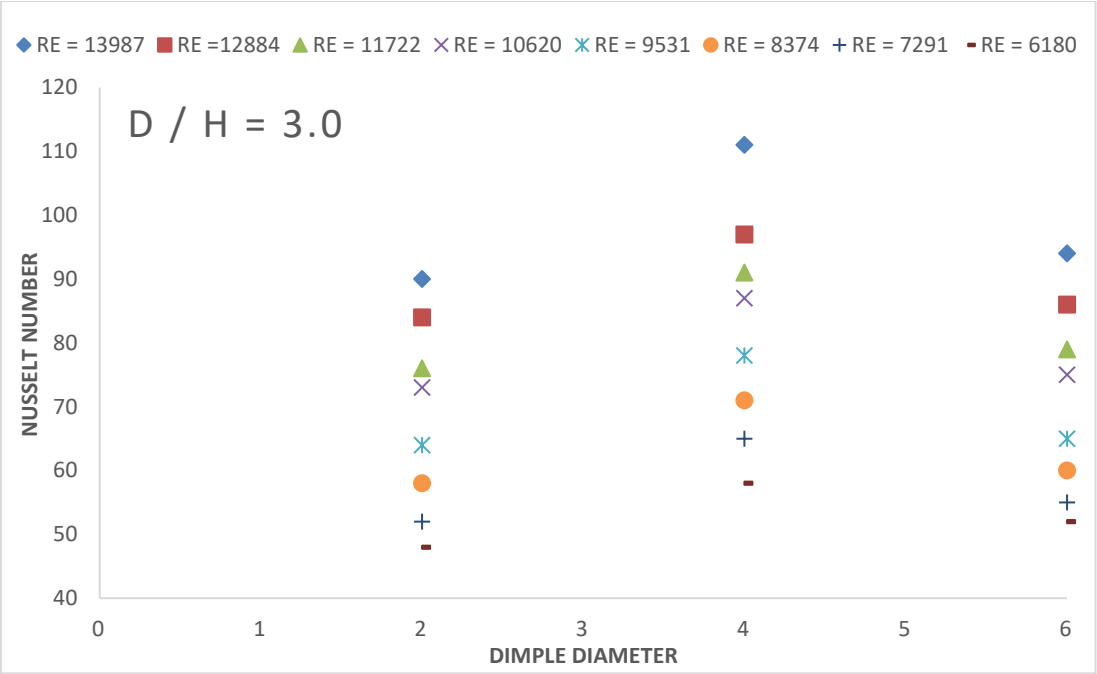

Fig.5.15 Nusselt number with Dimple diameter at various Reynolds number of Dimple Diameter to Depth Ratio (D/H) 3.0

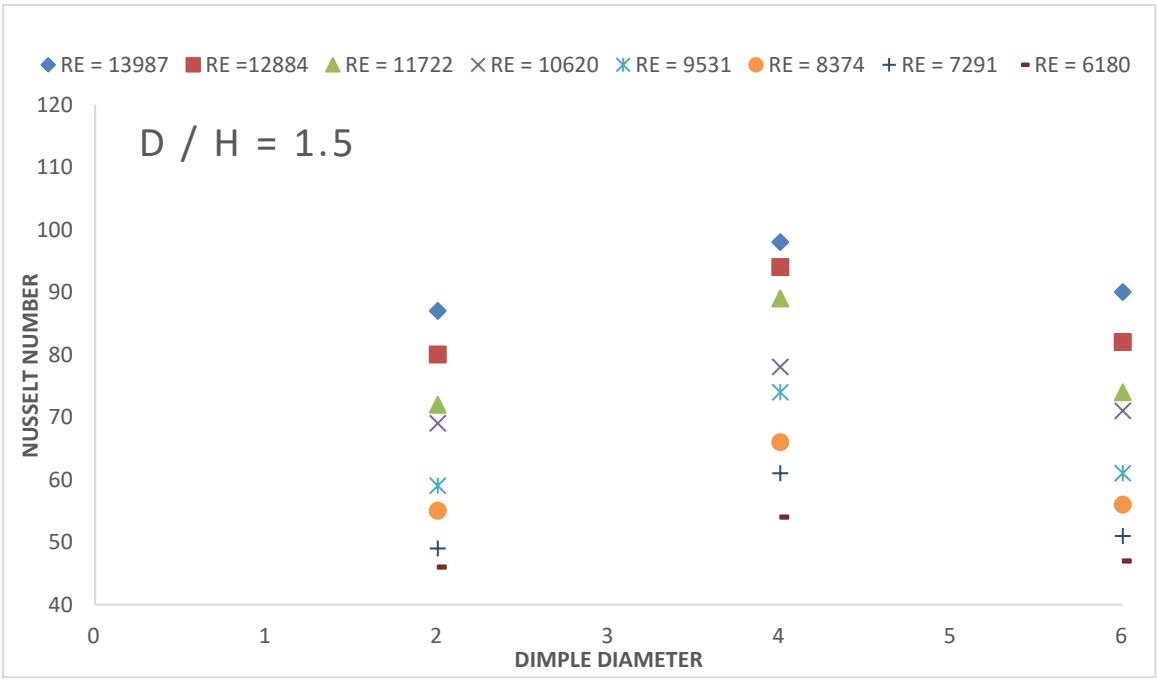

Fig.5.16 Nusselt number with Dimple diameter at various Reynolds number of Dimple Diameter to Depth Ratio (D/H) 1.5

The friction factor is inversely proportionate to dimple diameter (D) as well

dimple diameter to depth ratio (D/H)is directly proportionate to the dimple diameter (D) value of Reynolds number. This implies that friction factor decreases with increase in dimple diameter (D) in twisted tape and decreases with increase depth of dimple as well. The reduction in friction factor can be attributed to concavity of dimple, which reduces flow passage and increases contact surface resistance. Consequently, plain tube has minimum value of friction factor within examined dimple diameter (D) and dimple diameter to depth ratio (D/H) of dimple twisted tape, friction factor was identified lowest for twisted tape as dimple diameter (D) and dimple diameter to depth ratio (D/H) is 4 mm 4.5 respectively. Rate of friction factor aimed at plain tube is establish on 0.1033 (Reynolds number = 13987) and 0.1437 (Reynolds number = 6180) friction factor of without dimple twisted tape was 1.18–1.05 rates whereas twisted tape with dimple diameter (D) = 2 mm is 1.05–1.03 where dimple diameter to depth ratio (D/H) is 4.5, as well 1.08–1.19 where dimple diameter to depth ratio (D/H) is 3 and 1.32–1.39 where dimple diameter to depth ratio (D/H) is 1.5 rates more than friction factor is without twisted tape inserts. At next indicator, friction factor is dimple diameter with twisted tape dimple diameter (D) = 4 mm is found to be 1.18–1.05 where dimple diameter to depth ratio (D/H) is 4.5, as well 1.43–1.36 where dimple diameter to depth ratio (D/H) is 3 and 1.80–1.51 where dimple diameter to depth ratio (D/H) is 1.5 rates whereas dimple diameter (D) = 6 mm is measured to be 1.55–1.19 where dimple diameter to depth ratio (D/H) is 4.5, as well 1.77–1.70 where D/H is 3 and 2.16–1.95 where dimple diameter to depth ratio (D/H) is 1.5 rates correspondingly larger friction factor aimed at plain twisted tape. The friction factor increases along increasing dimple diameter (D) as well decreasing dimple diameter to depth ratio (D/H) where all ranges for Reynolds number. This means that friction factor is directly proportionate to dimple diameter (D) and inversely proportionate dimple diameter to depth ratio (D/H) is depicted in fig. 5.17. Figures.5.18, 5.19 and 5.20 shows the variation of friction factor indicates that there is an increase in friction factor as dimple diameter (D) rises from 2 to 4 mm, and another increase in friction factor as dimple diameter (D) further rises from 4 to 6 mm. For all values of Reynolds number dimple diameter (D) of 2 mm had less value of friction factor in comparison to the other two (2) dimple diameter (D).

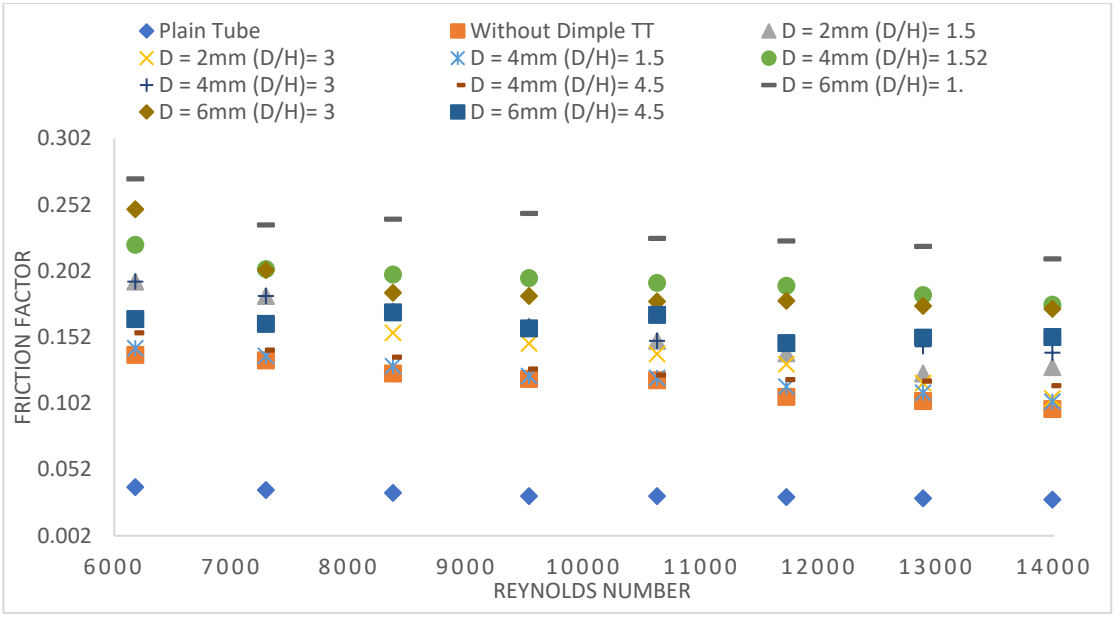

Fig: 5.17. Experimental values of friction factor Vs Reynolds number for Dimple Diameter to Depth Ratio (D/H) as well Dimple Diameter

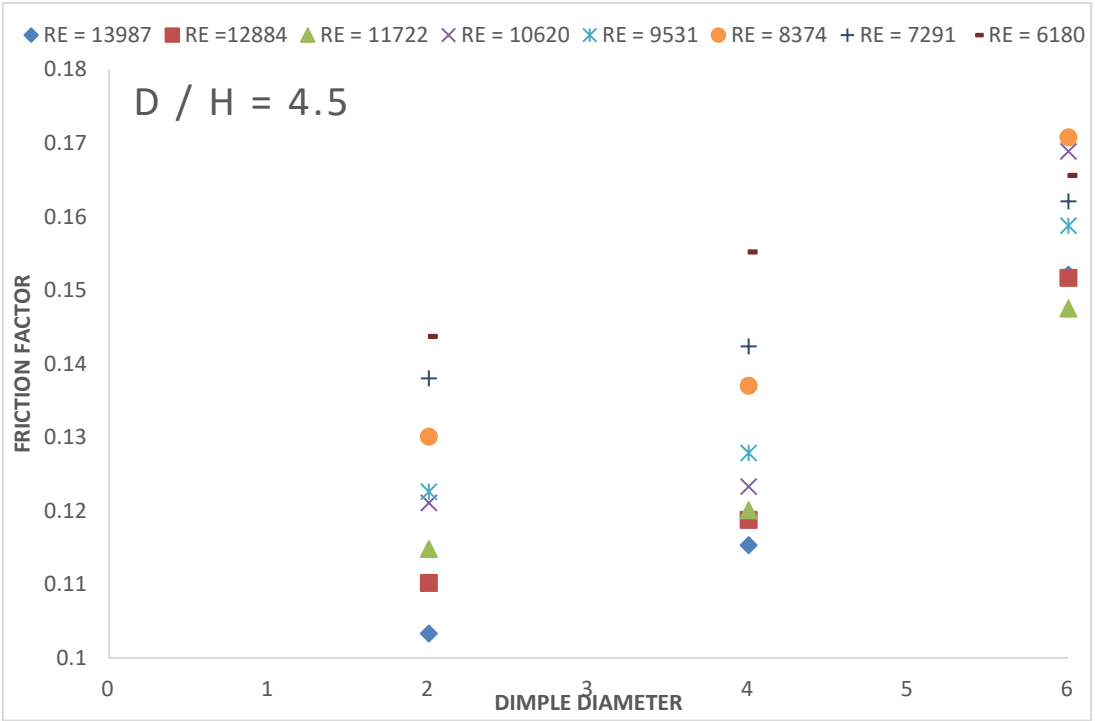

Fig.5.18 Friction Factor with Dimple diameter at various Reynolds number for Dimple Diameter to Depth Ratio (D/H) is 4.5

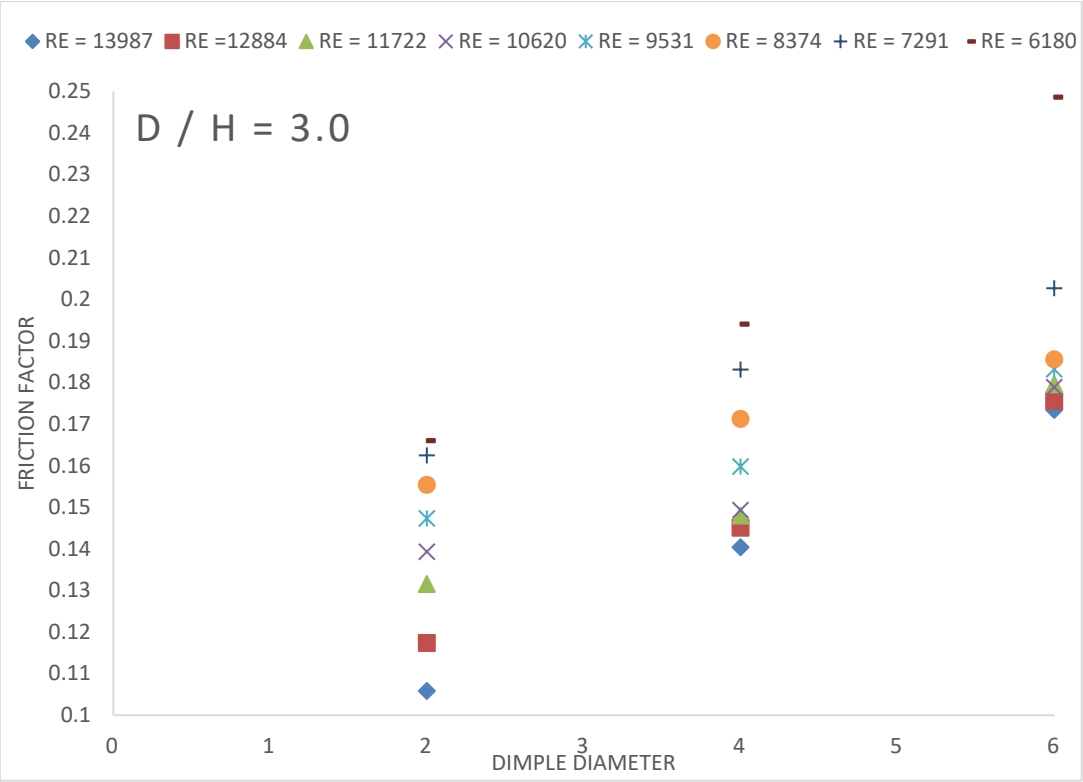

Fig.5.19 Friction Factor with Dimple diameter at various Reynolds number for Dimple Diameter to Depth Ratio (D/H) is 3

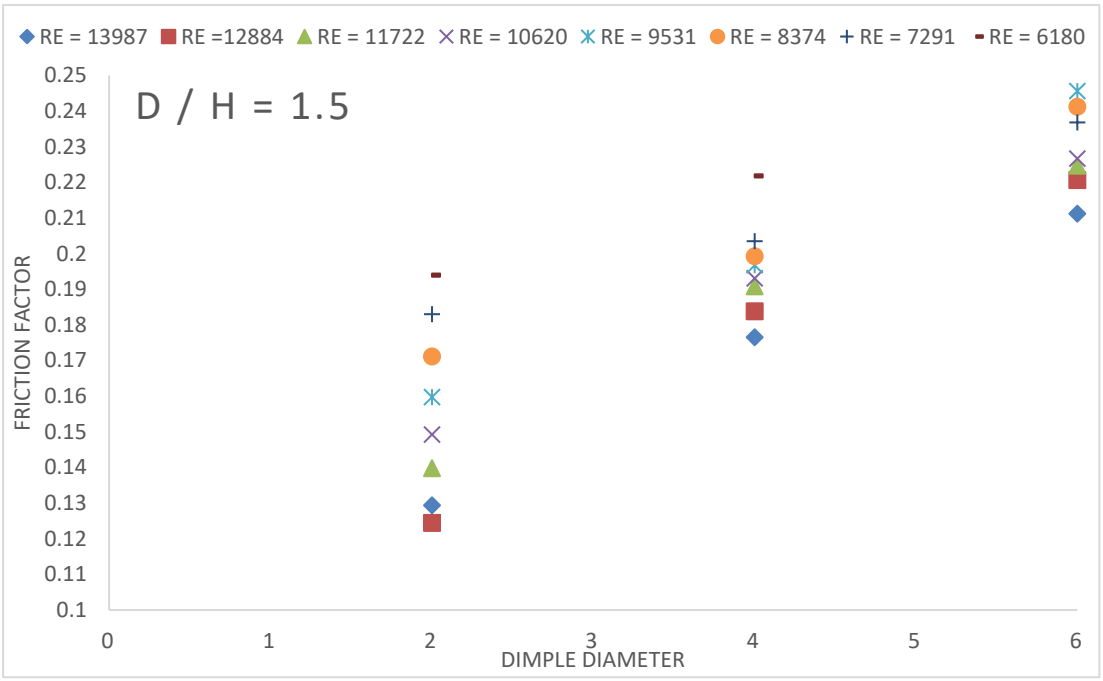

Fig.5.20 Friction Factor with Dimple diameter at various Reynolds number for Dimple Diameter to Depth Ratio (D/H) is 1.5

Objective: 3

5.5 To evaluate Performance Evaluation Criteria, in order to balance Ratio of Nusselt number as well friction factor with twisted tape inserts to plain twisted tape arrangement.

Ratio of Nusselt number in improved pipes to friction factor in enhanced tubes to plain tubes is the standard performance evaluation criteria. Ratio is main factor and reveals importance of heat transfer to pressure drop in Heat exchangers. It can be referred from figure 5.21 and Table. 5.7, that performance evaluation criteria decreases and as turbulence intensity increases, advantage of using twisted tape decreases. It can also observe that for a fixed value of Reynolds number, performance evaluation criteria is higher for higher dimple diameter to depth ratio (D/H), which indicates that twisted tape as well as higher dimple diameter to depth ratio (D/H) provides better heat transfer performance. Performance evaluation criteria is found Maximum at dimple diameter (D) = 4 mm on dimple diameter to depth ratio (D/H) = 4.5 for range of Reynolds number studied, with values 1.08796 (Reynolds number = 6180) as well 0.84075 (Reynolds number = 13987), as well 1.13-1.32 rates on dimple diameter to depth ratio (D/H) = 4.5, 1.19-1.30 times on dimple diameter to depth ratio (D/H) = 3, then 1.00-1.15 times on dimple diameter to depth ratio (D/H) = 1.5 twisted tape without dimples, respectively. As opposed to that, extreme rate of performance evaluation criteria is 1.05–1.18 for (dimple diameter to depth ratio (D/H) = 4.5), 1.06–1.13 on (dimple diameter to depth ratio (D/H) = 3), 1.00–1.03 on (dimple diameter to depth ratio (D/H) = 1.5) times more for dimple diameter (D) = 2 mm with dimple whereas it is 1.00–1.15 on (dimple diameter to depth ratio (D/H) = 4.5), 1.00–1.07 on (dimple diameter to depth ratio (D/H) = 3), 1.00–1.02 on (dimple diameter to depth ratio (D/H) = 1.5) times more for dimple diameter (D) = 6 mm correspondingly. Fig.5.22, 5.23 and 5.24 show the difference of performance evaluation criteria as a meaning of dimple diameter to depth ratio (D/H) of stable rate of dimple diameter (D) at 8 dissimilar Reynolds number rates. Detected those improvements from performance evaluation criteria on dimple diameter (D) = 2 to 4 mm as well falling from 4 to 6 mm and extreme rate for performance evaluation criteria is introduced for all Reynolds number values at dimple diameter (D) =4 mm corresponding to other

two (2) Dimeter meter in exclusively cases. Observed from results that performance evaluation criteria reductions with an rise in Reynolds number for all cases. This suggests that as Reynolds number increases, effect of friction factor becomes more significant compared to effect of Nusselt number. In other words, for range of Reynolds number studied, optimal configuration for double pipe heat exchanger with twisted tape inserts is a dimple diameter (D) of 4 mm and dimple diameter to depth ratio (D/H) of 4.5. This configuration resulted in highest value of performance evaluation criteria, indicating that enhancement in heat transfer (as measured by Nusselt number) is predominant over increase in pressure drop (as measured by friction factor). addition, it is found performance evaluation criteria where dimple diameter (D) and dimple diameter to depth ratio (D/H) is 4 mm and 4.5 respectively, is higher related to other two (2) dimple diameter (D) and dimple diameter to depth ratio (D/H) values for Reynolds number. This suggests that configuration provide best overall performance in terms of heat transfer enhancement and pressure drop penalty among tested.

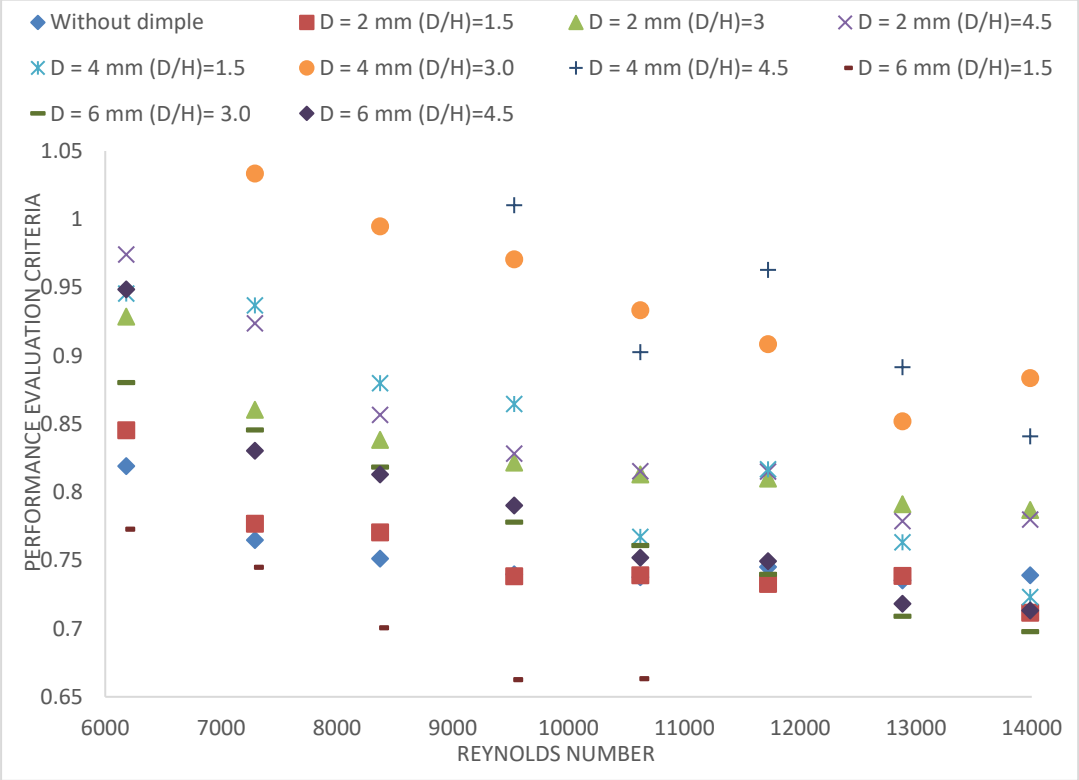

Fig: 5.21. Experimental values of Performance Evaluation Criteria Vs Reynolds number with Dimple Diameter to Depth Ratio (D/H) as well Dimple Diameter

Table 5.7. Calculation table for Performance evaluation criteria (PEC) with dimple configuration

Reynolds number	PEC									
	D =2mm			D =4mm			D =6mm			Without dimple twisted tape
	D/H=4.5	D/H=3	D/H=1.5	D/H=4.5	D/H=3	D/H=1.5	D/H=4.5	D/H=3	D/H=1.5	
13987	0.77991	0.78686	0.71164	0.84075	0.88358	0.72315	0.71317	0.69773	0.63138	0.73900
12884	0.77875	0.79116	0.73863	0.89154	0.85182	0.76323	0.71806	0.70898	0.62631	0.73531
11722	0.81499	0.80993	0.73269	0.96278	0.90839	0.81674	0.74943	0.73977	0.64339	0.74513
10620	0.81520	0.81304	0.73912	0.90266	0.93328	0.76728	0.75205	0.76076	0.66335	0.73768
9531	0.82831	0.82172	0.73829	1.01017	0.97058	0.86467	0.79009	0.77799	0.66247	0.73964
8374	0.85659	0.83837	0.77042	1.07045	0.99473	0.87979	0.81302	0.81823	0.70049	0.75132
7291	0.92374	0.86039	0.77690	1.08400	1.03355	0.93686	0.83036	0.84560	0.74491	0.76483
6180	0.97411	0.92872	0.84523	1.08796	1.06580	0.94541	0.94859	0.88038	0.77276	0.81897

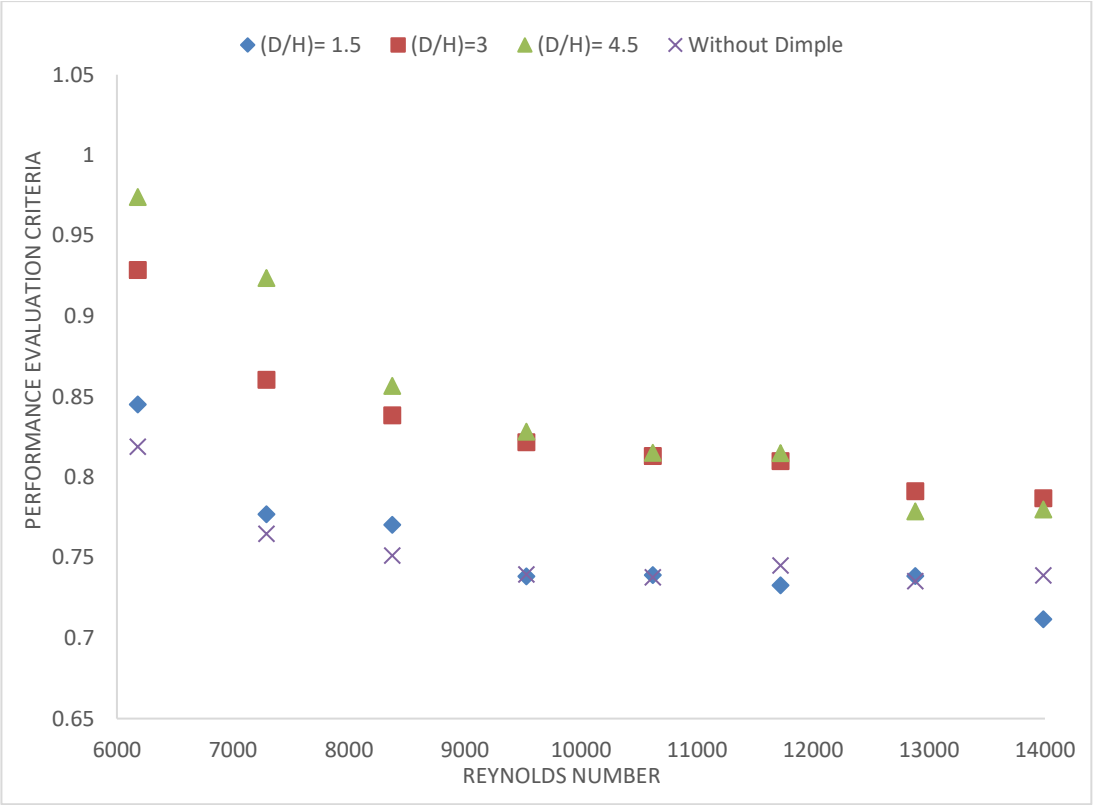

Fig. 5.22. Experimental values of Performance Evaluation Criteria Vs Reynolds number of D = 2 mm and various rate of Dimple Diameter to Depth Ratio (D/H)

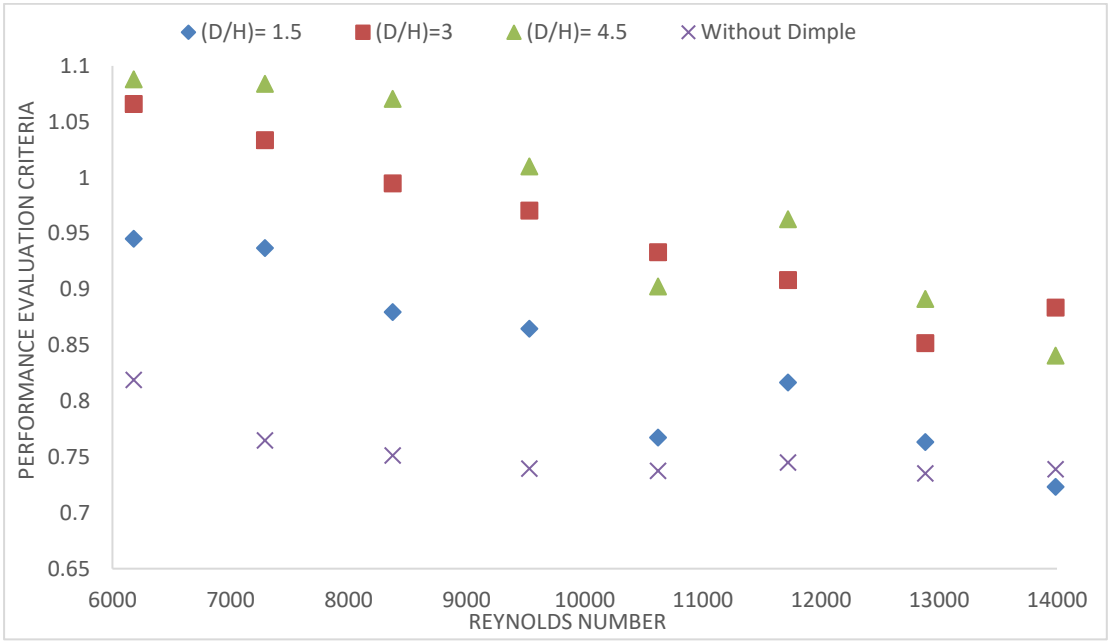

Fig. 5.23. Experimental values of Performance Evaluation Criteria Vs Reynolds number of D = 4 mm and various rate of Dimple Diameter to Depth Ratio (D/H)

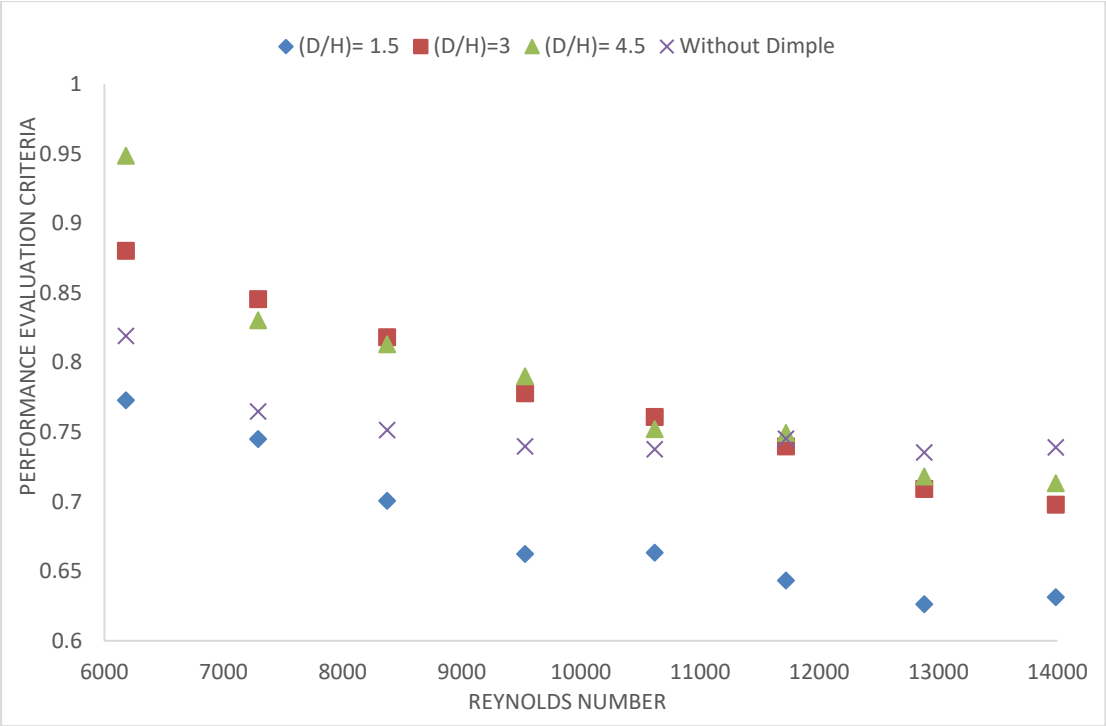

Fig. 5.24. Experimental values of Performance Evaluation Criteria Vs Reynolds number where (D = 6 mm) various rate of Dimple Diameter to Depth Ratio (D/H)

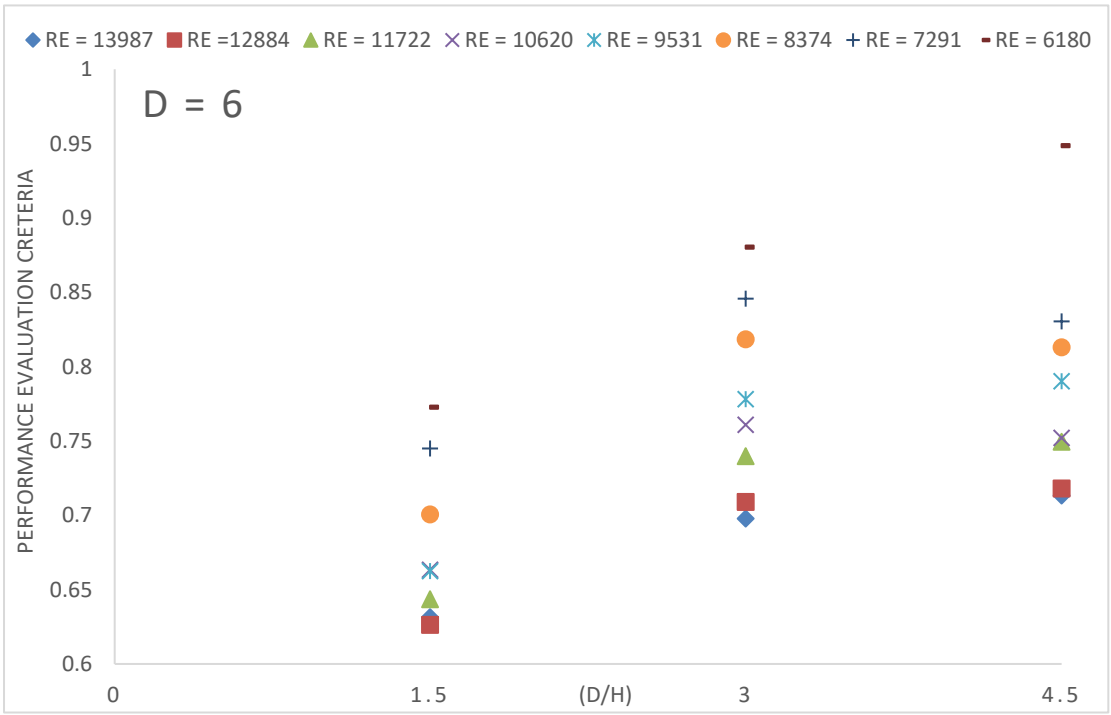

Fig. 5.25. Experimental values of Performance Evaluation Criteria Vs Dimple Diameter to Depth Ratio (D/H) where (D = 6 mm) with Reynolds number

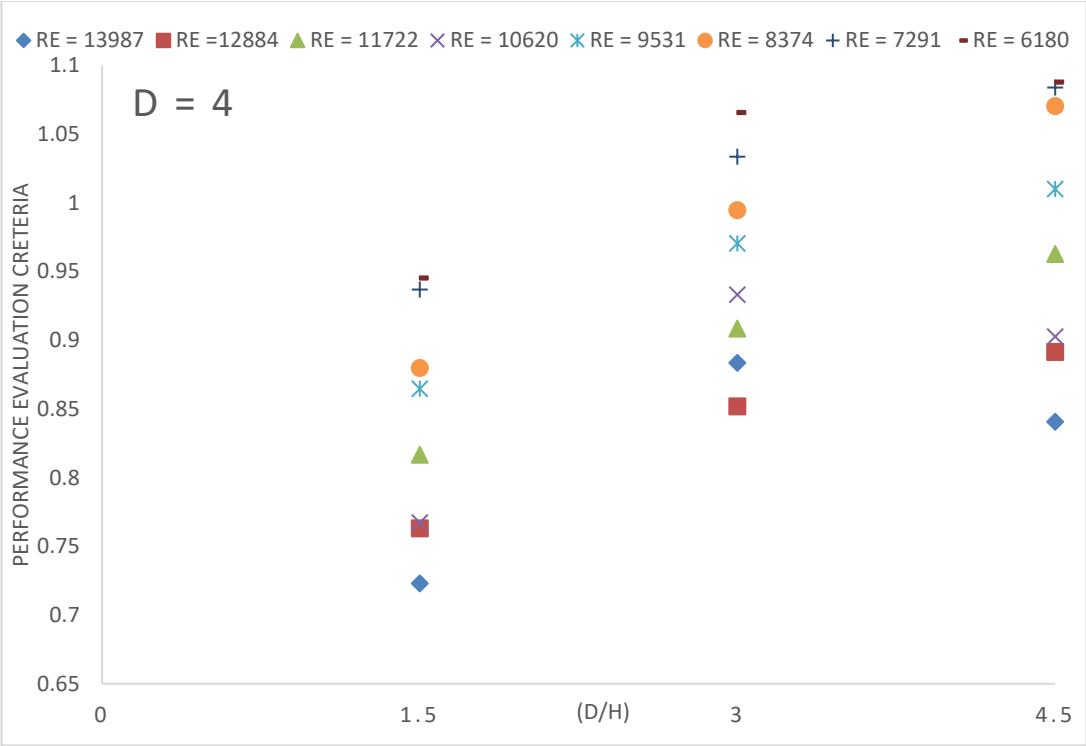

Fig. 5.26. Experimental values of Performance Evaluation Criteria Vs Dimple Diameter to Depth Ratio (D/H) where (D = 4 mm) with Reynolds number

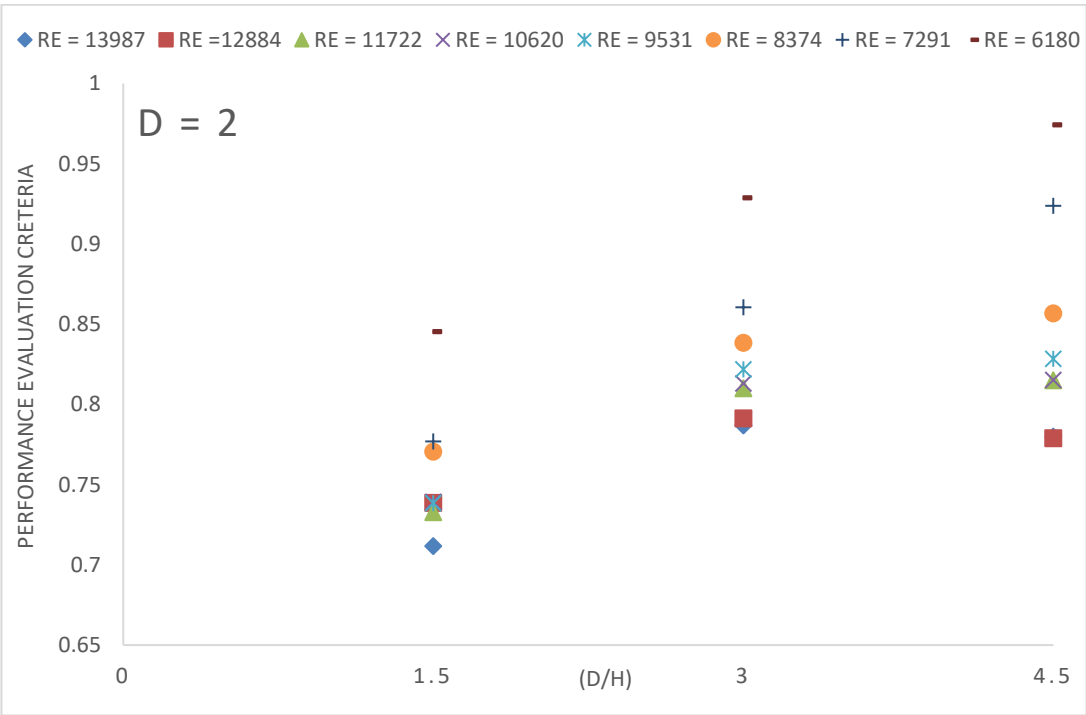

Fig. 5.27. Experimental values of Performance Evaluation Criteria Vs Dimple Diameter to Depth Ratio (D/H) where (D = 2 mm) with Reynolds number

Fig.5.25, 5.26 and 5.27 shows change of performance evaluation criteria, and it provides of dimple diameter (D) to dimple diameter to depth ratio (D/H) for a rigid value of dimple diameter (D) at eight other values of Reynolds number. The graph likely demonstrates how the performance evaluation criteria changes as the dimple diameter to depth ratio (D/H) increases or decreases at various Reynolds number. Performance evaluation criteria rises from dimple diameter to depth ratio (D/H) = 1.5 to 4.5, and then falling from dimple diameter to depth ratio (D/H) = 4.5 to 3. The maximum performance evaluation criteria is observed where dimple diameter to depth ratio (D/H) is 3 then to other two dimple diameter to depth ratio (D/H) values Reynolds number studied. Moreover, performance evaluation criteria value is found to be highest at a dimple diameter (D) of 4 mm and a dimple diameter to depth ratio (D/H) of 4.5 compared to the other two (2) dimple diameter (D) and dimple diameter to depth ratio (D/H) at all Reynolds number studied.

CHAPTER - 6

DEVELOPMENT OF CORRELATIONS FOR NUSSELT NUMBER AND FRICTION FACTOR

Objective: 4

6.1 Development of Correlation

The provide information on heat transfer enhancement and pressure drop, respectively. Correlations are useful in predicting performance of twisted tape with dimples under different operating conditions and geometrical parameters without the need for expensive and time-consuming experimentation. This can aid in design and optimization of Heat exchangers, heat transfer systems, and other applications that involve fluid flow and heat transfer. Functional relationship for Nusselt number and friction factor with working parameters such as Reynolds number, dimple diameter (D) and dimple diameter to depth ratio (D/H).

$$N_u = Nu\left\{Re, D, \frac{D}{H}\right\} \tag{6.1}$$

$$f = f\left\{Re, D, \frac{D}{H}\right\} \tag{6.2}$$

6.2 Correlation for Nusselt Number [4,14]

From the graph in figure. 6.1, observed linear relation with Nusselt number and Reynolds number for the range of parameters studied in experiment.

Regression analysis was performed on the plotted data of Nusselt number against Reynolds number for regulate mean slope for lines. Logarithmic values for Nusselt number “ln (Nu)” as well Reynolds number “ln (Re)” were used for curve fitting and it was observed that data varies linearly, as shown in fig. 6.1.

$$N_u = \mathrm{A}_0 Re^{0.7716} \tag{6.3}$$

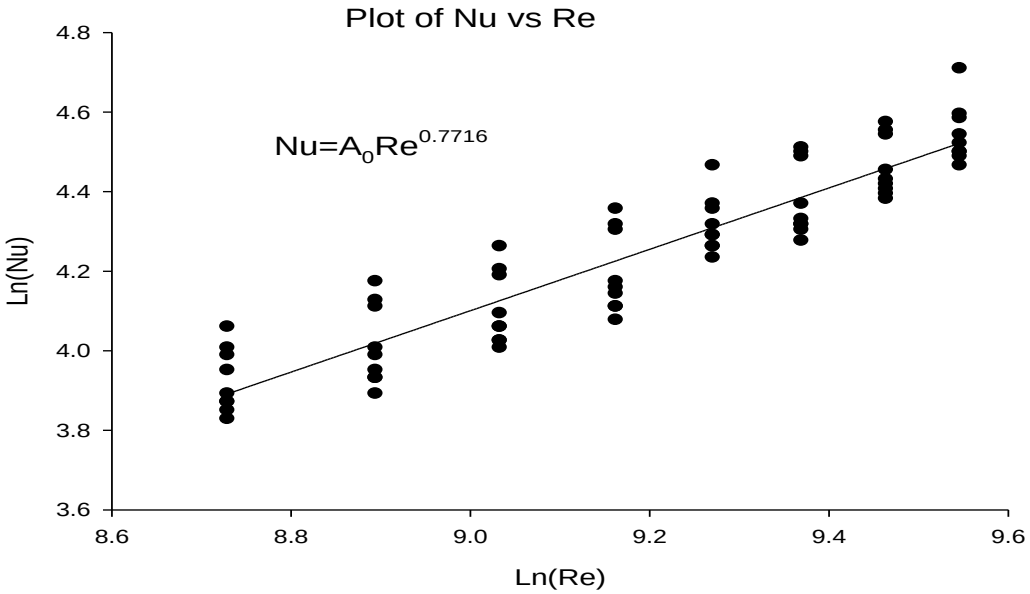

Fig. 6.1. Plot of $\log_e$ (Nusselt number) vs $\log_e$ (Reynolds number) for the experimental data

The coefficient A_0 in the generated equation (6.3) is a function of parameters. Now, the variation of $ln\frac{Nu}{Re^{0.7716}}$ function which is lnB_0 with the logarithmic value for dimple diameter to depth ratio (D/H) i.e.,ln(D/H) was plotted by fitting in second order quadratic equation as shown in Figures.6.2 and 6.3 the regression yield the following equation:

$$ln\left(\frac{Nu}{Re^{0.7716}}\right) = C_0\left(\frac{D}{H}\right)^{0.3141} Exp\left(-0.164\left(\left(ln\left(\frac{D}{H}\right)\right)^2\right)\right) \quad (6.4)$$

Value of the final constant can be used to write the final correlation i.e., C_0 is

$$N_u = 0.04632 \times Re^{0.7716}\left(\frac{D}{H}\right)^{0.3141} Exp\left(-0.164\left(ln\left(\frac{D}{H}\right)^2\right)\right) \quad (6.5)$$

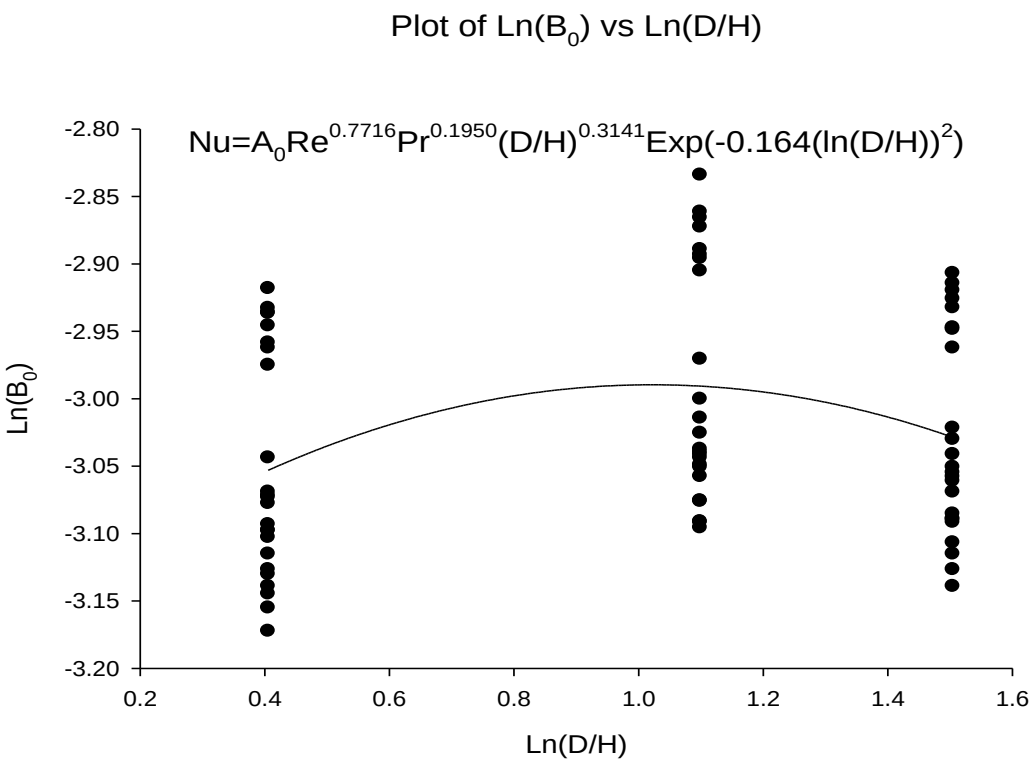

Fig. 6.2. Deviation for coefficient B_o and Dimple Diameter to Depth Ratio (D/H)

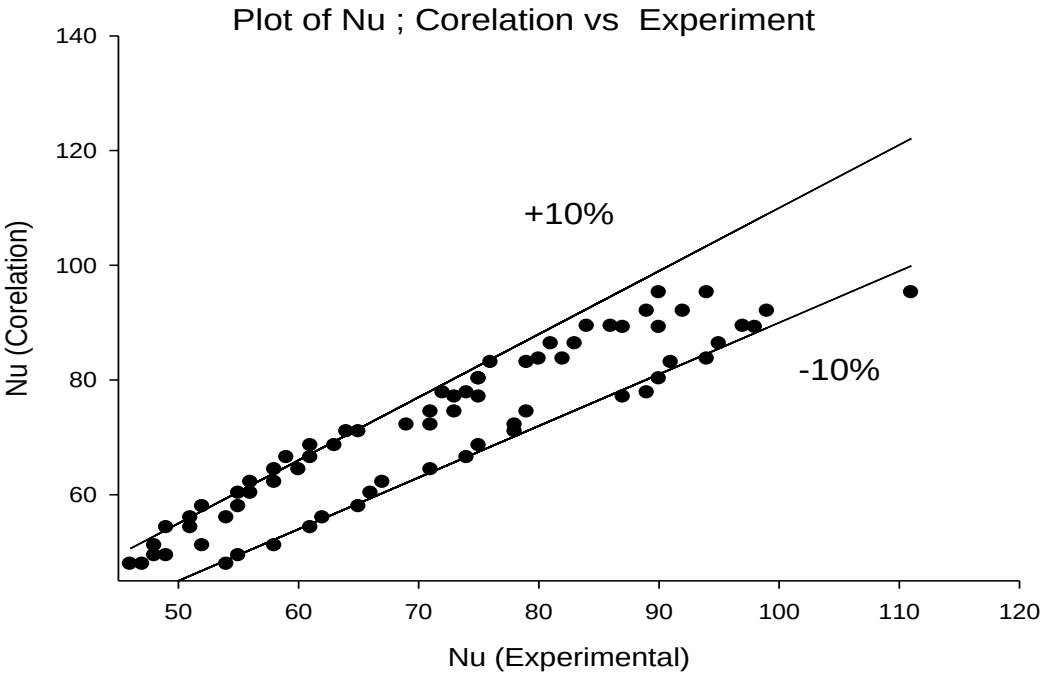

Fig. 6.3. Deviation for correlation and Nusselt number experimental

6.3 Experimental data collected for friction factor has been analyzed to obtain statistical correlations

To obtain geometric correlations for friction factor for experimentally attained data, regression analysis was performed in this section. The operating correlation between friction factor and Reynolds number was obtained by plotting values of $\log_e(f)$ and $\log_e(Re)$ for all data points as shown in figure 6.4.

Linear regression studied and curve fitting results in a straight line throughout the points:

$$f = A_1 Re^{-0.3583} \quad (6.6)$$

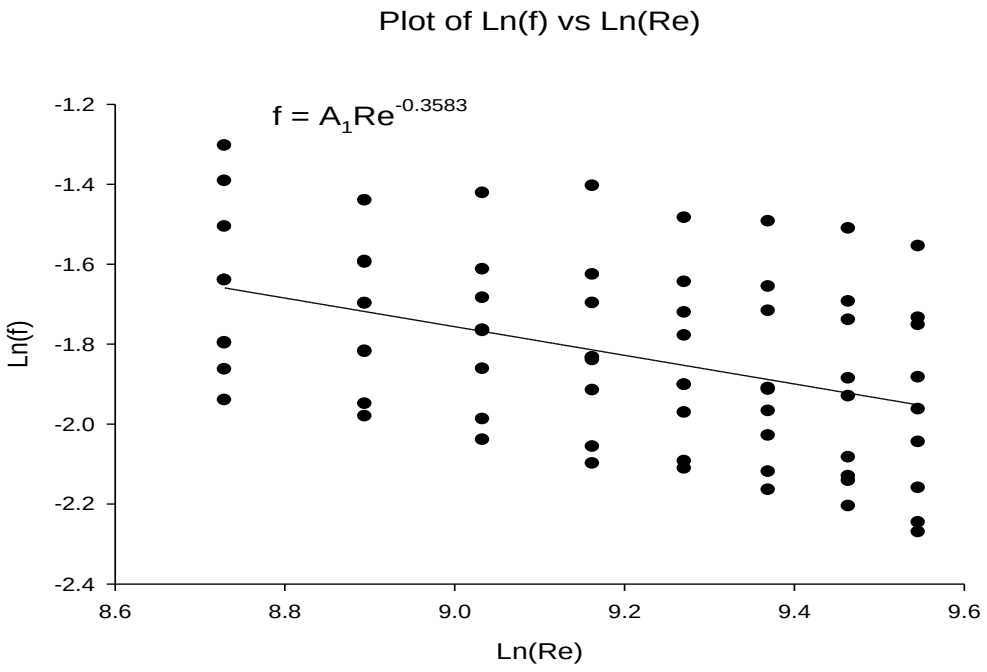

Figure 6.4. Experimental Change of friction factor and Reynolds number

The coefficient A_1 is greatly influenced by other geometrical specifications. Using the parameters dimple diameter (D), and dimple diameter to depth ratio (D/H), and values of $\frac{f}{Re^{-0.3583}} = A_1$ is graphically shown log-log scale as function for dimple diameter (D) to dimple diameter to depth ratio (D/H). This equation is derived from a regression study achieved for minimizing distance between curve and data.

Similarly, $ln\left(\frac{f}{Re^{-0.3583}}\right)$which is ln($B_1$) with the logarithmic dimple diameter to depth ratio (D/H) i.e., $\ln(D/H)$was plotted by fitting in second order quadratic equation as shown in Fig.6.5 and the regression yield the following equation

$$ln\left(\frac{f}{Re^{-0.3583}}\right) = C_1\left(\frac{D}{H}\right)^{-0.0026} Exp\left(0.1624\left(\frac{D}{H}\right)^2\right) \quad (6.7)$$

The final constant value can be used to express the final correlation. i.e., C_1 is written as

$$f = 1.7520 \times Re^{-0.3583}\left(\frac{D}{H}\right)^{-0.0026} Exp\left(0.1624\left(ln\left(\frac{D}{H}\right)^2\right)\right) \quad (6.8)$$

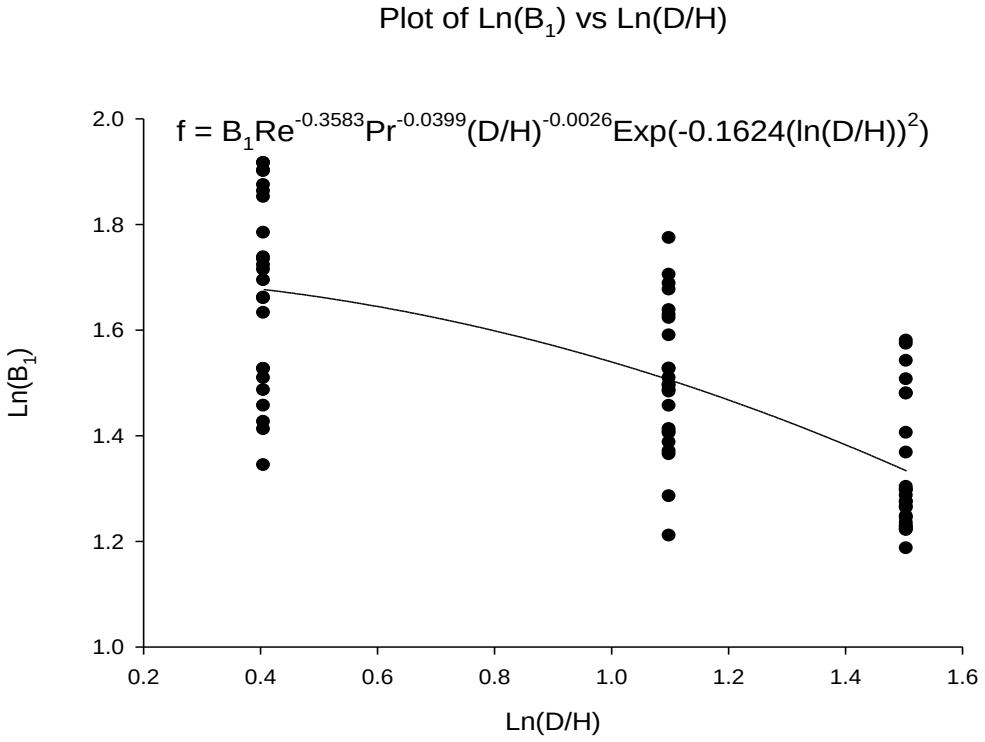

Figure 6.5. Deviation for coefficient B_1 and Dimple Diameter to Depth Ratio (D/H)

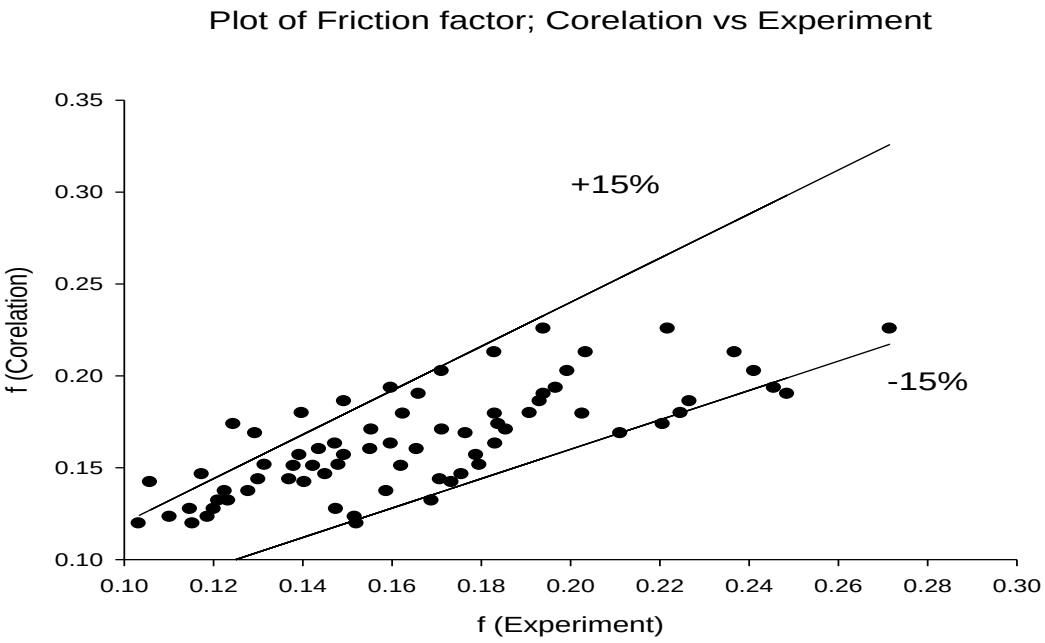

Figure 6.6. Deviation for correlation and friction factor Experimental

In order to validate correlations for Nusselt number and friction factor, data obtained from correlations plotted against experimental values shown in figure. 6.4 and 6.6. It is identified that majority of observed values of Nusselt number and friction factor using correlations developed. These correlations can be used by other investigators.

CHAPTER - 7

CONCLUSIONS AND FUTURE SCOPE

7.1. Conclusions

The impact of twisted tape inserts with different diameters and different dimple diameter to depth ratio (D/H) on Nusselt number & friction factor has been studied. According to experimental studies key findings are summarized as follows:

i. Identified that dimpled twisted tape inserts results in higher values of both Nusselt number and friction factor when compared to plain twisted tape inserts and plain tubes over the range of Reynolds number.

ii. It is evaluated that that the use of dimpled twisted tape inserts resulted in maximum values of Nusselt number and friction factor compared to plain twisted tape inserts and plain tubes across range of Reynolds number studied. Nusselt number was found to increase as the depth of the dimple increased where dimple diameter to depth ratio (D/H) is 1.5 to 3, and then decreased as the depth further increased where dimple diameter to depth ratio (D/H) is 3 to 4.5, for all cases.

iii. Effect of the dimple tape with twist on friction factor becomes more important at higher Reynolds number, leading to rise in friction factor with increasing thickness of dimple. This is because a deeper dimple reduces flow area and increases the contact surface area, resulting in more resistance to flow and higher friction factor. Moreover, Nusselt number increases with increasing depth of dimple at certain point, beyond which it starts to decrease. This is because the dimple obstructs the fluid flow, reducing heat transfer rate. Additionally, protrusion on convex side of the dimple separates the flow, leading to increased turbulence and elevated heat transfer rates.

iv. Performance Evaluation Criteria is a ratio of Nusselt number to friction factor, and it provides an overall assessment of the heat transfer augmentation and pressure drop penalty along with a particular heat transfer enhancement technique. In this study, examined that value of performance evaluation criteria is maximum for dimple diameter (D) = 4 mm and dimple diameter to depth ratio (D/H) = 4.5, which means that the increase in heat transfer due to the dimple geometry is more significant than

increase in pressure drop.

v. Correlations have been established for Nusselt number and friction factor using the results.

(a) Correlation for Nusselt number in terms of Reynolds number, dimple diameter (D) and dimple diameter to depth ratio (D/H) is given as.

(b) New correlation for friction factor in terms of Reynolds number, dimple diameter (D) and dimple diameter to depth ratio (D/H) is given as.

7.2 FUTURE SCOPE

This study Future research can explore various aspects of double pipe heat exchanger with twisted tape inserts, based on findings of this study and analysis

- The experiments involve testing the double pipe heat exchanger with the dimpled configuration twisted tape inserted in the inner tube. The selected nanofluid, which may consist of nanoparticles dispersed in a base fluid, is used as the working fluid. The relevant parameters, such as flow rates, temperatures, and pressure differentials, are measured to calculate the Nusselt number and friction factor.
- **Performance Optimization**: Further research can focus on optimizing the performance of double pipe heat exchanger with twisted tape inserts by investigating different geometries, configurations, and materials for the twisted tapes. This could involve studying the effects of varying twist ratios, tape dimensions, and angles of attack on heat transfer and pressure drop characteristics.
- **Heat Transfer Enhancement**: Future studies can explore advanced heat transfer enhancement techniques in double pipe heat exchanger using alternative types of inserts, such as vortex generators, wire coils, or nanofluids. Comparative studies can be conducted to evaluate the performance of different enhancement methods and identify the most effective ones.
- **Multi-Objective Optimization**: Researchers can employ multi-objective optimization techniques to simultaneously consider heat transfer

enhancement and pressure drop reduction in double pipe heat exchanger with twisted tape inserts. This can help identify optimal design configurations that achieve the best compromise between these conflicting objectives.

- **Flow Pattern Analysis**: Investigating the flow patterns inside the double pipe heat exchanger with twisted tape inserts can provide valuable insights into the fluid behaviour and heat transfer mechanisms. Computational fluid dynamics (CFD) simulations or experimental techniques, such as flow visualization, can be employed to study flow patterns, identify areas of recirculation or dead zones, and propose design modifications to enhance flow distribution.
- **Industrial Applications**: The practical application of double pipe heat exchanger with twisted tape inserts can be explored in various industrial sectors, including HVAC systems, chemical processes, power generation, and refrigeration. Future research can focus on evaluating the performance and feasibility of using double pipe heat exchanger with twisted tape inserts in real-world applications, considering factors such as fouling, scaling, and maintenance requirements.
- **Economic Analysis**: Future studies can investigate the economic viability and cost-effectiveness of employing double pipe heat exchanger with twisted tape inserts compared to traditional heat exchangers. This analysis can include factors such as manufacturing costs, installation expenses, energy savings, and overall system efficiency to provide a comprehensive economic assessment.

APPENDIX

APPENDIX - 1

Calibration of T-type thermocouple

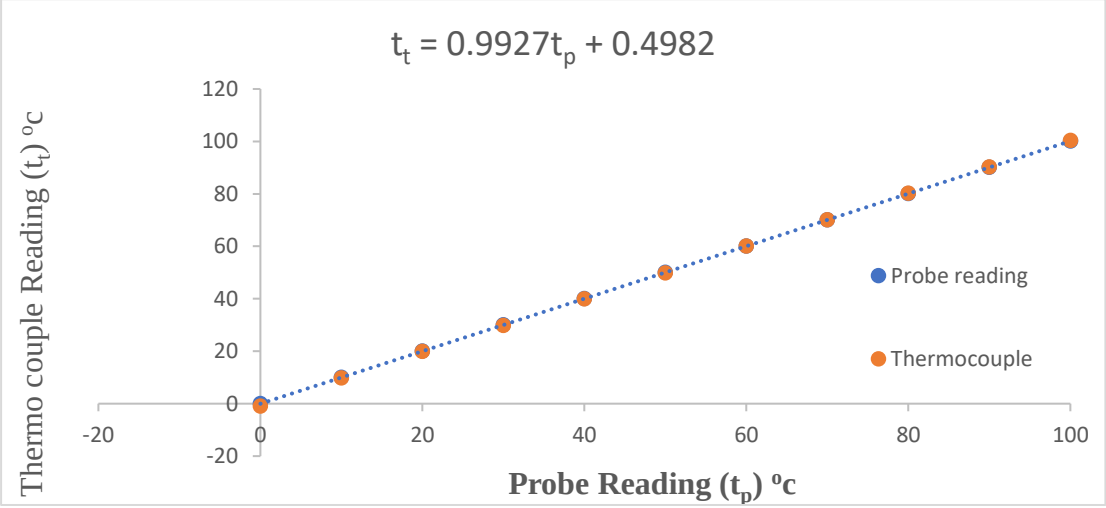

Fig.A.1.1 Calibration curve of thermocouple

Procedure to calibrate T-type thermocouple

T-type thermocouples consist of copper and nickel wire in which copper is act as positive terminal and nickel behaved as negative terminal. The thermocouple junctions are made by fusing the copper and nickel wires in the mercury bath while maintaining a potential difference of 20 volt by using variac transformer. Thermocouples calibrated in a lab setting against a dry block temperature calibrating system with a minimum count of 0.01 °C to determine temperature measurement accuracy. T thermocouple that needs to be calibrated is placed in a calibration bath where a constant temperature is maintained. A digital temperature indicator is used to display thermocouple's response to different present values of the standard probe, and readings from both the standard probe and thermocouple are recorded. If the limitation of thermocouple reading with regard to standard probe is less than tolerance limit of calibrator, then thermocouple is accepted. This process was repeated for increasing and decreasing temperature ranges. The plot of temperature measured by

standard thermometer as function of temperature measured by thermocouple is shown in Figure. A.1.1 and Table A.1.1. The average deviation of thermocouple reading with respect to the standard thermometer reading was found to be 0.5 and is having under acceptable limits.

Table – A.1.1. Probe vs Thermocouple reading

Sr. No.	Step of calibration (Pre-set value) (°C)	Probe reading (°C)	Thermocouple reading (°C)	Error (°C)
1	0	-0.04	-1.0	0.96
2	10	9.97	9.8	0.17
3	20	19.97	19.9	0.07
4	30	30.08	29.8	0.28
5	40	40.06	39.9	0.16
6	50	50.00	49.8	0.20
7	60	60.08	60.0	0.08
8	70	70.05	70.1	-0.05
9	80	80.10	80.2	-0.1
10	90	90.10	90.2	-0.1
11	100	100.12	100.3	-0.18

APPENDIX - 2

Calibration of RTD

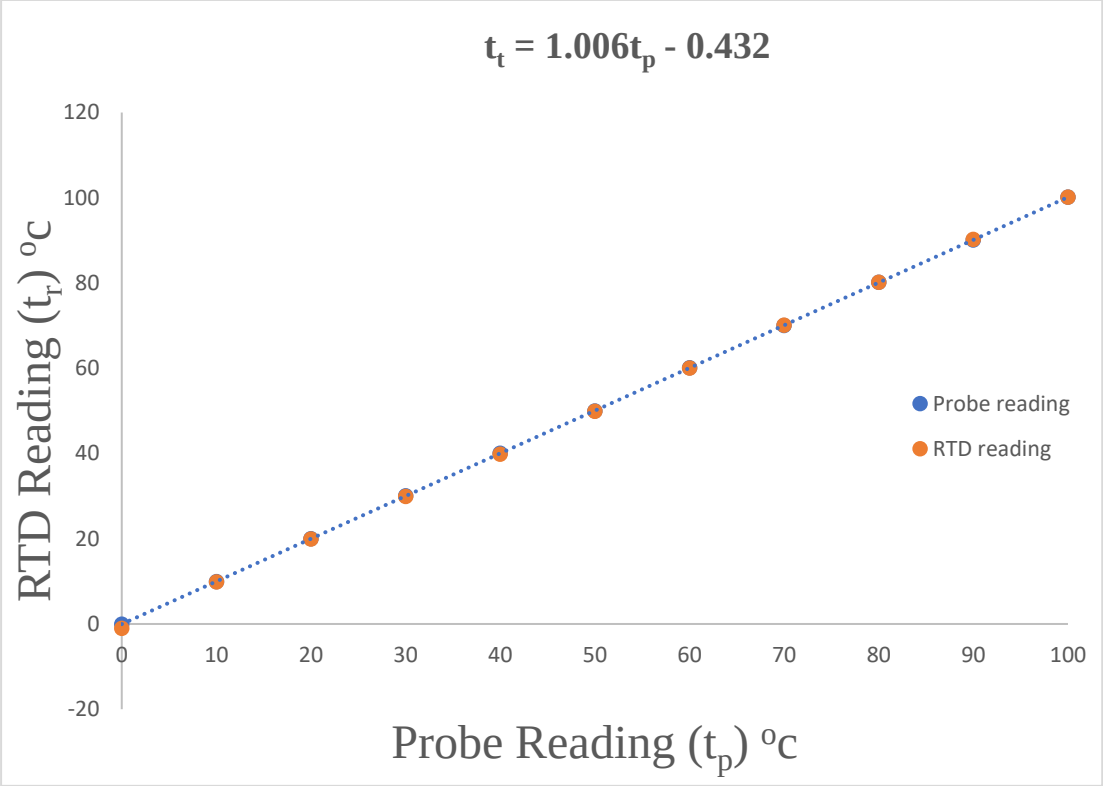

Fig.A.2.1. Calibration curve of RTD

Procedure to calibrate RTD

RTD calibrated in lab setting against a dry block temperature calibrating system with a minimum value of 0.01 °C to measure precision of temperature measurement. T thermocouple that needs to be calibrated is placed in the calibration bath, which maintains a constant temperature. A digital temperature indicator is used to display the response of the RTD and the standard probe for various pre-set values of the standard probe, and both the readings of the standard probe and RTD are recorded. RTD is acceptable if the RTD reading limit relative to the standard probe is smaller than calibrator's tolerance limit. Process repeated for increasing and decreasing temperature ranges. The plot of temperature measured by standard thermometer as

function of temperature measured by RTD is shown in Fig. A.2.1. and Table A.2.1. The average deviation of thermocouple reading with respect to the standard thermometer reading was found to be 0.5 and is having under acceptable limits.

Table – A.2.1. Probe vs RTD readings

Sr. No.	Step of calibration (Pre-set value) (°C)	Probe reading (°C)	PT-100(RTD) reading (°C)	Error (°C)
1	0	-0.06	-1.0	0.94
2	10	9.97	9.9	0.07
3	20	19.97	19.91	0.06
4	30	30.08	29.9	0.18
5	40	40.06	39.8	0.26
6	50	50.00	49.9	0.10
7	60	60.08	60.0	0.08
8	70	70.06	70.1	-0.06
9	80	80.15	80.2	-0.05
10	90	90.10	90.2	-0.1
11	100	100.12	100.18	-0.06

APPENDIX - 3

Calibration of Rotameter

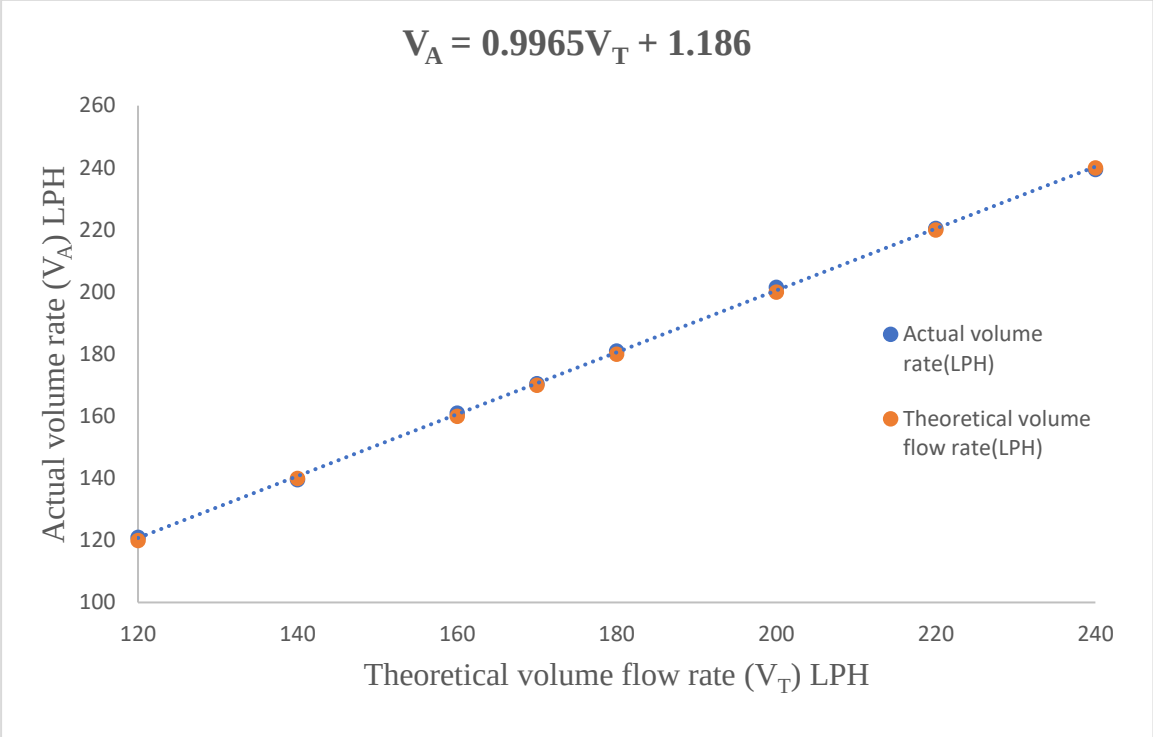

Fig.A.3.1 Calibration curve of Rotameter

Procedure to calibrate Rotameter

To calibrate rotameter, three sets of readings have been collected for each volume flow rate and average value of measured volume flow rate has been mentioned in table. During the experiment a bucket fitted with measuring scale of capacity 5000 ml has been used is shown in Table A.3.1 and figure A.3.1. As one end of the rotameter is connected with water tank and other end with measuring bucket and the volume flow rate of each set value for one minute time has been considered.

Table A 3.1 Actual discharge vs Theoretical discharge readings of rotameter

S.no	Theoretical volume flow rate (LPH)	Actual volume rate (LPH)	Error (LPH)
1	120	121	1.0
2	140	139.5	0.5
3	160	161	1.0
4	170	170.5	0.5
5	180	181	1.0
6	200	201.5	1.5
7	220	220.5	0.5
8	240	239.5	0.5

APPENDIX -4

UNCERTAINTY ANALYSIS

Uncertainty analysis involves predicting the range of uncertainty associated with an experimental result by considering the variability observed in the raw data used to calculate the result. It takes into account the scatter or variability observed in the data to estimate the uncertainty interval associated with the final experimental outcome. The term "scatter" is a qualitative description of the variance in data, the extent to which the individual values differ from the mean is shown in Table A 4.1.

Kline and McClintock [84] was proposed methodology for predicting the uncertainty of experimental results, which is particularly valuable in analyzing the errors arising from deviations in primary measurements during experimental work. This approach allows for a comprehensive assessment of the uncertainties associated with the final results, taking into account the potential variations and inaccuracies in the primary measurements conducted.

X=Y ± Z, (10 to 1) (1)

$$\frac{\delta y}{y} = \left\{\left[\left(\frac{\partial y}{\partial x_1}\right)\delta x_1\right]^2 + \left[\left(\frac{\partial y}{\partial x_2}\right)\delta x_2\right]^2 + \left[\left(\frac{\partial y}{\partial x_3}\right)\delta x_3\right]^2 + \cdots \ldots \cdots \cdots\right\}^{\frac{1}{2}} \quad (2)$$

Where δ X_1, δ X_2, δ X_3,…… are the Uncertainty in measurement of X_1, X_2,X_3,…….

δY= absolute uncertainty

Δy/y= relative uncertainty

- $R_e = \frac{Ud}{v}$ (3)

- Heat transfer coefficient $h = \frac{mC_{p(T_{hi}-T_{ho})}}{A_{s(T_h-T_s)}}$ (4)
- Nusselt number $N_u = \frac{hd}{k}$ (5)
- Friction factor $f = \frac{2d(\Delta P)}{4\rho LV^2}$ (6)

Illustrative Methodology for Uncertainty Analysis

Table A.4.1. Parameters and test data used for Uncertainty analysis

Parameters	**Symbol**	**Data**
Test section length	L	1500 mm
Tube diameter	d	16 mm
U- tube manometer reading	h*	2.2 mm of Hg
Hot water temp at outlet	t_{ho}	63.3°C
Hot water temp at inlet	t_{hi}	73.8°C
Hot water temp drop	t_{hi}- t_{ho}	10.5°C
Hot water bulk temp	t_h	68.55°C
Inlet temperature of cold water	t_{ci}	25.2°C
Outlet temperature of cold water	t_{co}	51.8°C
The bulk temperature of cold water	t_c	38.5°C
Average surface temperature of inner tube	t_w	62.45°C
Volume flow	V	240 lph
Specific heat at Hot water	C_{Ph}	4066 J/Kg K
Hot water of Thermal conductivity	K	0.66153 W/m K
Density of hot water at inlet temperature	ρ_{in}	975.1 kg/m^3
Density of hot water at bulk temperature	ρ_h	978.2 kg/m^3
Density of cold water at bulk temperature	ρ_c	992.36 kg/m^3
Kinematic viscosity of hot water at bulk temp	υ	3.12 x10^{-7}m^2/sec

Specific heat of cold water	C_{Pc}	4067.6 J/Kg K
Mean velocity of hot water	U_h	0.33069 m/s
Reynolds number of hot water	R_e	12884
Heat released by hot water	Q_h	2784.566W
Heat gain by cold water	Q_c	1491.27 W
Average heat flow rate	Q	2137.919 W
Convective heat transfer coefficient	h_i	2824.326 W/m^2 K
Nusselt number	Nu	68.31
Friction factor	f	0.0304

1. Test tube surface area

$A_s = \pi dL$

$$\delta A_s = \left[\left(\frac{\delta A_s}{\delta d} \times \delta d\right)^2 + \left(\frac{\delta A_s}{\delta L} \times \delta L\right)^2\right]^{0.5}$$

$$\delta A_s = [(\pi L \times \delta d)^2 + (\pi d \times \delta L)^2]^{0.5}$$

$$\frac{\delta A_s}{A_s} = \left[\left(\frac{\delta d}{d}\right)^2 + \left(\frac{\delta L}{L}\right)^2\right]^{0.5}$$

$$\frac{\delta A_s}{A_s} = \left[\left(\frac{0.1}{16}\right)^2 + \left(\frac{1}{1500}\right)^2\right]^{0.5}$$

$$\frac{\delta A_s}{A_s} = [3.906 \times 10^{-5} + 4.444 \times 10^{-7}]^{0.5}$$

$$\frac{\delta A_s}{A_s} = 0.0062533$$

2. Cross sectional area

$A = \frac{\pi}{4} d^2$

$$\frac{\delta A}{\delta d} = \frac{2\pi d}{4}$$

$$\delta A = \left[\left(\frac{\delta A}{\delta d} \times \delta d\right)^2\right]^{0.5}$$

$$\delta A = \left[\left(\frac{\pi d}{2} \times \delta d\right)^2\right]^{0.5}$$

$$\delta A = \frac{\pi d}{2} \times \delta d$$

$$\frac{\delta A}{A} = \frac{\frac{\pi d}{2} \times \delta d}{\frac{\pi}{4} d^2}$$

$$\frac{\delta A}{A} = \frac{2\delta d}{d}$$

$$\frac{\delta A}{A} = \frac{2 \times 0.1}{16} = 0.0125$$

3. Mass flow rate

$$m = \frac{V_{\text{flow}}}{3600} \times \rho$$

$$\frac{\delta m}{m} = \left[\left(\frac{\delta V_{\text{flow}}}{V_{\text{flow}}}\right)^2 + \left(\frac{\delta \rho}{\rho}\right)^2\right]^{0.5}$$

$$\frac{\delta m}{m} = \left[\left(\frac{0.00277}{0.06666}\right)^2 + \left(\frac{0.1}{978.2}\right)^2\right]^{0.5}$$

$$\frac{\delta m}{m} = [1.736 \times 10^{-3} + 1.045 \times 10^{-8}]^{0.5}$$

$$\frac{\delta m}{m} = 0.041665$$

4. Velocity of water

$$\mathrm{U} = \frac{m}{\rho A}$$

$$\frac{\delta U}{U} = \left[\left(\frac{\delta m}{m}\right)^2 + \left(\frac{\delta \rho}{\rho}\right)^2 + \left(\frac{\delta A}{A}\right)^2\right]^{0.5}$$

$$= [(0.041665)^2 + (1.022 \times 10^{-4})^2 + (0.0125)^2]^{0.5}$$

$$\frac{\delta U}{U} = 0.043499$$

5. Heat transfer rate

$Q_{\text{water}} = mC_p\Delta T$

$$\frac{\delta Q_{\text{water}}}{Q_{\text{water}}} = \left[\left(\frac{\delta m}{m}\right)^2 + \left(\frac{\delta C_p}{C_p}\right)^2 + \left(\frac{\delta(\Delta T_w)}{\Delta T_w}\right)^2\right]^{0.5}$$

$$\frac{\delta Q_{\text{water}}}{Q_{\text{water}}} = \left[(0.041665)^2 + \left(\frac{0.1}{4066}\right)^2 + \left(\frac{0.1}{10.5}\right)^2\right]^{0.5}$$

$$\frac{\delta Q_{\text{water}}}{Q_{\text{water}}} = [1.73 \times 10^{-3} + 6.046 \times 10^{-10} + 9.06 \times 10^{-5}]^{0.5}$$

$$\frac{\delta Q_{\text{water}}}{Q_{\text{water}}} = 0.0426$$

6. Heat transfer coefficient

$$h = \frac{Q_{\text{water}}}{A_s(T_h - T_s)} = \frac{Q_{\text{water}}}{A_s(\Delta T)}$$

$$\frac{\delta h}{h} = \left[\left(\frac{\delta Q_{\text{water}}}{Q_{\text{water}}}\right)^2 + \left(\frac{\delta A_s}{A_s}\right)^2 + \left(\frac{\delta(\Delta T)}{\Delta T}\right)^2\right]^{0.5}$$

$$\frac{\delta h}{h} = \left[(0.0426)^2 + (0.0062533)^2 + \left(\frac{0.1}{6.1}\right)^2\right]^{0.5}$$

$$\frac{\delta h}{h} = [(0.0426)^2 + (0.0062533)^2 + (0.01639)^2]^{0.5}$$

$$\frac{\delta h}{h} = 0.04606$$

7. Reynolds number

$$R_e = \frac{Ud}{v}$$

$$\frac{\delta R_e}{R_e} = \left[\left(\frac{\delta U}{U}\right)^2 + \left(\frac{\delta d}{d}\right)^2 + \left(\frac{\delta v}{v}\right)^2\right]^{0.5}$$

$$= \left[(0.043499)^2 + \left(\frac{0.1}{16}\right)^2 + \left(\frac{0.1 \times 10^{-7}}{4.1064 \times 10^{-7}}\right)^2\right]^{0.5}$$

$$= [(0.043499)^2 + (0.00625)^2 + (0.0243)^2]^{0.5}$$

$$\frac{\delta R_e}{R_e} = 0.050216$$

8. Nusselt number

$$N_u = \frac{hd}{k}$$

$$\frac{\delta N_u}{N_u} = \left[\left(\frac{\delta h}{h}\right)^2 + \left(\frac{\delta d}{d}\right)^2 + \left(\frac{\delta k}{k}\right)^2\right]^{0.5}$$

$$= \left[(0.04607)^2 + (0.00625)^2 + \left(\frac{0.00001}{0.66153}\right)^2\right]^{0.5}$$

$$= \left[(0.04607)^2 + (0.00625)^2 + \left(\frac{0.00001}{0.66153}\right)^2\right]^{0.5}$$

$$\frac{\delta N_u}{N_u} = 0.04649$$

9. Friction factor

$$f = \frac{2d(\Delta P)}{4\rho L V^2}$$

$$\frac{\delta f}{f} = \left[\left(\frac{\delta d}{d}\right)^2 + \left(\frac{\delta \rho}{\rho}\right)^2 + \left(\frac{\delta L}{L}\right)^2 + \left(\frac{\delta U}{U}\right)^2 + \left(\frac{\delta(\Delta P)}{(\Delta P)}\right)^2\right]^{0.5}$$

$$\frac{\delta f}{f} = [(0.00625)^2 + (1.022 \times 10^{-4})^2 + (4.166 \times 10^{-4})^2 + (0.043499)^2 + (0.004545)^2]^{0.5}$$

$$\frac{\delta f}{f} = 0.04418$$

10. Dimple diameter

$$\frac{\delta d}{d} = \left[\left(\frac{\delta d}{d}\right)^2\right]^{0.5}$$

$$\frac{\delta d}{d} = \left[\left(\frac{0.01}{6}\right)^2\right]^{0.5} = 0.001643$$

Table A 4.2. Measured quantities

S. No.	Details	Uncertainty
1	Test tube Surface area	± 0.625 %
2	Test-tube cross-sectional area	±1.25 %
3	Water mass flow	± 4.16 %
4	Test tube Velocity in water	± 4.34 %
5.	Dimple diameter	± 0.16 %

Table A 4.2. Calculated quantities

S. No.	Details	Uncertainty
1	Coefficient of heat transfer	± 4.60 %
2	Reynolds number	± 5.02 %
3	Nusselt number	± 4.64%
4	friction factor	± 4.41 %
5	Heat gain by water	± 4.26 %

APPENDIX - 5

Heat transfer data pertaining to various configurations have been collected and presented in the tables below.

Table A 5.1. Observation table for plain tube

S.No.	V_h (LPH)	t_{hi}(^{O}C)	t_{ho}(^{O}C)	t_{ci}(^{O}C)	t_{co}(^{O}C)	t_1(^{O}C)	t_2(^{O}C)	t_3(^{O}C)	t_4(^{O}C)	t_5(^{O}C)	t_6(^{O}C)	h_1(mm)
1	120	73.4	57.7	25.2	45.8	55.4	54.6	54.4	55.3	55.3	55.2	0.7
2	140	73.5	59.2	25.5	47.5	57.4	56.7	56.5	57.4	57.4	57.4	0.9
3	160	73.5	59.9	25.6	48.3	58.3	57.5	57.4	58.2	58.2	58.1	1.1
4	180	73.7	61.3	25.8	49.7	60.1	59.4	59.2	60.0	60.0	59.9	1.3
5	200	73.7	61.8	25.4	50.4	61.1	60.4	60.5	61.0	61.0	60.9	1.5
6	220	73.7	62.3	25.5	50.9	61.6	60.9	60.6	61.6	61.6	61.4	1.9
7	240	73.8	63.3	25.2	51.8	62.7	62.0	62.0	62.7	62.7	62.6	2.2
8	260	73.8	63.6	24.8	52.1	63.2	62.4	62.6	63.2	63.2	63.1	2.5

Table A 5.2 Observation table for twisted tape (without dimples)

S.No.	V_h (LPH)	t_{hi} (^OC)	t_{ho} (^OC)	t_{ci} (^OC)	t_{co} (^OC)	t_1(^OC)	t_2(^OC)	t_3(^OC)	t_4(^OC)	t_5(^OC)	t_6(^OC)	h_1(mm)
1	120	71.4	57.5	33.4	51	58.9	58.4	58.6	58.8	58.8	58.8	3
2	140	71.5	58.9	33.8	51.9	60.2	59.7	59.9	60.1	60	60.0	4
3	160	71.7	60.2	33.7	52.7	61.1	61.2	61.1	61	60.8	61.2	5
4	180	71.8	61.2	33.7	53.2	61.9	62.0	62.0	61.8	61.6	62.6	6
5	200	72.2	62.1	33.7	53.5	62.8	62.9	63.0	62.8	62.6	63.0	7
6	220	72.1	62.7	34.1	54.1	63.4	63.5	63.5	63.2	63.1	63.5	7.8
7	240	72.1	63.2	34	54.4	63.8	63.8	64.0	63.8	63.6	64.0	9
8	260	72.2	63.9	34.8	55.3	64.5	64.5	64.5	64.4	64.2	64.6	10

Table A 5.3 Observation table for twisted tape (D=2 mm), where dimple diameter to depth ratio (D/H)=4.5

S.No.	V_h (LPH)	t_{hi} (^OC)	t_{ho} (^OC)	t_{ci} (^OC)	t_{co} (^OC)	t_1(^OC)	t_2(^OC)	t_3(^OC)	t_4(^OC)	t_5(^OC)	t_6(^OC)	h_1(mm)
1	120	71.2	58.7	37.7	53.8	59	59.5	59.8	59	60	59	2
2	140	71.5	60.3	37.6	54.7	61.7	60.6	61.1	60.9	61.4	61.3	3
3	160	71.8	61.2	37.4	55.4	62.3	62.8	61.9	61	61.7	61.7	4
4	180	71.9	62.7	37.4	56.3	62.8	62.6	62.7	62.1	62.5	62.5	5
5	200	72.3	63.1	37.3	56.7	63.6	63.3	63.6	63.7	63.6	63.6	6.4
6	220	72.5	64.4	37.3	57.5	64.7	64.1	64.2	64.3	64.5	64.5	8
7	240	71.7	64.6	37.2	57.7	65.1	64.5	64.7	64.6	64.7	64.9	9.5
8	260	71.6	64.3	36.1	56.9	64.8	64.1	64.3	64.3	64.5	64.3	10.5

Table A 5.4 Observation table for twisted tape (D=2 mm), where dimple diameter to depth ratio (D/H)= 3

S.No.	V_h (LPH)	t_{hi} (^OC)	t_{ho} (^OC)	t_{ci} (^OC)	t_{co} (^OC)	t_1(^OC)	t_2(^OC)	t_3(^OC)	t_4(^OC)	t_5(^OC)	t_6(^OC)	h_1(mm)
1	120	70.6	57.6	36.5	51.6	59	58	58.3	58.4	58.8	58.8	2
2	140	70.5	59.2	36.4	53.1	60.3	59.5	60.2	60.4	60	60.2	3
3	160	70.7	60.7	35.8	54.4	61.0	60.4	61	61.3	61.4	61.6	4
4	180	71.1	61.5	35.1	55.2	62.4	61.2	61.8	62.1	62.6	62	5.5
5	200	71.3	62.9	36.6	56.4	63.4	62.8	62.5	63.4	63.4	63.2	6.4
6	220	71.1	63.2	36.2	56.2	63.5	63.1	62.8	63.2	63.6	63.6	7.8
7	240	71.4	63.4	36.8	56.8	63.9	63.5	63.5	63.6	64.1	63.9	9.4
8	260	70.9	64	36.6	57.0	64.1	63.8	63.9	64	64.4	64.4	10.8

Table A 5.5 Observation table for twisted tape (D=2 mm), where dimple diameter to depth ratio (D/H)= 1.5

S.No.	V_h (LPH)	t_{hi} (^OC)	t_{ho} (^OC)	t_{ci} (^OC)	t_{co} (^OC)	t_1(^OC)	t_2(^OC)	t_3(^OC)	t_4(^OC)	t_5(^OC)	t_6(^OC)	h_1(mm)
1	120	70.8	58.8	36.4	54	60.3	59.6	59.5	60.2	60.2	60.2	3.2
2	140	70.9	59.5	36.3	54.8	61.1	61.2	61.3	61.5	61.5	61.5	4.3
3	160	71.1	60.5	36.2	55.2	62.5	61.4	61.9	62.2	62.2	62	5
4	180	71.3	61.6	36.6	56.5	63	62.1	63	63.4	63.6	62.7	6
5	200	71.8	62.8	36.5	56.7	63.8	63.3	63.4	64	64	63.5	7.8
6	220	71.7	63.2	35.6	56.8	64.5	63.5	63.5	64.2	64.2	63.8	8.6
7	240	71.6	63.5	36.3	57.5	64.7	64.6	64.5	64.3	64.6	64.2	10
8	260	71.9	64	35.7	57.1	65.2	64.8	64.6	65.2	65	64.6	10.6

Table A 5.6 Observation table for twisted tape (D=4 mm), with dimple diameter to depth ratio (D/H)= 4.5

S.No.	V_h (LPH)	t_{hi} (^OC)	t_{ho} (^OC)	t_{ci} (^OC)	t_{co} (^OC)	t_1(^OC)	t_2(^OC)	t_3(^OC)	t_4(^OC)	t_5(^OC)	t_6(^OC)	h_1(mm)
1	120	71.3	58.5	36.6	53.5	60	59.5	60	60	60	60	3.2
2	140	71.4	60	36.4	54	61	60.2	60.5	60.5	60.4	60.4	4
3	160	71.5	60.4	36.2	54.6	61.4	61.3	61	61.6	61.6	61.4	4.6
4	180	71.8	62.2	36.1	55	62.6	62.5	62.2	62.5	62.3	62.4	5.2
5	200	71.9	62.8	36.6	55.6	63.4	63	63.4	63.4	63	63.2	6
6	220	71.8	63.1	36.4	56.4	63.5	63.5	63.5	63.6	63.4	63.5	7.2
7	240	71.8	63.5	36.5	56.6	64.2	63.6	63.8	64.2	64.3	63.8	8
8	260	71.9	64	35.5	57	64.6	63.8	64.3	64	64.2	64	10.2

Table A 5.7 Observation table for twisted tape (D=4 mm), where dimple diameter to depth ratio (D/H)= 3

S.No.	V_h (LPH)	t_{hi} (^OC)	t_{ho} (^OC)	t_{ci} (^OC)	t_{co} (^OC)	t_1(^OC)	t_2(^OC)	t_3(^OC)	t_4(^OC)	t_5(^OC)	t_6(^OC)	h_1(mm)
1	120	71.7	59.6	37.4	55.4	61.8	60.5	60.5	61.4	61	61	2
2	140	71.8	60.8	37.3	56.6	62.2	61.9	62	62	62.5	62.3	3.8
3	160	71.8	61.4	37.1	57.2	63	62.4	62.4	62.6	63	62.6	5
4	180	72	62.6	37.4	57.6	63.6	63.1	63.1	63	63.4	63	6.5
5	200	72.1	63.2	37.3	58.6	64.4	64	64	64.1	64	64.6	7
6	220	72.2	64.4	37.9	59.2	65	64.6	64.5	64.9	65.3	65	8.5
7	240	72.4	64.6	38.2	59.8	65.5	65	65	65.2	65.6	65.6	10.7
8	260	72.5	65	37.7	60	66	65.5	65.6	65.8	66.2	66.3	11.8

Table A 5.8 Observation table for twisted tape (D=4 mm), where dimple diameter to depth ratio (D/H)= 1.5

S.No.	V_h (LPH)	t_{hi} (OC)	t_{ho} (^{O}C)	t_{ci} (^{O}C)	t_{co} (^{O}C)	t_1(^{O}C)	t_2(^{O}C)	t_3(^{O}C)	t_4(^{O}C)	t_5(^{O}C)	t_6(^{O}C)	h_1(mm)
1	120	70.7	57.4	36.5	52.6	58.9	58.5	59	58.8	58.6	58.6	3
2	140	71	59.2	36.7	53.7	59.7	60	59.7	60	60	60	4
3	160	71.1	60.5	36.4	54	61	60.6	60.5	60.6	60.6	60.6	6
4	180	71.6	61	37	55	62.	62	62	62.5	62	62	8
5	200	72	63	37.5	56.5	63.6	63.4	63.5	63.1	63.1	63.3	10.6
6	220	71.7	63.4	38	56.4	63.7	63.8	63.3	63.6	63.6	63.5	12.6
7	240	72	63.8	37.5	57	64.1	64	64	64	64.7	64.3	13.8
8	260	72.3	64.5	37	57.5	64.7	64.5	64.8	64.5	64.9	64.5	15

Table A 5.9 Observation table for twisted tape (D=6 mm), where dimple diameter to depth ratio (D/H)= 4.5

S.No.	Vh (LPH)	t_{hi} (^{O}C)	t_{ho} (^{O}C)	t_{ci} (^{O}C)	t_{co} (^{O}C)	t_1(^{O}C)	t_2(^{O}C)	t_3(^{O}C)	t_4(^{O}C)	t_5(^{O}C)	t_6(^{O}C)	h1(mm)
1	120	71	59.5	38	55.5	61	60.5	60.6	60.8	60.5	60.7	3.5
2	140	71.1	61	37.8	56.1	61.8	61.8	61	62	62	62	4.8
3	160	71.2	61.6	37.5	56.6	62.5	62	62.5	62.5	62.5	62.4	6
4	180	71.5	63.5	38.6	58	63.8	63.5	63.6	64.3	64	63.6	7.2
5	200	71.6	63.6	38.1	58.2	64.2	64	64	64.1	64.5	64	8.9
6	220	71.5	64	38	58.4	64.3	64.5	64.5	64.5	64.8	64.6	9.6
7	240	71.6	63.9	37.4	57.5	64.4	64	64.5	64.8	64.5	64.7	11.2
8	260	71.8	64	36.1	58.3	65	64.5	65	65	65	65	13.5

Table A 5.10 Observation table for twisted tape (D=6 mm), where dimple diameter to depth ratio (D/H)= 3

S. No	V_h (LPH)	t_{hi} (^{O}C)	t_{ho} (^{O}C)	t_{ci} (^{O}C)	t_{co} (^{O}C)	t_1(^{O}C)	t_2(^{O}C)	t_3(^{O}C)	t_4(^{O}C)	t_5(^{O}C)	t_6(^{O}C)	h_1(mm)
1	120	71	57.4	36	52.5	59.7	59	58.9	59.7	59.5	59.7	4.2
2	140	71.1	58.8	35.8	53	60.9	60.1	60.2	60.5	60	60	5
3	160	71.2	60	35.6	53.5	61.5	60.9	61	61.6	61.4	61.5	6.5
4	180	71.3	60.6	35.4	54.1	62.7	61.7	61.7	62.1	62.4	62.3	8
5	200	71.5	62	36	55.3	63	62.5	62.6	63.5	63.7	63.5	9.4
6	220	71.7	62.7	35.8	55.6	63.8	63.5	63.5	63.9	63.9	63.7	11
7	240	71.8	63.5	36.5	56.5	64.5	64.3	64.3	64	64	64	13.4
8	260	71.8	64.1	36.2	57	64.8	64.6	64.5	64.8	64.6	64.6	15.2

Table A 5.11 Observation table for twisted tape (D=6 mm), where dimple diameter to depth ratio (D/H)= 1.5

S. No	V_h (LPH)	t_{hi} (^OC)	t_{ho} (^OC)	t_{ci} (^OC)	t_{co} (^OC)	t_1(^OC)	t_2(^OC)	t_3(^OC)	t_4(^OC)	t_5(^OC)	t_6(^OC)	h1(mm)
1	120	71.1	57.3	36.6	53.5	59.9	59.5	59.5	59.5	59.6	59.5	4.8
2	140	71.2	59	37.5	54	60.5	60	60	60.7	60.9	60.5	6.2
3	160	71.3	60.5	37.7	55.7	61.7	61.7	61.5	61.5	61.5	61.4	9
4	180	71.5	61.6	37.6	55.9	62.5	62.6	62.3	62.3	62.5	62.2	10.7
5	200	71.8	63	38	56.6	63.3	63.3	63.8	63.5	63.9	63	13
6	220	71.6	63.5	38.1	56.9	64.2	63.8	63.5	63.9	64	63.5	14.7
7	240	71.8	64	38.7	57.5	64.8	64.6	64.2	64.8	64.9	64.2	16.1
8	260	71.6	64.5	38	58	65	64.8	64.8	64.5	65.3	64.5	18.3

PUBLICATIONS FROM THIS WORK

S. No.	Objectives	PublicationTitle	Journal Name	Year	DOI	Volume / Issue	Journal / Conference
1.	1,2,3	Experimental evaluation and thermal performance analysis of a twisted tape with dimple configuration in a heat exchanger	CSTE	2023	https://doi.org/10.1016/j.csite.2023.103003	46(2023) 103003	ELSEVIER
2.	4	Develop a New Correlation between Thermal Radiation and Heat Source in Dual-Tube Heat Exchanger with a Twist Ratio Insert and Dimple Configurations: An Experimental Study	MPDI	2023	https://doi.org/10.3390/pr11030860	11 (2023) 860	SCI Journal
3.	Related to Research work	Optimization and comparison of performance parameters of a double pipe heat exchanger with dimpled twisted tapes using CFD and ANN	JPME	2024	https://doi.org/10.1177/095440892312235	-	SCI Journal
4.	Review Paper	Heat Transfer and Friction Factor Augmentation Using Twisted Tape in a Double Pipe Heat Exchanger: A Critical Review	AIP	2022	https://doi.org/10.1063/5.0163080	*AIP Conf. Proc.* 2800, 020008 (2023)	Conference
5.	Related to Research work	Experimental Investigation of Heat Transfer and Friction Factor Enhancement in a Double Pipe Heat Exchanger Using Twisted Tape Inserts with Dimple Configurations	ICET-2023	2023	NA	NA	Springer

References

[1] Kumar, Prashant, and R. M. Sarviya. "Experimental investigation on effect of perforated double V-cut twisted tape on thermo-hydraulic characteristics of heat exchanger tube." Energy Sources, Part A: Recovery, Utilization, and Environmental Effects 46, no. 1 (2024): 3228-3244.

[2] Jawarneh, Ali M., Mohamad Al-Widyan, and Zain Al-Mashhadani. "Experimental study on heat transfer augmentation in a double pipe heat exchanger utilizing jet vortex flow." Heat Transfer 52, no. 1 (2023): 317-332.

[3] Mohamed, Hozaifa A., Majed Alhazmy, F. Mansour, and El-Sayed R. Negeed. "Enhancing Heat Transfer Inside a Double Pipe Heat Exchanger Using Al2O3 Nanofluid, Experimental Investigation Under Turbulent Flow Conditions." Journal of Nanofluids 12, no. 2 (2023): 356-371.

[4] Dandoutiya, Bhrant Kumar, and Arvind Kumar. "Study of thermal performance of double pipe heat exchanger using W-cut twisted tape." Energy Sources, Part A: Recovery, Utilization, and Environmental Effects 45, no. 2 (2023): 5221-5238.

[5] Ilikan, Ayhan Nazmi. "Heat transfer enhancement in a tube with a twisted tape inserted for various length ratios." Energy Sources, Part A: Recovery, Utilization, and Environmental Effects 45, no. 2 (2023): 3602-3616.

[6] Soltani, Mohammad Mohsen, Mofid Gorji-Bandpy, Ahmad Vaisi, and Rouhollah Moosavi. "Heat transfer augmentation in a double-pipe heat exchanger with dimpled twisted tape inserts: An experimental study." Heat and Mass Transfer 58, no. 9 (2022): 1591-1606.

[7] Zheng, Dan, Jianqiang Du, Wei Wang, Jiří Jaromír Klemeš, Jin Wang, and Bengt Sundén. "Analysis of thermal efficiency of a corrugated double-tube heat exchanger with nanofluids." Energy 256 (2022): 124522.

[8] Noorbakhsh, Mehdi, Seyed Soheil Mousavi Ajarostaghi, Mohammad Zaboli, and Behnam Kiani. "Thermal analysis of nanofluids flow in a double pipe heat exchanger with twisted tapes insert in both sides." Journal of Thermal Analysis and Calorimetry (2021): 1-12.

[9] Chen, Ke, Jia Zheng, Juan Li, Jingli Shao, and Qiulan Zhang. "Numerical study on the heat performance of enhanced coaxial borehole heat exchanger and double U borehole heat exchanger." Applied Thermal Engineering 203 (2022): 117916.

[10] Ding, Zi, Cong Qi, Tao Luo, Yuxing Wang, Jianglin Tu, and Chengchao Wang. "Numerical simulation of nanofluids forced convection in a corrugated double-pipe heat exchanger." The Canadian Journal of Chemical Engineering 100, no. 8 (2022): 1954-1964.

[11] Dagdevir, Toygun, and Veysel Ozceyhan. "An experimental study on heat transfer enhancement and flow characteristics of a tube with plain, perforated and dimpled twisted tape inserts." International Journal of Thermal Sciences 159 (2021): 106564.

[12] Subasi, Abdussamet, and Kasim Erdem. "An integrated optimization methodology for heat transfer enhancement: a case study on nanofluid flow in a pipe equipped with inserts." International Journal of Heat and Mass Transfer 172 (2021): 121187.

[13] Nakhchi, M. E., Mohammad Hatami, and Mohammad Rahmati. "Experimental investigation of performance improvement of double-pipe heat exchangers with novel perforated elliptic turbulators." International Journal of Thermal Sciences 168 (2021): 107057.

[14] Singh, Sanjay Kumar, and Arvind Kumar. "Experimental study of heat transfer and friction factor in a double pipe heat exchanger using twisted tape with dimple inserts." Energy Sources, Part A: Recovery, Utilization, and Environmental Effects (2021): 1-30.

[15] Chaurasiya, Prem Kumar, Sanjay Kumar Singh, Piyush Kumar Jain, Upendra Rajak, Tikendra Nath Verma, A. K. Azad, Keshavendra Choudhary, Abeer M. Alosaimi, and Anish Khan. "Heat transfer and friction factor correlations for double pipe heat exchanger with inner and outer corrugation." Energy Sources, Part A: Recovery, Utilization, and Environmental Effects (2021): 1-28.

[16] Suri, Amar Raj Singh, Anil Kumar, and Rajesh Maithani. "Heat transfer enhancement of heat exchanger tube with multiple square perforated twisted tape inserts: experimental investigation and correlation

development." Chemical Engineering and Processing: Process Intensification 116 (2017): 76-96.

[17] Samruaisin, P., W. Changcharoen, C. Thianpong, V. Chuwattanakul, M. Pimsarn, and S. Eiamsa-Ard. "Influence of regularly spaced quadruple twisted tape elements on thermal enhancement characteristics." Chemical Engineering and Processing-Process Intensification 128 (2018): 114-123.

[18] Chamoli, Sunil, Peng Yu, and Shimin Yu. "Multi-objective shape optimization of a heat exchanger tube fitted with compound inserts." Applied Thermal Engineering 117 (2017): 708-724.

[19] Lin, Zhi-Min, Liang-Bi Wang, Mei Lin, Wei Dang, and Yong-Heng Zhang. "Numerical study of the laminar flow and heat transfer characteristics in a tube inserting a twisted tape having parallelogram winglet vortex generators." Applied Thermal Engineering 115 (2017): 644-658.

[20] Man, Changzhong, Xiaogang Lv, Jingwei Hu, Peiyan Sun, and Yunbang Tang. "Experimental study on effect of heat transfer enhancement for single-phase forced convective flow with twisted tape inserts." International Journal of Heat and Mass Transfer 106 (2017): 877-883.

[21] Man, Changzhong, Jinyu Yao, and Chong Wang. "The experimental study on the heat transfer and friction factor characteristics in tube with a new kind of twisted tape insert." International Communications in Heat and Mass Transfer 75 (2016): 124-129.

[22] Tamna, Sombat, et al. "Heat transfer enhancement in tubular heat exchanger with double V-ribbed twisted-tapes." Case studies in thermal engineering 7 (2016): 14-24.

[23] Singh, Vijaypal, Sunil Chamoli, Manoj Kumar, and Alok Kumar. "Heat transfer and fluid flow characteristics of heat exchanger tube with multiple twisted tapes and solid rings inserts." Chemical Engineering and Processing: Process Intensification 102 (2016): 156-168.

[24] Nanan, K., N. Piriyarungrod, C. Thianpong, K. Wongcharee, and S. Eiamsa-ard. "Numerical and experimental investigations of heat transfer enhancement

in circular tubes with transverse twisted-baffles." Heat and Mass Transfer 52 (2016): 2177-2192.

[25] Skullong, Sompol, Pongjet Promvonge, Nuthvipa Jayranaiwachira, and Chinaruk Thianpong. "Experimental and numerical heat transfer investigation in a tubular heat exchanger with delta-wing tape inserts." Chemical Engineering and Processing-Process Intensification 109 (2016): 164-177.

[26] Hasanpour, A., M. Farhadi, and K. Sedighi. "Experimental heat transfer and pressure drop study on typical, perforated, V-cut and U-cut twisted tapes in a helically corrugated heat exchanger." International Communications in Heat and Mass Transfer 71 (2016): 126-136.

[27] Patil, Suhas, and P. Vijay Babu. "Experimental heat transfer and friction factor studies through a square duct fitted with helical screw tapes." The Canadian Journal of Chemical Engineering 92.4 (2014): 663-670.

[28] Eiamsa-ard S., Kongkaitpaiboon V., Nanan K. Thermohydraulics of Turbulent Flow Through Heat Exchanger Tubes Fitted with Circular-rings and Twisted Tapes. Chinese J. Chem. Eng. 21 (2013) 585-593.

[29] Zhang Z., Yang W., Guan C., Ding Y., Li F., Yan H. Heat transfer and friction characteristics of turbulent flow through plain tube inserted with rotor-assembled strands. Exp. Therm. Fluid Sci. 38 (2012) 33-39.

[30] Murugesan P., Mayilsamy K., Suresh S. Turbulent Heat Transfer and Pressure Drop in Tube Fitted with Square-cut Twisted Tape. Chinese J. Chem. Eng. 18 (2010) 609-617.

[31] Sarada, S. Naga, AV Sita Rama Raju, K. Kalyani Radha, and L. Shyam Sunder. "Enhancement of heat transfer using varying width twisted tape inserts." International Journal of Engineering, Science and Technology 2, no. 6 (2010).

[32] Eiamsa-ard, Smith, Chinaruk Thianpong, and Petpices Eiamsa-ard. "Turbulent heat transfer enhancement by counter/co-swirling flow in a tube fitted with twin twisted tapes." Experimental Thermal and Fluid Science 34.1 (2010): 53-62.

[33] Yadav A.S. Effect of half-length twisted-tape turbulators on heat transfer and pressure drop characteristics inside a double pipe u-bend heat exchanger. Jordan J. Mech. Ind. Eng. 3 (2009).

[34] Krishna, Siva Rama, Govardhan Pathipaka, and P. Sivashanmugam. "Heat transfer and pressure drop studies in a circular tube fitted with straight full twist." Experimental Thermal and Fluid Science 33.3 (2009): 431-438.

[35] Promvonge, Pongjet. "Thermal augmentation in circular tube with twisted tape and wire coil turbulators." Energy Conversion and Management 49.11 (2008): 2949-2955.

[36] Li, Q., D. Chen, and Y. Xiang. "Crystallized salty in heat transfer tube spiral rotation cleaning technology study." J Therm Sci Tech–Jpn 7 (2008): 217-220.

[37] Chang, Shyy Woei, Tsun Lirng Yang, and Jin Shuen Liou. "Heat transfer and pressure drop in tube with broken twisted tape insert." Experimental Thermal and Fluid Science 32.2 (2007): 489-501.

[38] Promvonge, Pongjet, and Smith Eiamsa-Ard. "Heat transfer behaviors in a tube with combined conical-ring and twisted-tape insert." International Communications in Heat and Mass Transfer 34.7 (2007): 849-859.

[39] Mengna, Hong, D. E. N. G. Xianhe, Kuo Huang, and L. I. Zhiwu. "Compound heat transfer enhancement of a converging-diverging tube with evenly spaced twisted-tapes." Chinese Journal of Chemical Engineering 15, no. 6 (2007): 814-820.

[40] Naphon, Paisarn. "Heat transfer and pressure drop in the horizontal double pipes with and without twisted tape insert." International Communications in Heat and Mass Transfer 33.2 (2006): 166-175.

[41] Noothong, Watcharin, Smith Eiamsa-Ard, and Pongjet Promvonge. "Effect of twisted-tape inserts on heat transfer in a tube." The 2nd joint international conference on “sustainable energy and environment (see 2006). 2006.

[42] Yu, Xiumin, Tianlan Yu, Deqi Peng, S. Jiang, and J. Luo. "Twisted strip with oblique teeth to efficiently remove fouling and enhance heat transfer at low flowing velocity." Journal of Chemical Industry and Engineering Beijing 56, no. 4 (2005): 744-747.

[43] Zheng, Lu, Yonghui Xie, and Di Zhang. "Numerical investigation on heat transfer performance and flow characteristics in circular tubes with dimpled twisted tapes using Al2O3-water nanofluid." International Journal of Heat and Mass Transfer 111 (2017): 962-981.

[44] Suri A.R.S., Kumar A., Maithani R. Heat transfer enhancement of heat exchanger tube with multiple square perforated twisted tape inserts: experimental investigation and correlation development. Chem. Eng. Process.: Process Intensif. 116 (2017) 76-96.

[45] Suri A.R.S., Kumar A., Maithani R. Effect of square wings in multiple square perforated twisted tapes on fluid flow and heat transfer of heat exchanger tube. Case Stud. Therm. Eng. 10

[46] Zhang X., Liu Z., Liu W. Numerical studies on heat transfer and flow characteristics for laminar flow in a tube with multiple regularly spaced twisted tapes. Int. J. Therm. Sci. 58 (2012) 157-67.

[47] Hong Y., Deng X., Zhang L. 3D Numerical Study on Compound Heat Transfer Enhancement of Converging-diverging Tubes Equipped with Twin Twisted Tapes. Chinese J. Chem. Eng. 20 (2012) 589-601

[48] Mokkapati V., Lin S. Numerical study of an exhaust heat recovery system using corrugated tube heat exchanger with twisted tape inserts. Int. Commun. Heat Mass Transf. 57 (2014) 53-64.

[49] Zhang C., Wang D., Ren K., Han Y., Zhu Y., Peng X., et al. A comparative review of self-rotating and stationary twisted tape inserts in heat exchanger. Renew. Sust. Energ. Rev. 53 (2016) 433-449.

[50] Nanan K., Yongsiri K., Wongcharee K., Thianpong C., Eiamsa-ard S. Heat transfer enhancement by helically twisted tapes inducing co- and counter-swirl flows. Int. Commun. Heat Mass Transf. 46 (2013) 67-73.

[51] Promvonge P., Suwannapan S., Pimsarn M., Thianpong C. Experimental study on heat transfer in square duct with combined twisted-tape and winglet vortex generators. Int. Commun. Heat Mass Transf. 59 (2014) 158-165.

[52] Suhas P., Vijay Babu P. Experimental heat transfer and friction factor studies through a square duct fitted with helical screw tapes. Canadian J. Chem. Eng. 92 (2014) 663-670.

[53] Eiamsa-ard P., Piriyarungroj N., Thianpong C., Eiamsa-ard S. A case study on thermal performance assessment of a heat exchanger tube equipped with regularly-spaced twisted tapes as swirl generators. Case Stud. Therm. Eng. 3 (2014) 86-102.

[54] Sun B., Zhang Z., Yang D. Improved heat transfer and flow resistance achieved with drag reducing Cu nanofluids in the horizontal tube and built-in twisted belt tubes. Int. J. Heat Mass Transf. 95 (2016) 69-82.

[55] Seemawute P., Eiamsa-ard S. Thermohydraulics of turbulent flow through a round tube by a peripherally-cut twisted tape with an alternate axi s. Int. Commun. Heat Mass Transf. 37 (2010) 652-659.

[56] Eiamsa-ard S., Wongcharee K., Eiamsa-ard P., Thianpong C. Thermohydraulic investigation of turbulent flow through a round tube equipped with twisted tapes consisting of centre wings and alternate-axes. Exp. Therm. Fluid Sci. 34 (2010) 1151-1161.

[57] Eiamsa-ard S., Promvonge P. Thermal characteristics in round tube fitted with serrated twisted tape. Appl. Therm. Eng. 30 (2010) 1673-1682.

[58] Chang S.W., Guo M.H. Thermal performances of enhanced smooth and spiky twisted tapes for laminar and turbulent tubular flows. Int. J. Heat Mass Transf. 55 (2012) 7651-7667.

[59] Eiamsa-ard S., Somkleang P., Nuntadusit C., Thianpong C. Heat transfer enhancement in tube by inserting uniform/non-uniform twisted-tapes with alternate axes: Effect of rotated-axis length. Appl. Therm. Eng. 54 (2013) 289-309.

[60] Bhuiya M.M.K., Chowdhury M.S.U., Shahabuddin M., Saha M., Memon L.A. Thermal characteristics in a heat exchanger tube fitted with triple twisted tape inserts. Int. Commun. Heat Mass Transf. 48 (2013) 124-132.

[61] Murugesan P., Mayilsamy K., Suresh S., Srinivasan P.S.S. Heat transfer and pressure drop characteristics in a circular tube fitted with and without V-cut twisted tape insert. Int. Commun. Heat Mass Transf. 38 (2011) 329-334.

[62] Bhuiya M.M.K., Sayem A.S.M., Islam M., Chowdhury M.S.U., Shahabuddin M. Performance assessment in a heat exchanger tube fitted with double counter twisted tape inserts. Int. Commun. Heat Mass Transf. 50 (2014) 25-33.

[63] Bhattacharyya S., Saha S., Saha S.K. Laminar flow heat transfer enhancement in a circular tube having integral transverse rib roughness and fitted with centre-cleared twisted-tape. Exp. Therm. Fluid Sci. 44 (2013) 727-735.

[64] Maddah H., Alizadeh M., Ghasemi N., Alwi S.R.W. Experimental study of Al2O3/water nanofluid turbulent heat transfer enhancement in the horizontal double pipes fitted with modified twisted tapes. Int. J. Heat Mass Transf. 78 (2014) 1042-1054.

[65] Murugesan P., Mayilsamy K., Suresh S. Heat Transfer and Friction Factor Studies in a Circular Tube Fitted with Twisted Tape Consisting of Wire-nails. Chinese J. Chem. Eng. 18 (2010) 1038-1042.

[66] Salam B., Biswas S., Saha S., Bhuiya M. Heat Transfer Enhancement in a Tube using Rectangular-cut Twisted Tape Insert. Procedia Eng. 56 (2013) 96-103.

[67] Omidi M., Farhadi M., Jafari M. A comprehensive review on double pipe heat exchangers. Appl. Therm. Eng. 110 (2017) 1075-90.

[68] Yang L., Du K. A comprehensive review on heat transfer characteristics of TiO_2 nanofluids. Int. J. Heat Mass Transf. 108 (2017) 11-31.

[69] Sundar L.S., Otero-Irurueta G., Singh M.K., Sousa A.C. Heat transfer and friction factor of multi-walled carbon nanotubes–Fe_3O_4 nanocomposite nanofluids flow in a tube with/without longitudinal strip inserts. Int. J. Heat Mass Transf. 100 (2016) 691-703.

[70] Vashistha C., Patil A.K., Kumar M. Experimental investigation of heat transfer and pressure drop in a circular tube with multiple inserts. Appl. Therm. Eng. 96 (2016) 117-129.

[71] Man, C., Yao, J., & Wang, C. (2016). The experimental study on the heat transfer and friction factor characteristics in tube with a new kind of twisted tape insert. International Communications in Heat and Mass Transfer, 75, 124-129.

[72] Chougule S.S., Sahu S.K. Heat transfer and friction characteristics of Al2O3/water and CNT/water nanofluids in transition flow using helical screw tape inserts – a comparative study. Chem. Eng. Process.: Process Intensif. 88 (2015) 78-88.

[73] Omidi M., Farhadi M., Jafari M. A comprehensive review on double pipe heat exchangers. Appl. Therm. Eng. 110 (2017)1075-90.

[74] Zhang X., Liu Z., Liu W. Numerical studies on heat transfer and flow characteristics for laminar flow in a tube with multiple regularly spaced twisted tapes. Int. J. Therm. Sci. 58 (2012) 157-67.

[75] Saha S., Saha S.K. Enhancement of heat transfer of laminar flow of viscous oil through a circular tube having integral helical rib roughness and fitted with helical screw-tapes. Exp. Therm. Fluid Sci. 47 (2013) 81-9.

[76] Zhang C., Wang D., Ren K., Han Y., Zhu Y., Peng X., et al. A comparative review of self-rotating and stationary twisted tape inserts in heat exchanger. Renew. Sust. Energ. Rev. 53 (2016) 433-449.

[77] Song S., Liao Q., Shen W. Laminar heat transfer and friction characteristics of microencapsulated phase change material slurry in a circular tube with twisted tape inserts. Appl. Therm. Eng. 50 (2013) 791-798.

[78] B.L. Zapata, R. Escobar, M.A. Medina, C. Zaragoza, State variables estimation for a counter-flow double-pipe heat exchanger using multi-linear model, in: Proceedings of the IEEE Electronics, Robotics and Automotive Mechanics Conference, Cuernavaca, Morelos, Brazil, 2009, pp. 22–25.

[79] Yu L., Liu D. Study of the Thermal Effectiveness of Laminar Forced Convection of Nanofluids for Liquid Cooling Applications. IEEE Trans. Compo. Package. Manuf. Technol. 3 (2013) 1693-1704.

[80] Tala, JV Simo, et al. "Investigation of the flow characteristics in a multirow finned-tube heat exchanger model by means of PIV measurements." Experimental Thermal and Fluid Science 50 (2013): 45-53.

[81] Nikuradse, Johann. "Laws of flow in rough pipes." (1950).

[82] Abdelghani-Idrissi, Moulay Ahmed, Farid Bagui, and L. Estel. "Analytical and experimental response time to flow rate step along a counter flow double pipe heat exchanger." International Journal of Heat and Mass Transfer 44.19 (2001): 3721-3730.

[83] Yang L., Du K. A comprehensive review on heat transfer characteristics of TiO2 nanofluids. Int. J. Heat Mass Transf. 108(2017) 11-31.

[84] Kline, Stephen J. "Describing uncertainty in single sample experiments." Mech. Engineering 75 (1953): 3-8.

[85] Zhang, Cancan, et al. "A comparative review of self-rotating and stationary twisted tape inserts in heat exchanger." Renewable and Sustainable Energy Reviews 53 (2016): 433-449.

[86] Liu, Shuli, and M. Sakr. "A comprehensive review on passive heat transfer enhancements in pipe exchangers." Renewable and sustainable energy reviews 19 (2013): 64-81.

[87] Garg, M. O., Himanshu Nautiyal, Sourabh Khurana, and M. K. Shukla. "Heat transfer augmentation using twisted tape inserts: a review." Renewable and Sustainable Energy Reviews 63 (2016): 193-225.

[88] Bhuiya, M. M. K., A. K. Azad, M. S. U. Chowdhury, and M. Saha. "Heat transfer augmentation in a circular tube with perforated double counter twisted tape inserts." International Communications in Heat and Mass Transfer 74 (2016): 18-26.

[89] Lin, Zhang, Y. K. You, H. W. Qian, Y. Liu, and X. M. Yu. "and Yu, XM," Experimental research of self-preventing fouling technology for the self-rotating twisted tape in heat exchangers." Chemical Engineering 34 (2006): 16-19.

[90] Saha, S. K., A. Dutta, and S. K. Dhal. "Friction and heat transfer characteristics of laminar swirl flow through a circular tube fitted with regularly spaced twisted-tape elements." International Journal of Heat and Mass Transfer 44.22 (2001): 4211-4223.

[91] Liao, Q., and M. D. Xin. "Augmentation of convective heat transfer inside tubes with three-dimensional internal extended surfaces and twisted-tape inserts." Chemical Engineering Journal 78.2-3 (2000): 95-105.

[92] Hong, Yuxiang, Juan Du, and Shuangfeng Wang. "Experimental heat transfer and flow characteristics in a spiral grooved tube with overlapped large/small twin twisted tapes." International Journal of Heat and Mass Transfer 106 (2017): 1178-1190.